UNIVERSITY OF TASMANIA

Overgrowth Mutants of Barley and Wheat with Increased Gibberellin Signalling

By

Seyedeh Asemeh Miraghazadeh (M.Sc)

School of Biological Sciences

In collaboration with CSIRO Plant Industry, Black Mountain, Canberra

Submitted in fulfilment of the requirements for the degree of Doctor of Philosophy

University of Tasmania, August 2014

Dedication

To Dad, Mom and Javad

Statements and Declarations

Declaration of originality

This thesis contains no material which has been accepted for a degree or diploma by the University of Tasmania or any other institution. To the best of my knowledge and belief, this thesis contains no material previously published or written by another person except where due acknowledgement is made in the text, nor does this thesis contain any material that infringes copyright.

August 2014

Seyedeh Asemeh Miraghazadeh
School of Plant Science
University of Tasmania

Statement regarding published work contained in thesis and authority of access

This thesis may be available for loan and limited copying in accordance with the Copyright Act 1968.

August 2014

Seyedeh Asemeh Miraghazadeh
School of Plant Science
University of Tasmania

Acknowledgements

I would like to gratefully and sincerely thank Dr Peter M. Chandler, my principal supervisor (at CSIRO) for his scientific advice and many insightful discussions, also for his understanding, support and patience. I appreciate all his guidance throughout my thesis. For everything you have done for me Peter, I thank you. I would like to express my deep gratitude and respect to Associate Professor John J. Ross, my academic supervisor at UTAS, whose knowledge, advice and constant encouragement and support were invaluable for me. I would like to thank you John for having time always for me.

I would like to acknowledge Dr Wolfgang Spielmeyer, who always had time to answer my questions. I would like to extend my gratitude to Graduate Coordinator Associate Professor Mark Hovenden for his support that helped my PhD research going smoothly at CSIRO Plant Industry in Canberra.

There were a number of people who helped me with various aspects of my PhD. I would like to say thanks to Carol A. Harding, for her great help that she often provided for my laboratory work, and also to Shek Hossain for his help in glasshouse and field experiments. I appreciate Jess Hyles for her technical advice. I would like to thank my friend, Robin Chapple for support she provided to me during my PhD. I would also like to thank the Grain Research and Development Corporation for providing my PhD scholarship.

I would especially like to thank my family. Dad, thank you for your encouragement, support and patience. I hope this achievement will complete the dream you had for me. Mom and Javad, you have supported and encouraged me throughout my whole degree. There have been moments during the long journey of my PhD that it was impossible to move forward without your kind support. I am forever indebted to you for what you have done for me.

Abstract

DELLA proteins are a key component in the gibberellin (GA) signaling pathway that negatively regulates plant growth. In model plant systems such as Arabidopsis and rice, mutagenesis and screens for GA response mutants have led to the characterization of genes important in GA biosynthesis and GA signalling. In barley and wheat, screening for overgrowth mutants in a dwarf background (suppressor screen) resulted in the isolation of many mutants potentially involved in GA signalling. Characterization of these mutants showed that in barley and wheat nearly all of the mutations represent new *Della* alleles (Chandler and Harding 2013). This PhD project characterizes many of these overgrowth alleles, and addresses their potential application in cereal breeding.

In barley, overgrowth mutants were isolated using dwarf mutants of the variety 'Himalaya' as starting material. They were characterized as plants with enhanced growth, which varied in extent among different mutants, but all retained the original dwarfing gene. These mutants carried new mutations elsewhere in the genome that resulted in enhanced GA signalling. Some overgrowth alleles led to the formation of larger grains, a trait that is important in barley breeding. To assess the effects of overgrowth alleles on grain size, they were back-crossed to a commercial variety (Sloop). In this thesis the agronomic characteristics of BC_3F_4 sister lines (homozygous for either the WT or mutant *Della/Spy1* gene) were studied in detail in glass house and field experiments. The results indicated that overgrowth alleles were able to improve grain size of the commercial variety by about 22% across a range of environments compared to the wild type, but there was also a reduction in grain yield. The hormone physiology of overgrowth mutants was also investigated. Some alleles resulted in a high degree of resistance to growth inhibition caused by applied ABA. This result means that some selected overgrowth alleles are interesting material for studies on tolerance to factors such as drought.

In wheat, overgrowth mutants were isolated as suppressors of the *Rht-B1c* dwarfing gene, which results from a 30 amino acid insertion in the DELLA protein encoded by the B-genome. The new mutants grew faster than the dwarf parent and at maturity they had a range of heights from slightly taller than *Rht-B1c* to as tall as *Rht-B1a* (tall isoline). More detailed characterization of these mutants showed that faster growth resulted from single nucleotide mutations in the dwarfing gene, or altered splicing of the transcript. This class of mutant includes about 15 different alleles that are semi-dwarf alleles of the *Rht-1* gene, similar to *Rht-B1b* and *Rht-D1b* which formed the basis of the Green Revolution. Studies commenced with the characterization of overgrowth alleles that had single amino acid substitutions in the DELLA protein. Semi-dwarf overgrowth alleles with improved dormancy have been characterized. These mutants have significantly higher dormancy than *Rht-B1b* allele. This characteristic is important for wheat breeding in humid environment, where pre-harvest sprouting is a major issue.

The screen for overgrowth mutants in wheat also resulted in 'tall' mutants that appeared to lack the *Rht-B1* gene. Deletion of this gene was confirmed by Southern blot analysis. The extent of deletion in such lines is of interest since isolation of 4B deletion lines

has not been very successful in other wheat genetic backgrounds. We used a newly developed technology, Single Nucleotide Polymorphism (SNP) chip analysis to assess the size of deletions. The results allowed us to classify the deletion lines into three classes: (i) interstitial deletions of 4BS (short arm of chromosome 4B), ranging from small to large deletions, (ii) lines that have lost all 4BS markers, but retain 4BL (long arm of chromosome 4B) markers, and (iii) lines that have lost all 4BS and all 4BL markers. Mutants that lacked the short arm and those that lacked the whole 4B chromosome were also studied with FISH (Fluorescent In Situ Hybridization) analysis (part of a collaborative cytogenetic study). Microscopy clearly showed the presence of acro-/telocentric 4B chromosomes for class (ii) mutants, while mutants in class (iii) had a chromosome count of 40, instead of 42, indicating the complete loss of 4B.

The *Rht-B1c* allele contains one intron, and some overgrowth mutations have occurred in the nucleotides immediately flanking the exon-intron junction, making them potential splice site mutations. The expression of the *Rht-B1c* gene in these mutants was studied with semi-quantitative and real-time PCR techniques. The results of semi-quantitative PCR showed that splicing site alleles had less normal *Rht-B1c* mRNA relative to *Rht-B1c* (dwarf parent), and they also had mRNAs that differed in length. It was also shown that different-sized mRNAs in some cases resulted in a change of the open reading frame. qPCR showed that splicing site mutants had reduced expression levels of the gene, similar to *Rht-B1c*. However, some mutants had longer stem length (about 84% of the tall parent) which is difficult to reconcile with the similar gene expression levels of the dwarf parent (dwarf stem length is 42% of tall isoline). Our results suggested that altered *Rht-B1c*transcripts produce DELLA proteins with less activity compared to the wild type, which in turn had less effect on growth repression.

Overgrowth alleles enhance growth due to changes in DELLA proteins, one of the key components of the GA signalling pathway. These mutations might result in DELLA proteins with reduced activity in terms of their physical interactions with other proteins important in growth responses. They are also potentially useful in barley and wheat breeding, offering a range of semi-dwarf plants with characteristics important in breeding such as grain size (in barley) and improved dormancy (in wheat).

Reference:

CHANDLER, P. M. & HARDING, C. A. 2013. 'Overgrowth' mutants in barley and wheat: new alleles and phenotypes of the 'Green Revolution' Della gene. *Journal of Experimental Botany,* 64**,** 1603-1613.

Table of Contents

List of Figures

List of Tables

CHAPTER 1

General Introduction

1.1.Gibberellins

The class of plant hormone known as gibberellins (GA), comprise a large family of diterpenoid carboxylic acids that have been well characterized, with their best known function being the regulation of stem elongation in plants. GAs were first isolated from a pathogenic fungus, *Gibberella fujikuroi*, which caused rice plants to grow too tall, without seed production. All higher plants produce GA hormones and certain GAs are characterized as endogenous growth regulators. GAs are also found in some species of endophytic free-living bacteria, several fungal species, and some lower plants, but their functions are unclear. Currently 136 different GA structures have been identified from all sources, but few of them are biologically active in higher plants. The principal biologically active GAs are GA_1, GA_3 and GA_4. They control diverse aspects of plant growth and development. They play roles as growth regulators by enhancing cell elongation, and in some cases cell division (Smith *et al.* 1992; Gendreau *et al.* 1997). GAs are involved in certain developmental transitions, and in different species they promote the switch between seed dormancy and germination, juvenile and adult growth phases, and vegetative and reproductive development (Evans and Poethig 1995; Tanaka *et al.* 2012).

In the pathways by which plants respond to environmental and developmental signals, GAs can be important molecules. The responses involve the regulation of GA biosynthesis, deactivation, perception and signal transduction.

GA biosynthesis

GAs are biosynthesised from trans-geranylgeranyl diphosphate (GGDP), a common C20 precursor of diterpenoids. The pathway to bioactive GAs can be divided into three stages that take place in the plastid, endoplasmic reticulum (ER) and cytosol respectively, each involving a different class of enzyme. In plastids, the linear molecule GGDP is converted into a tetracyclic compound, *ent*-kaurene, in two steps catalyzed by *ent*-copalyl-diphosphate synthase (CPS) and *ent*-kaurene synthase (KS). These enzymes belong to the first group of

enzymes in the pathway, called terpene synthases. In the second stage the intermediate *ent*-kaurene is converted into GA_{12}, the common precursor for all GAs. This requires six oxidative steps, and the two enzymes involved are *ent*-kaurene oxidase (KO) and *ent*-kaurenoic acid oxidase, both of which belong to the cytochrome P450 group of enzymes. These enzymes are localized in the plastid envelope and endoplasmic reticulum.

The third stage occurs in the cytosol; the common GA_{12} precursor is a substrate for two branches of oxidations involving hydroxylation at C-13 and/or C-20. In the early 13-hydroxylation pathway GA_{12} is converted into GA_{53}. GA_{12} and GA_{53} are both oxidized at C-20 by GA20-oxidase (GA20ox), and through a series of parallel oxidative reactions these substrates are converted to GA_9 and GA_{20} respectively(Hedden and Thomas 2012). The final step to bioactive GAs is 3-oxidation of GA_9 and GA_{20} to form their 3βOH derivatives GA_4 and GA_1 respectively, catalyzed by GA 3-oxidases (GA3ox). The 20-oxidase and 3-oxidase enzymes are representatives of the third group of enzymes in GA biosynthesis, the soluble 2-oxoglutarate-dependent dioxygenase (2ODD) class of enzymes.

GA deactivation

Deactivation is an important mechanism by which plants maintain bioactive GA concentrations at levels appropriate for optimum growth and development. It enables a controlled reduction in active GA content in response to changing environment, and along with homeostatic regulation, balances the synthesis of bioactive GA. The principal enzymes involved in this mechanism are GA 2-oxidases (GA2ox), which are also 2ODDs. GA2oxs catalyse 2β-hydroxylation of bioactive GAs, GA_4 producing inactive GA_{34} and GA_1 producing inactive GA_8. They can also potentially catalyse the 'inactivation' (2-oxidation) of precursors to bioactive GAs. The consequence is that the deactivation mechanism affects bioactive GA synthesis by limiting the precursor pool, and less bioactive GA is synthesized (Thomas *et al.* 1999; Yamaguchi 2008). GA2oxs are known as the major enzyme for GA deactivation, although it is clear that there are additional pathways.

Another mechanism by which GAs are catabolised was revealed in a rice mutant, *elongated uppermost internode* (*eui*). The *Eui* gene encodes a cytochrome P450 monooxygenase that catalyzes the 16α, 17-epoxidation of non-13-hydroxylated GAs, which reduces the content of GA_4 in rice. Mutant *eui*plants are taller than the WT, because they accumulate a large amount of bioactive GAs in the uppermost internode, in turn because EUI

(GA-deactivating enzyme) is defective in these mutants. Consistent with that, overexpression of EUI in transgenic rice caused dwarfism and a reduction in GA_4 content in the uppermost internode (Zhu *et al.* 2006).

Regulation of GA biosynthesis

The content of bioactive GA is maintained at appropriate levels in cells for its role in regulating plant growth and development. It is likely that transcriptional and post-transcriptional events that affect the expression of genes encoding enzymes essential for GA biosynthesis are involved in this process. To achieve this, there is evidence for different mechanisms that regulate the balance between GA biosynthesis and catabolism. Although environmental factors and developmental stage of the plant affect GA biosynthesis (and GA signal transduction), feedback and feedforward mechanisms have been suggested to control GA homeostasis.

Feedback mechanism

Biochemical and gene expression studies of GA biosynthesis and GA-response mutants provided evidence of feedback regulation of bioactive GA. In these studies the GA levels before and after GA treatment were compared between the mutants and their respective wild-type line, and it was demonstrated that GA levels are controlled through this regulatory process (Thomas *et al.* 2005). Further attempts in cloning of genes encoding GA biosynthesis enzymes led to the demonstration that this regulation was mediated through the transcriptional control of specific ODDs (Hedden and Thomas 2012).

There is a tendency to maintain the normal content of bioactive GA using feedback mechanisms that operate at the levels of GA biosynthesis, GA deactivation and GA signalling. The role of GA signalling in such mechanisms will be discussed later in the section on GA signalling(p. 6). In feedback regulatory systems the content of GA is negatively regulated by bioactive GA 'action' itself, this action reflecting the ability of a plant to respond to GA (Hedden and Kamiya 1997).

Feedback regulation was studied originally by comparing GA contents in GA biosynthesis and GA response mutants and the respective wild type. In maize, *d1* mutants accumulated high levels of GA_{20}, but had lower levels than expected of GA_{53} and GA_{19}. Due to the defective 3-oxidation of GAs in this mutant, it is not able to effectively convert GA_{20} to bioactive GAs such as GA_1 and GA_3 (via GA_5). Application of GA restored the levels of GA_{53}

and GA_{19} close to those in the wild type (Hedden and Croker 1992). They proposed that GA 20-oxidase is the primary target for feedback regulation. Further studies on transcriptional control of specific ODDs provided more information about feedback mechanism and GA 20-oxidase regulation. In Arabidopsis, GA_3application led to reduced expression levels of *AtGA20ox1, AtGA20ox2* and *AtGa20ox3* genes (Phillips *et al.* 1995; Xu *et al.* 1995). Interestingly, later studies showed that *AtGA20ox4, AtGA20ox5* and *AtGA3ox2* genes are apparently not under the same regulatory mechanism; however they confirmed that *GA20ox1-3* were negatively regulated by GA (Yamaguchi *et al.* 1998; Rieu *et al.* 2008b).

The Arabidopsis *ga4-1* mutant, which has a single nucleotide substitution in its *GA*4 gene, has reduced 3β-hydroxylase activity, and has high levels of GA_9 and GA_{20} together with reduced levels of GA_4 and GA_1. Overexpression of the *GA4* gene in the *ga4-1* mutant resulted in more abundant *AtGA4* mRNA, two to three fold elevated compared with the wild type. Treating *ga4-1* plants with GA_3 repressed levels of the overexpressed *ga4* transcript, indicating that expression of *AtGA3ox1* is also under feedback control by bioactive GAs (Chiang *et al.* 1995). Consistent with this observation, Yamaguchi *et al.* (1998) also confirmed that *AtGA3ox1* is under feedback regulation in germinating seeds. They showed that *AtGA3ox1* and *AtGA3ox2* (former *GA4* and *GA4H*) genes are expressed in germinating seed. In a GA-deficient mutant (*ga1-3*) the mRNA expression of these two genes increased during imbibition in water (12 to 24 hrs in constant light), however the abundance of *AtGA3ox1* mRNA was very high compared with *AtGA3ox2* mRNA. Application of GA_4 (100µM) reduced the expression level of the *AtGA3ox1* gene, but increased expression of *AtGA3ox2* particularly at 24 and 36 hrs after imbibitions. This study showed different behaviour of these genes in feedback regulation.

Changes in the expression of GA 3-oxidase mRNA were also studied in germinated grains of rice. The expression of *OsGA3ox2* mRNA was altered significantly after applying GA or uniconazole, a GA inhibitor. It was decreased after GA_3 treatment, but increased after treatment with GA biosynthesis inhibitor. However there were no changes in the expression of *OsGA3ox1* mRNA, and it seems that regulation of this gene is not subject to feedback mechanism (Itoh *et al.* 2001).

These observations indicate that only specific ODDs are regulated by feedback. It might be caused by their distinct expression in specific cells and organs, suggesting separate physiological roles during plant growth and development. Therefore, in different plant growth stages there might be a need for plasticity in generating bioactive GA with regards to the

different environmental signals. These genes might also have other functions in addition to GA metabolism which possibly gives them alternative regulation.

Feedforward mechanism

GA deactivation (catabolism) also plays an important role in maintaining an appropriate level of active GA. In this mechanism, feedforward regulation, active GAs up-regulate expression of GA 2-oxidase genes. Among a number of mechanisms known to inactivate GAs (Zhu *et al.* 2006; Varbanova *et al.* 2007), the most widespread mechanism in many plant species was suggested to be through 2-oxidation. Genes encoding GA 2-oxidases were identified by screening cDNA expression libraries for 2β-hydroxylase activity (Lester *et al.* 1999; Thomas *et al.* 1999). The enzyme activity was demonstrated *in vivo* by overexpressing the gene in Arabidopsis, which resulted in a dwarf plant with low bioactive GA levels (Rieu *et al.* 2008a). It was shown that 2-oxidation played a major role in regulating GA content in different stages of growth and development (Thomas *et al.* 1999; Elliott *et al.* 2001;Rieu *et al.* 2008a).

In *ga1-2*, a GA-deficient mutant of Arabidopsis due to a defect in the CPS enzyme, the abundance of different *GA2ox* gene transcripts was assessed by RNA blots after applying GA_3. It was demonstrated that expression of both *AtGA2ox1* and *AtGA2ox2*, which can 2-hydroxylate both C20-GAs and C19-GAs, is up-regulated in response to increased bioactive GA_3. In contrast, *AtGA20ox2* and the GA 3β-hydroxylase gene *AtGA3ox1* were both expressed at high levels in this mutant and reduced remarkably after GA_3 treatment. This provided evidence for feedforward and feedback mechanisms respectively that would tend to maintain active GA concentrations at constant levels (Thomas *et al.* 1999). Further studies by Rieu *et al*. (2008a) showed that other GA 2-oxidases, *AtGAox4, AtGAox6, AtGAox7* and *AtGAox8* were also up-regulated in response to applied GA, however *AtGA2ox3* was not, and is therefore an exception to this feedforward mechanism. This shows the complexity of regulation in a gene family.

In rice, *OsGA2ox3* was proposed as the 2-oxidase responsible for homeostatic regulation of the concentration of bioactive GA, and it was expressed in every tissue (Sakai *et al.* 2003). They showed that the transcript level of *OsGA2ox3* was low in the WT and in plants treated with uniconazol, but GA_3 application increased the expression of the gene rapidly. It was also reported earlier that ectopic expression of *OsGA2ox1* in transgenic rice resulted in a low content of endogenous GA_1 (less than one-fourth of the wild type GA_1 content), however, *OsGA2ox1* transcript level was not affected by GA_3 (Sakamoto *et al.* 2001).

This result also indicated that, similar to Arabidopsis, only some of the GA 2-oxidase genes are subject to feedforward regulation.

1.2.GA signalling

During the past decade studies of GA response mutants have brought great progress in understanding the molecular basis of GA signal transduction. GA-insensitive mutants are dwarf, similar to GA biosynthesis mutants, but their phenotype cannot be rescued by hormone (GA) application. This lack of response to GA suggested that these plants are unable to perceive the GA signal. Genetic and molecular studies, mainly in Arabidopsis and rice, have identified major genes playing key roles in GA signalling. These genes encode proteins that determine GA response capacity (Hartweck and Olszewski 2006; Daviere and Achard 2013). Key components include the GA receptor *GIBBERELLIN INSENSITIVEDWARF 1* (*GID1*), the DELLA growth inhibitors (DELLAs) and F-box proteins *SLEEPY1* (*SLY1*) and *SNEEZY* (*SNE*) in Arabidopsis and *GIBBERELLIN INSENSITIVE DWARF 2* (*GID2*) in rice (Achard and Genschik 2009).

The basic model of GA signalling proposes that the accumulation of DELLA proteins inhibits growth, and that the GA signal removes this inhibition by destabilizing DELLAs (Ueguchi-Tanaka *et al.* 2007). Other studies provide evidence suggesting that there might be additional mechanisms, independent of DELLA destruction, and these will be discussed later. In this section the molecular basis of the basic GA signalling model will be reviewed, together with genetic and biochemical evidence from studies of GA-signalling mutants.

GA receptor

It is widespread in hormone systems for target cells to have specific receptors that detect a complementary chemical signal, usually the hormone or a related molecule. Receptors are proteins that specifically and reversibly bind to the hormone. Then, through a conformational change, receptor molecules are transformed to an active form, which initiates a molecular program that ultimately leads to a characteristic response. One of the major hormone transduction pathways in animal systems is perception of hormones by plasma membrane-localized receptors e.g. G protein-coupled receptors and tyrosine kinase receptors. These receptors respond to external hormone and transduce the signal into intracellular signals. They might directly interact with DNA sequences of target genes and this interaction results in altered patterns of gene transcription (Libbenga *et al.* 1986).In fact, some members of

membrane-localized mammalian receptors have been detected in the nucleus, and it is suggested that they might act as regulatory proteins (Johnson *et al*., 2004).

Plant hormone receptor research aims to identify the initial events of perception and transduction of the hormone signal, similar to what is known from animal models (not necessarily identical). GA was one of the earliest hormone systems studied, in part because a well-defined target tissue was available. The induction of hydrolytic enzymes following GA treatment of aleurone layers of cereal grains is a characteristic GA response. It was demonstrated that α-amylase can be induced in aleurone protoplasts in a GA-dependent manner(Hooley *et al.* 1991). Later it was reported that when GA_4 was injected into the cytoplasm of barley aleurone there was no α-amylase induction in the aleurone cells (Gilroy and Jones 1994). Therefore biochemical experiments suggested that the GA perception site is on the plasma membrane. Based on these observations attempts were made to detect a GA receptor on the membrane of oat aleurone by the photoaffinity-labeling method. These led to the identification of two putative GA binding proteins from the plasma membrane fraction (Lovegrove *et al.* 1998). Although partial amino acid sequences of these proteins were identified, there was little follow-up work published.

The successful identification of the GA receptor came from map-based cloning of a dwarf mutant gene. Ueguchi-Tanaka e*t al*. (2005) characterized *gid1-1*, a GA-insensitive mutant in rice, which led to the discovery of the GA receptor. In contrast to the previous reports (Hooley *et al*., 1991), GID1 is a soluble protein contained within the nucleus (Nakajima *et al.* 2006). They isolated four different alleles of the *gid1* locus and the corresponding phenotypes were all very dwarf with dark-green leaves, which is a typical GA mutant phenotype. They did not show any response to GA_3 treatment i.e. no α-amylase was produced when embryo-less half seeds were treated with GA_3, and the second leaf sheath did not elongate in response to GA, in contrast to wild type seedlings. Endogenous GA levels were measured in *gid1* mutants and on average they had 100 times more endogenous GA_1 than the wild type.

It was known that DELLA proteins suppress GA signalling, because their degradation triggers a range of GA responses *in planta* (Itoh *et al.* 2003). Therefore the relationship between SLR1, a rice DELLA protein, and GID1 was tested. SDS-polyacrylamide gel electrophoresis showed a very strong band for SLR1 in the *gid1* mutant compared with the wild type. GA_3 treatment did not diminish the amount of the SLR1 in the mutant, whereas it did in the wild type. The stability of DELLA proteins in *gid1* mutants was confirmed in transgenic plants producing SLR1-GFP. The GFP signals were detected in nuclei of *gid1* cells after GA_3 treatment, but the

wild type did not show any signals. This observation demonstrated that GID1 is essential for SLR1 degradation.

The involvement of GID1 in GA perception was shown by interaction between recombinant GST-GID1 and radio-labelled GA. GST-GID1 showed high affinity for biologically active GAs (GA_1, GA_3, and GA_4). Single amino acid substitutions introduced into the fusion proteins GST-GID1-1 and GST-GID1-2 or a deletion in GST-GID1-3 caused a lack of GA binding and resulted in GA insensitivity. Transgenic plants with over-expression of GID1 also resulted in a GA-hypersensitive phenotype i.e. tall plants with light green leaves and poor fertility (Ueguchi-Tanaka *et al.* 2005). Therefore if GID1 is a GA receptor, this perception of GA should be transduced to SLR1 by GID1 proteins. Indeed they showed GID1 interacted with SLR1 in yeast cells in a GA-dependent manner. The interaction of DELLA proteins and GID1 was tested by a yeast two-hybrid assay. In the presence of GA_3, GID1 interacted directly with the rice DELLA protein SLR1 (Ueguchi-Tanaka *et al.* 2005).

In Arabidopsis three GA receptor genes (*AtGID1a, AtGID1b* and *AtGID1c*), all closely related to rice *OsGID1,* were cloned (Nakajima *et al.* 2006). Their GA-binding activities were confirmed by *in vitro* assays, and the yeast two-hybrid system showed interaction between AtGID1 and Arabidopsis DELLA proteins that was dependent on GA, similar to the rice system. The expression of each *AtGID1* gene in the rice *gid1* mutant rescued the GA-insensitive dwarf phenotype to normal. These results demonstrated that all AtGID1s function as GA receptors in Arabidopsis (Nakajima *et al*., 2006; Griffiths *et al*., 2006; Willige *et al*., 2007; Iuchi *et al*., 2007).

Chandler *et al*. (2008) identified a putative barley GA receptor, based on barley ESTs related to the *OsGID1* sequence. A collection of barley GA insensitive mutants was used to confirm the putative receptor role in GA signalling. In addition, there was perfect linkage in segregating populations between the new mutations and the *gse1* phenotype, suggesting that the putative *HvGID1* sequence in barley corresponds to the *Gse1* locus. *Gse1* mutants showed a higher content of GA_1 and they had a reduced sensitivity to low concentration of exogenous GA_3 compared with the wild type.

The comparison between barley GA receptor mutants and rice *gid1* mutants revealed that different species might show differences in their GA hormonal physiology. All of the barley GA receptor (*Gse*) alleles were self-fertile and showed a range in heights from severe dwarf to mild dwarf. In contrast, Ueguchi-Tanaka *et al*. (2005) reported that only the mild dwarf mutant of rice (*Osgid1-2*) produced fertile flowers. Rice GA receptor mutants did not respond (leaf sheath elongation or half grain α-amylase production) to GA_3, whereas barley

mutants which were insensitive to low concentrations of GA_3 gave substantial growth and considerable α-amylase production at very high concentrations of GA_3 (1mM). GA_1 contents of the barley mutants showed a modest increase (about 4-fold) whereas in rice it was 95- to 125-fold (Ueguchi-Tanaka *et al.* 2005) and it was also reported as 16-fold in Arabidopsis (Griffiths *et al.* 2006). Among the 16 barley GA receptor mutants similar to *gid1* mutants in rice, none showed complete GA insensitivity. There was also no correlation between the degree of GA response and the degree of dwarfism in *gse1* mutants i.e. there were severe dwarfs with large GA responses and mild dwarfs with small GA responses. These observations leave open the possibility that there might be a second GA signalling mechanism that leads to GA responses at high concentration of GA_3 in barley (Chandler *et al.* 2008).

Recently Li *et al*. (2013) studied *GID1*-related genes in hexaploid wheat. Three *TaGID1* genes, related to rice *OsGID1,* were isolated and their expression levels studied in the heading stage. Real-time PCR results showed that all putative GA receptor genes, *TaGID1-A1*, *TaGID1-B1* and *TaGID1-D1*, had similar expression patterns in flag leaves, young spikes, peduncles and the third and fourth internodes. The interaction of these putative GA receptors with wheat DELLA proteins was tested in yeast two hybrid assays. The three TaGID1 proteins shared strong interaction with TaRHT-1 (wheat DELLA protein) in the presence of GA_3, but not in its absence. Moreover, over-expression of *TaGID1* genes in the Arabidopsis double mutant *gid1a/gid1c* partially rescued the GA-insensitive dwarf phenotype, with height increasing from less than 15 cm to about 27 cm, contrasting with the control line at about 40 cm. All three TaGID1 genes restored height of the double mutants, demonstrating that all TaGID1 genes are functional (Li *et al.* 2013). Their identification of GID1-related proteins as the GA receptor in the species described above suggests that there is a common mechanism in GA signalling which has been conserved among species.

The primary structure of GID1 is similar to the hormone-sensitive lipase (HSL) protein family (Yeaman 2004). The HSL family contains an α/β-hydrolase fold of distinct topology and the catalytic centre contains Ser-His-Asp amino acids. It also has a mobile lid that controls access to the active site of a lipid in a lipase reaction. The similar structures of GID1 and HSLs raised the question of how different isGID1 from HSLs, enabling GID1 to specifically interact with bioactive GAs while maintaining the conserved structure of the HSL family (Shimada *et al*., 2008; Murase *et al*., 2008).

The GID1 structure contains a GA-binding pocket and an N-terminal lid that is mainly α-helix and β-scaffold, but it also consists of loops. Inside the pocket, a bioactive GA_4 is held by several hydrogen bonds by means of water molecules. The molecular shape and the basal

skeleton of GAs also contribute to keeping GA_4 firmly in the pocket by non-polar interactions. Both faces of the gibberellin molecule rings interact with central amino acid residues of GID1, and each residue comes into contact with some of the C positions in the GA_4 molecule. It was suggested that GA_4 possibly acts to close the N-terminal lid over the binding pocket. The N-terminal lid amino acid chains on the molecular surface are suggested to be involved in OsGID1-GA interaction with SLR1 proteins. Replacement of these residues diminished interaction of OsGID1 with DELLA proteins in yeast cells, but did not interfere with GA-binding activity (Murase *et al.* 2008; Shimada *et al.* 2008).

Shimada *et al*. (2008) produced 17 OsGID1 mutants, in which different amino acid residues that were proposed (by structural analyses) to be important residues for GA binding, were replaced with Ala. In all cases the GA-binding activity was reduced significantly. This result confirmed that these amino acids are important to give GID1 its GA receptor role, and differentiate it from the HSL family. This observation suggests that GID1 originated from the HSL family, with a Ser residue adapted specifically in GID1 for GA binding ability. Some of the N-terminal lid residues have also become specialized for holding the GA molecule. They proposed a model and described how GID1 discriminates and becomes activated by bioactive gibberellin for specific binding to DELLA proteins.

In this model GID1, but not DELLA, is responsible for GA perception. The GID1 core domain forms a deep pocket and accommodates GA_3 or GA_4 inside. The N-terminal lid of the GID1 molecule then covers the bioactive GA, so there is no direct interaction between the hormone and the DELLA domain.

DELLA proteins

DELLA proteins are localized in cell nuclei and are a subfamily of GRAS (GAI, RGA and SCR) proteins, but interact with GID1. These plant-specific proteins are suggested to function as transcriptional regulators with important roles in signal transduction pathways (Pysh *et al*.,1999); however so far there was no report of their DNA-binding site. All subgroups in this family share the C-terminal GRAS domain that is involved in transcriptional regulation and is characterised by two leucine heptad repeats (LHRI and LHRII) and three conserved motifs, VHIID, PFYRE and SAW (Bolle 2004). DELLAs are different to other members of the GRAS protein family, because of the N-terminal DELLA domain (they have been named after this motif) and their TVHYNP domain. They are highly conserved among different species, including Arabidopsis, wheat, maize, rice and barley (Peng *et al.* 1997; Peng *et al.* 1999; Ikeda *et al.* 2001;Chandler *et al.* 2002). (Figure 1.1)

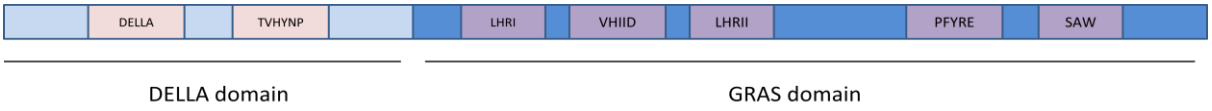

Figure 1.1. DELLAs are a subset of the plant-specific GRAS family of transcriptional regulators. DELLAs share a conserved C-terminal GRAS domain, and a specific N-terminal GA perception domain.

Several studies have provided evidence that DELLAs are repressors of plant growth, following earlier suggestions that GA signal transduction might be regulated through such repressors (Potts *et al.* 1985; Chandler 1988; Lanahan and Ho 1988; Croker *et al.* 1990; Harberd *et al.* 1998). Peng *et al.* (1997) reported that GAI is involved in the GA signalling pathway and that it negatively regulate GA responses e.g. stem growth. They studied GA responses in *gai*, a GA insensitive mutants of Arabidopsis. About the same time Silverstone *et al.* (1998) were able to isolate mutants of RGA that rescued the dwarf phenotype of *ga1-3*, a GA biosynthesis mutant of Arabidopsis. They isolated the RGA gene and it showed a high degree of identity with GAI. So, it was suggested that RGA might be another negative regulator of GA signalling. They also detected the signal of green fluorescent protein-RGA in the nucleus. Later studies showed that Arabidopsis has five DELLA-encoding genes that all produce growth repressors including *GAI, RGA, RGL1, RGL2* and *RGL3* (Silverstone *et al*., 1998; Wen and Chang , 2002; Lee *et al*., 2002).

Peng *et al*.(1999) reported that the *Reduced Height-1* (*Rht-1*) loci in wheat are related to the Arabidopsis *GAI* gene. The proteins encoded by these genes had very similar carboxy-terminal amino acid sequences, equivalent to a region of a candidate transcription factor from Arabidopsis. There is more than 90% similarity between the COOH-terminal 60% of RHT-1 and GAI amino acid sequences; and it is even higher (more than 98%) between the three *Rht-1* homoeologues in wheat. The N-terminal region of the RHT-1 protein is less conserved compared with the C-terminal domain; however it still contains two motifs that are closely related to those in GAI and RGA i.e. DELLA and TVHYNP (Peng 1997, Silverstone 1998). It was suggested that these might be responsible for the GA response regulation of these proteins. Mutation of this motif leads to generation of gain-of-function mutants and leads to a GA-insensitive phenotype (Dill *et al.* 2001), whereas loss-of-function mutants cause a constitutive GA-response phenotype (Sun and Gubler 2004).

In other species like rice it was also reported that there was a GAI-like gene closely related to *AtGAI* (Ogawa *et al.* 2000). The *OsGAI* gene was isolated and showed 53-55% identity to GAI and RGA from Arabidopsis. High levels of *OsGAI* transcripts were found in tissues such as nodes and internodes where GA induces cell elongation and cell division. Later, the constitutive GA response mutant, *slr1-1* was mapped to *OsGAI*. This mutant does not respond to uniconazole, the GA biosynthesis inhibitor, and its aleurone layers produced α-amylase even when GA was absent. When the content of endogenous GA was measured there was a very low level of GA_1 compared with the wild type. These observations indicated that the product of the *SLR1* gene might play a role in the GA signalling pathway (Ikeda *et al.* 2001). Moreover, introducing the wild type *SLR* gene into the *slr1-1* mutant restored GA sensitivity to normal. It was proposed that OsGAI be renamed SLR1. This protein contained the DELLA motif which was believed to be a GA response domain (Peng *et al*. 1999).

It was shown in barley that two different mutations in the *Sln1* gene resulted in either a dwarf, GA-insensitive phenotype or in a 'slender' phenotype. A dominant dwarf mutant of barley (*Hordeum vulgare*), (*Sln1d)* shows a slight growth response to GA_3 at very high concentrations; in contrast a recessive mutant (*sln1c*) generates a different phenotype, tall and GA hypersensitive slender type, which resembles a normal plant treated with high doses of GA_3 (Chandler *et al.* 2002). The slender phenotype is due to a loss of function of the wild type *Sln1* gene, and it was suggested that the product of the *Sln1* locus is a negative regulator or "repressor" of GA responses (Chandler and Robertson 1999). Immunoblotting studies showed that in growing leaves SLN1 protein localized to the leaf elongation zone. The two mutants, *Sln1d* and *sln1c* are different in their abundance and distribution of SLN1 protein, and also in the amount of bioactive GAs as well as their precursors and catabolites. These results indicated that leaf elongation rate in barley depends on GA content, activity of SLN1 protein and their interaction. It also suggested a feedback regulation of GA biosynthesis resulted from excessive SLN1 activity. The *Sln1* gene encodes a DELLA protein and loss- or gain-of-function mutants of this gene alter GA responses in barley. The *Slender1* gene is related to Arabidopsis *GAI* and *RGA*, wheat *Rht-1* and rice *Slr1*.

In fact the DELLA domains are essential motifs that critically determine the binding affinity to the complex formed between an active GA and the GA receptor. They stabilize GA binding to the receptor by interacting with the GID1 extended lid on 'top' of GA and trapping the hormone inside the GID1 molecule (Fleet and Sun 2005). Subsequent degradation of the DELLA proteins triggers GA responses such as stem growth and grain germination. Therefore

DELLA proteins are key molecules in GA signalling that negatively regulate GA responses (Itoh *et al*., 2003).

F-Box subunits

As discussed above, DELLA proteins are negative regulators of GA signalling. Much of our understanding of how GA represses DELLA activity came from the observations of Silverstone *et al*. (2001). Using the GFP-RGA fusion gene and anti-RGA antibodies, they demonstrated that GA stimulates rapid disappearance of DELLA proteins (in 30 min) in Arabidopsis. Their observation suggested that ubiquitin-mediated proteolysis might be involved in controlling the levels of DELLA proteins in the cell (Callis and Vierstra 2000; Karniol and Chamovitz 2000, McGinnis *et al*., 2003; Sasaki *et al*., 2003).

Indeed characterization of rice GID2 and Arabidopsis SLY1 F-box proteins provided evidence for the involvement of the ubiquitin/proteosome pathway in GA signalling. The *gid2* mutant is a severe GA-insensitive dwarf mutant of rice. It shows very little response to even very high concentrations of GA_3 (100μM), and there was no GA-dependent induction of α-amylase mRNA. The level of bioactive GA was 100 times higher than that detected in the wild type (Sasaki *et al.* 2003). Moreover, they showed that the GA-dependent degradation of the SLR1 protein did not occur in *gid2* mutants, and suggested that DELLA accumulation caused the dwarf phenotype of this mutant.

In Arabidopsis *sly1* mutants have been reported with similar characteristics to *gid2* in rice. The *sly1* mutants were GA-insensitive and dwarf. Loss of SLY1 function results in increased seed dormancy, dark green dwarfism and delayed flowering. The accumulation of RGA was reported in *sly* mutants even in the presence of GA_4 (McGinnis *et al.* 2003). Two loss-of-function mutants of F-box proteins *AtSLY1* and *OsGID2* were dwarf and GA treatments did not rescue their phenotype, similar to DELLA gain-of-function mutants (McGinnis *et al.* 2003; Sasaki *et al.* 2003).

These two genes, *GA-INSENSITIVEDWARF2 (GID2)* and *SLEEPY1 (SLY1)* encode F-box domain-containing proteins in rice and Arabidopsis respectively. F-box proteins are a component of the SCF (SKPI, CULLIN,F-BOX) E3 ubiquitin-ligase complex, that catalyses the attachment of polyubiquitin chains to target proteins for their subsequent degradation by the 26S proteasome (Lechner *et al.* 2006).

The hypothesis that GA-dependent degradation of DELLA is caused by 26S ubiquitination was tested by immunoblot analysis. In contrast to wild type, SLR1that was polyubiqutinated in the presence of GA, in *gid2-1* (a GA-insensitive mutant), SLR1 protein

was not ubiquitinated with or without the presence of GA (Sasaki *et al.* 2003).High levels of DELLA were detected in *gid2-1* which demonstrated that the *GID2* gene encodes a positive regulator of GA signalling. The double mutant constructed from *gid2-1* and loss-of-function *slr1-1* showed the slender phenotype of *slr1-1*, indicating that the F-box functions upstream of SLR1 (Sasaki *et al.* 2003; Dill *et al.* 2004).

The molecular mechanism for GA-dependant degradation of DELLA via the 26S ubiquitination pathway was described in detail by Hirano *et al*. (2010). They characterised a rice *Slr-d4* mutant that had a mutation in the GRAS domain (in the SAW motif). This mutant is dwarf and GA insensitive, and immunoblot analysis and yeast-two hybrid assay showed that the DELLA protein with the mutation was stable even in the presence of high concentrations of GA_3, because it did not bind to GID1. They suggested that the GA-GID1-DELLA complex induced conformational changes in the GRAS domain of DELLA and enhanced recognition between VHIID and LHRII motifs of DELLA and the F-box protein SLY1/GID2 (Hirano *et al.* 2010). Then the $SCF^{SLY1/GID2}$ complex promotes the ubiquitination and subsequent degradation of DELLA by 26S proteasome (McGinnis *et al.* 2003; Sasaki *et al.* 2003; Dill *et al.* 2004).

In other species also, a similar model for GA signalling was suggested. The molecular mechanism for GA-dependent destabilizing of DELLA was studied in barley. The results suggested a 26S- proteasome-mediated degradation of the barley DELLA protein, SLN1. A 26S proteasome inhibitor blocked GA-promoted leaf one expansion and α-amylase production in wild type barley while it has no effect on *sln1c*, a loss-of-function mutant in barley with constitutive response to GA (Chandler and Robertson 1999) and it showed that DELLA is a specific target for the 26S proteasome in the DELLA degradation model (Fu *et al.* 2002).

GA signalling model

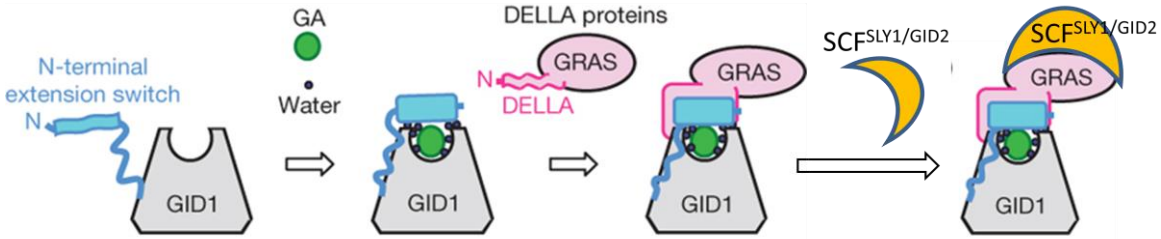

Figure1.2. GA is perceived by a soluble receptor, GID1. The binding of bioactive GA to GID1 induced a conformational change in the N-terminal extension domain of GID1 enabling DELLA to interact. The formation of GA-GID1-DELLA complex promotes interaction between DELLA and the E3 ubiquitin ligase $SCF^{SLY/GID2}$, leading to polyubiquitination and subsequent degradation of DELLA by the 26S proteasome pathway. (This Figure was modified from Murase *et al*., 2008)

When GID1 binds to bioactive GA, it gains the ability to interact with DELLA proteins. The GID1 molecule is like a pocket with GA placed in its central deep cleft (Murase *et al.* 2008). The N-terminal amino acids of the GID1 receptor protein fold over the top of the GA molecule and, like a lid, close the pocket and conceal the GA inside (Murase *et al.* 2008; Shimada *et al.* 2008). The allosteric activity of GA allows a change in the shape of GID1 and prepares the receptor molecule to interact with DELLA proteins. There is no direct contact between the hormone and the DELLA protein (Murase *et al.* 2008). The N-domain of the DELLA protein has an intrinsically disordered structure that possesses binding-induced folding properties(Sun *et al.* 2010a). This domain contains DELLA and VHYNP motifs that directly interact with the GA-bound receptor GID1, and play a critical role in molecular recognition events (Murase *et al.* 2008; Sun *et al.* 2010a). Binding of GA to GID1 results in rapid degradation of DELLA. The GA-GID1-DELLA complex allows F-box proteins to recognize DELLA proteins by binding to VHIID and LHRII motifs of the GRAS domain of the DELLA proteins (Hirano *et al.* 2010). A specific ubiquitin E3 ligase complex recruits DELLAs for polyubiquitination and subsequent degradation by the 26 proteasome (Sun 2010).

Possible exceptions to the GA signalling model

Although the molecular events involving GID1, DELLA and F-box proteins described above (Figure 1.2) are now accepted as the fundamental model of GA signalling, this is not necessarily the complete picture of regulating DELLA function because there are exceptions to the model in which GID1-DELLA interaction might be independent of bioactive GA. For instance, one unique GID1 protein in Arabidopsis (AtGID1b) can interact with GAI and RGA in the absence of GA (Griffiths *et al.* 2006; Nakajima *et al.* 2006). Further studies in rice using suppressor screen method (Carol *et al*., 1995; Wilson and Somerville, 1995; Silverstone *et al.*, 1997; Peng *et al*., 1999) resulted in isolation of *Sgd-1*, a mutant with reduced binding of GID1 to GA. This mutant has a substitution of Pro_{99} with Ser in the loop region of OsGID1 that partially suppressed the *gid1-8* phenotype because of a higher affinity to SLR1 in the low GA_4 condition. Moreover substitution of this proline residue with alanine conferred a new GA-independent DELLA protein interaction with GID1(Yamamoto *et al.* 2010). They showed that the GID1 loop structure is important in determining GA-dependant or -independent GID1-DELLA interaction in any GID1 protein. They suggested that in this mutant the GID1 lid tends to be closed even in the absence of GA, which leads to enhanced interaction with SLR1 (Figure 1.2).

The other mechanism that possibly modulates DELLA function independent of GA is *O*-linked *N*-acetylglucosaminyl transferase (OGT) encoded by the *SPINDLY (SPY)* gene (Jacobsen and Olszewski 1993; Silverstone *et al.* 2007). OGTs catalyse O-linked N-acetylglucosamine (O-GlcNac) modification of target Ser/Thr residues of regulatory proteins. SPY negatively regulates GA signalling in Arabidopsis, rice and barley (Robertson *et al.* 1998; Swain *et al.* 2001; Shimada *et al.* 2006;Silverstone *et al.* 2007). Loss-of-function *spy* alleles partially suppress the dwarf phenotype of GA-deficient mutants despite the accumulation of DELLA proteins (Shimada *et al.* 2006; Silverstone *et al.* 2007). A *spy* mutant of barley partially rescued the phenotypes of GA biosynthesis, GA receptor and DELLA dwarf mutants (Chandler and Harding 2013). These results indicate that *spy* mutants promote GA signalling independently of DELLA destruction.The biological function of SPY in addition to DELLA was suggested to be (i) enhancing the repression activity of DELLA in the GA signalling pathway, or (ii) increasing DELLA stability by protecting it from interaction with the proteasome pathway. However, there is more evidence to support the first possibility, because *spy* mutants in a defective GA signalling background showed enhanced GA signalling in terms of elongated leaves, and decreased *GA20ox* expression. There were changes in the phosphorylation state of DELLA, but no change in DELLA amount (Shimada *et al.* 2006; Silverstone *et al.* 2007). It was suggested that less SPY1 activity results in less *O*-GlcNAcylation of DELLA, and conversely more phosphorylation of DELLA which decreases DELLA function (Fu *et al.* 2002; Sasaki *et al.* 2003; Wells *et al.* 2004; Itoh *et al.* 2005; Shimada *et al.* 2006).

The suggested model is that, as in mammals, *O*-GlcNAcylation competes with phosphorylation for modification of the same Ser/Thr residues. In loss-of-function *spy* mutants, the *O*-GlcNAcylation of DELLAs is decreased, resulting in phosphorylation of DELLA and consequently decreased DELLA function (Wells *et al.* 2004; Shimada *et al.* 2006;Silverstone *et al.* 2007). Although it has not been clearly demonstrated at the biochemical level that DELLA is *O*-GlcNAcylated, or that the SPY protein has *O*-GlcNAcylation activity, some studies provide evidence for phosphorylation/dephosphorylation of DELLA. It was shown recently that Ser/Thr protein casein kinase I encoded by rice *EARLY FLOWERING1* (*EL1*) regulates DELLA (SLR1) through direct protein phosphorylation and also regulates gibberellin signalling in rice (Dai and Xue 2010). Taken together these studies suggest that post-translational modifications of DELLAs are important and that DELLA activity can be modified by this mechanism.

How do DELLA proteins exert their suppressive function?

DELLA proteins are growth repressors that are located in the nucleus, suggesting that they might function as transcription factors (Ogawa *et al.* 2000). Several genes were identified as DELLA target genes and *SCARECROW-LIKE 3* (*SCL3*) was found to be a direct target gene. The expression of this gene was up-regulated by DELLA and was inhibited by GA. Transient expression, ChIP, and co-IP studies showed that *SCL3* auto-regulates its own transcription by directly interacting with DELLA (Zhang *et al.* 2011). However, attempts to find a clear DNA binding domain in DELLA proteins have not succeeded so far. The suggested mechanism is that this repressor might regulate the expression of the target genes by associating with their promoters and that this might involve additional factors (Levesque *et al.* 2006).The more robust evidence in support of this notion will be discussed later in the "DELLA interaction with other proteins" section.

Recent studies in rice showed that the repressive function of DELLA proteins required their transactivation activity (Hirano *et al.* 2012). They overexpressed FLAG-tagged SLR1 fused to VP16, a protein derived from herpes simplex virus that has strong transactivation activity in plants as well as other species (Sadowski *et al.* 1988; Liang *et al.* 2006). Results showed that this transformed plant was a severe dwarf. Next, they showed that DELLA and TVHYNP motifs contributed to the transactivation activity of SLR1. GA-dependent GID1-SLR1 interaction diminished this activity, because *gid1/slr1* plants transformed with SLR1 lacking the DELLA or TVHYNP motifs had more severe dwarf phenotypes than plants transformed with other truncated SLR1 proteins. They also provided evidence that suppression of SLR1 activity does not necessarily require SLR1 degradation, and that interaction of SLR1 with GID1 *per se* is sufficient (Ueguchi-Tanaka *et al.* 2008; Hirano *et al.* 2012). The over-expression of wild type SLR1 and mutated $SLR1^{P96L}$ was studied in *gid2* mutants that are incapable of SLR1 degradation. The $SLR1^{P96L}$ mutant had weak interaction with GID1 and in the presence of GA_4 retained its transactivation activity. Expression of FLAG-tagged wild-type SLR1 in the *gid2* mutant resulted in a dwarf phenotype, while $SLR1^{P96L}$ resulted in more severe dwarf than wild type SLR1.

All the *slr1* loss-of-function mutations possess mutations in the GRAS domain but not in the N-terminal portion (Ikeda *et al.* 2001).This suggests that the GRAS domain of DELLA is necessary for growth suppression in rice. Various mutations were introduced into the GRAS domain of SLR1 and the constructs were transformed into *slr1* mutant. It was indicated that LHRI and SAW motifs alter the repressive effects of SLR1 without affecting its

transactivation activity, because mutations in those regions led to slender phenotypes (Hirano *et al.* 2012).

These studies suggest that the C-terminal GRAS domain of SLR1 exhibits a suppressive function on plant growth, possibly by direct or indirect interactions with the promoter region of target genes. It was also demonstrated that the N-terminal region of SLR1 has two roles in GA signalling: interaction with GID1 and transactivation activity (Hirano *et al.* 2012).

The role of DELLAs in GA homeostasis

Recent studies (above) have improved our understanding of GA signal transduction, and provided insight into the mechanisms responsible for GA homeostasis. There is evidence to show that the GA signalling pathway mediates feedback and feedforward regulation of GA metabolism. It was demonstrated that DELLA protein levels play crucial roles in these processes.

The role of DELLA proteins in feedback mechanisms regulating GA metabolism was clearly illustrated in gain-of-function and loss-of-function DELLA mutants. The first evidence of feedback regulation was provided by *Rht3* and *gai* gain-of-function DELLA mutants in wheat and Arabidopsis respectively (Talon *et al.* 1990; Appleford and Lenton 1991). In these studies the level of GA_1 and its precursors was determined, and in both cases the mutants had significantly higher contents of bioactive GA compared with the wild type. Loss-of-function DELLA mutants *la* and *cry-s* in pea were reported to have a great reduction in the expression of GA biosynthesis genes (*PsGA20ox1*, *PsGA3ox1* and *PsGA3ox2*) compared with the wild type pea (Weston *et al.* 2008). In Arabidopsis also, expression levels of the *GA4* GA biosynthesis gene (which encodes GA 3β-hydroxylase) was reported to be very low in double *rga/ga1-3* and triple *rga-24/gai-t6/ga1-3* mutants compared with *ga1*-3, a mutant with defective GA biosynthesis (Dill and Sun 2001; Silverstone *et al.* 2001). Further studies using RNA gel blot analysis also showed triple mutants accumulated lower levels of *GA4* mRNA compared with wild type in the absence of exogenous GA_3 (Dill and Sun 2001).

Transcript analysis of DELLA target genes in Arabidopsis has shown that most genes that are up-regulated by DELLA are down-regulated by GA (Zentella *et al.* 2007; Cao *et al.*, 2006). In order to define early GA-regulated genes and early DELLA-regulated genes, wild-type and mutant seedlings of Arabidopsis were studied under normal and GA treatment conditions (Zentella *et al.* 2007). They studied the GA deficient mutant (*ga1-3*) and dominant

DELLA mutant (*rga-Δ17*) that had a DELLA motif deletion and was resistant to GA-induced degradation and conferred an extreme dwarf phenotype. Microarray and q-PCR studies indicated 14 overlapping genes in these two sets of analysis. It showed that transcript levels of GA biosynthetic genes, such as *GA20ox* and *GA3ox*, showed a rapid decline with GA treatment whereas the expression of *GA2ox*, a GA catabolic gene, was up-regulated. Microarray and q-PCR analysis showed that the GID1 gene was also under feedback regulation. Transcript levels of all GA receptors in wild type Arabidopsis were down-regulated under GA treatment, and were elevated in *ga1-3* and *rga-Δ17* mutants in the same condition. It is concluded that GA biosynthesis genes and the GA receptor gene(s) may be direct DELLA targets and that DELLA's involvement in GA homeostasis is by regulating transcription levels of these genes.

Studies on pea DELLA mutants (*lacrys*) showed strong promotion of the deactivation genes *PsGA2ox1* and *PsGA2ox2;* this study demonstrated that GA-mediated feed forward regulation is also controlled by DELLA protein levels (Weston *et al.* 2008).

Several studies reported feedback regulation in mutants that lack normal GA signalling components including GID1 and GID2/SLY1. These components are required for GA-dependent DELLA destruction; hence DELLA proteins are accumulated in these mutants. High levels of bioactive GA were detected in these mutants, and gene expression studies showed up-regulated *GA3ox* and *GA20ox* genes (McGinnis *et al*., 2003; Sasaki *et al.* 2003; Ueguchi-Tanaka *et al.* 2005; Griffiths *et al.* 2006;Chandler *et al.* 2008) .

1.3.DELLA interactions with other proteins

DELLA proteins are nuclear localized and because of the homology that their GRAS domain has with signal transducer and activators of transcription (STAT) factors, it was suggested that DELLA proteins regulate transcription (Darnell 1997; Peng *et al.* 1997; Silverstone *et al.* 1998; Richards *et al.* 2000; Ikeda *et al.* 2001). Recent studies have shown that DELLA proteins are able to interact with regulatory proteins from the signalling pathways of other hormones. These proteins control gene transcription from other pathways to transmit external cues and integrate different signalling activities. Recent studies on Arabidopsis have shown that DELLAs control gene transcription through direct protein-protein interaction with many specific transcriptions factors (Hauvermale *et al.* 2012).

DELLA-PIF interaction and hypocotyl elongation

Hypocotyl elongation is one of the best characterised DELLA responses. DELLA proteins modulate light and GA effects on this process by interactions with regulatory molecules (Alabadi *et al.* 2004; Achard *et al.* 2007). It was shown that GA promoted hypocotyl elongation in the dark, and this was suppressed in the light by DELLA proteins (Alabadi *et al.*2004; Achard *et al.* 2007). PIF3 is a photomorphogenesis related transcription factor that mediates signalling between light and gene expression. This protein is a member of the bHLH family of transcription factors that bind directly to DNA (Toledo-Ortiz *et al.* 2003) and it interacts with the active form of phytochrome B (phyB) (Ni *et al.* 1999; Zhu *et al.* 2000). PIF3 promotes hypocotyl elongation in red light before dawn– the opposite effect compared with DELLA. The short hypocotyl phenotype of *pif3-1* mutants is resistant to applied GA_3, but hypersensitive to the GA inhibitor paclobutrazol (PAC). In contrast, PIF3 over-expression lines show a long hypocotyl, similar to GA-treated plants and *della* mutants that are insensitive to PAC (Feng *et al.* 2008). It was proposed that DELLA negatively regulates PIF3 in the control of hypocotyl elongation, and suggested that this regulation is probably mediated through direct physical interaction between PIF3 and DELLA proteins (de Lucas *et al.* 2008; Feng *et al.* 2008). When the DELLA protein content is high, it sequesters PIF3 so that it no longer binds DNA. But when DELLA protein abundance is low, for instance after proteasomal degradation of DELLA that occurs with GA signalling, the interacting protein partners e.g. PIF3 are released, and PIF3 can then bind to target promoters and regulate expression of genes involved in hypocotyl cell elongation (de Lucas *et al.* 2008; Feng *et al.* 2008). Therefore, DELLA blocks the transcriptional activity of PIF3 and interferes with down-stream regulation of target genes inducing hypocotyl elongation through direct interaction with these proteins (Figure 1.3).

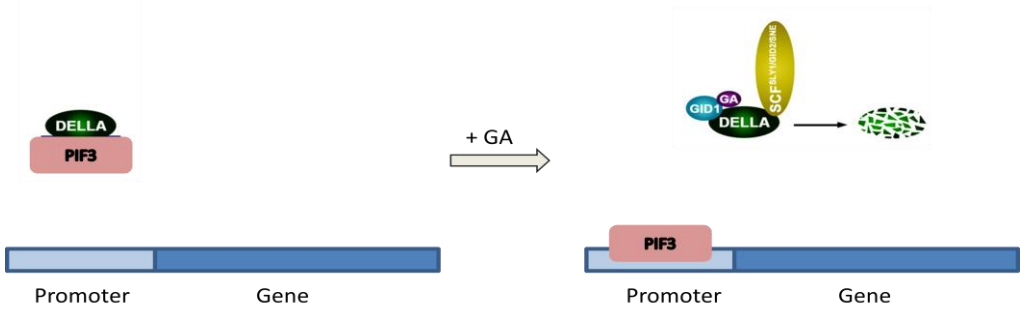

Figure 1.3. A model of GA-dependent interaction of DELLA and PIF3. When GA is absent, free DELLAs interact with PIF3 a transcription factor. GA-dependent degradation of DELLA results in free PIF3 and subsequent regulation of its target genes. This Figure was modified from Gao *et al.*, 2011.

Another member of the PIF family is PIF4, which behaves in a very similar way to PIF3 in regulating hypocotyl growth. De Lucas *et al.* (2008) suggested that PIF4 is negatively regulated by DELLA in a similar way to PIF3. PIF4 was over-expressed in a GA20-oxidase mutant background and in *gai*, a GA-insensitive mutant that lacks the DELLA domain. The partial GA deficient and GA insensitive mutants had hypocotyl lengths of 1mm and 3 mm respectively in 5 d old germinants, whereas the over-expression of PIF4 increased hypocotyl lengths significantly to 6mm and 11 mm in these mutant backgrounds.

DELLA-BZR1-PIF4 is a core transcription module in the hypocotyl elongation system

Previously, it was mentioned that other factors regulate hypocotyl elongation. One example of DELLA-mediated regulation of hypocotyl elongation will be discussed in more detail. Recently Bai *et al.* (2012)showed that brassinosteroid (BR) also regulates hypocotyl elongation. Their studies provide evidence of cross talk between GA and BR regulation involving DELLA proteins.

The relationship between GA and BR regulation of hypocotyl length was investigated using a mutant-based approach. Applied GA_3 increased hypocotyl length in the wild type, but the BR deficient mutant *det2-1* and the BR-insensitive mutant *bri1-119* did not respond to the exogenous GA_3. Applied BR was able to restore a GA response in *det2-1* over a range of different concentrations of GA_3. BR did not restore a GA response in the BR-insensitive mutant *bri1-119*. However, a dominant gain-of-function mutant, *bzr1-1D,* which has active BRASSINAZOLE RESISTANT1 (BZR1), one of the major transcription factors of BR-induced responses, showed longer hypocotyls in this mutant. The recovery of long hypocotyls by *bzr1-1D* was also seen in the GA-deficient *ga1-3* mutant and in wild type plants treated with PAC. These results suggested that BR or active BZR1 is necessary for the GA promotion of hypocotyl elongation.

The requirement of BR-activated BZR1 for GA/DELLA regulation of hypocotyl elongation raises the possibility that DELLAs directly repress BZR1. Indeed, yeast two-hybrid assays showed a direct interaction between RGA and BZR1. Furthermore, deletion of the DELLA domain had no effect on BZR1 binding, suggesting interaction with the GRAS domain, rather than with DELLA. Further studies showed that the dimerisation and SAW domains are important in RGA for its binding to BZR1 and suppression of plant growth. Since the GRAS domain is conserved in all members of the DELLA family, BZR1 is likely to interact with RGA, GAI, RGL1, RGL2 and RGL3.

Further investigation showed that BZR1 binding to promoters of its target genes (*PRE1, PRE5, IAA19, SAUR-AC1* and *DWF4* (Sun *et al.* 2010b) was increased after GA treatment, presumably through GA dependant DELLA degradation. So, it is suggested that DELLA proteins inhibit the transcriptional activity of BZR1 by blocking its DNA-binding activity. In vitro DNA-binding assays have shown that incubation of recombinant maltose-binding proteins (MBP)-BZR1 with MBP-RGA led to a significant reduction in BZR1 binding to DNA. Consistent with this result, GA_3 treatment of seedlings and also GA-signalling mutant *rga-24/gai-t6* did not affect the abundance of active BZR1 proteins.

Both DELLA and BZR1 interact with PIF4 (Feng *et al.* 2008; Oh *et al.* 2012). PIF4 and BZR1 bind to the promoters of their target genes to function as transcription factors. PIF4 and BZR1 together bind to a large number of common promoters in the genome (Feng *et al.* 2008; Oh *et al.* 2012). ChIP data and micro array expression profiling data showed that genes regulated by PIFs and/or BZR1 included a higher percentage of GA-regulated genes compared with genes not regulated by BZR1 and PIF4. Common target genes co-regulated by BZR1 and PIF4 also included the highest percentage of GA-regulated genes.

The combined model for hypocotyl elongation shows that GA-promoted hypocotyl elongation requires brassinosteroid-activator BZR1 and phytochrome-interacting factors (PIFs). GA signalling involves DELLA degradation; and this presumably releases BZR1 and PIFs which stimulate expression of their target genes (Figure 1.4).

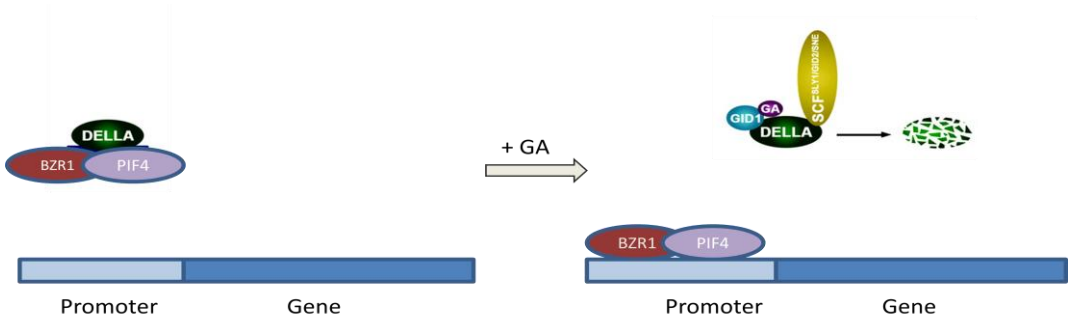

Figure 1.4. A model of GA-dependent regulation of BZR1-PIF4 target genes. BZR1 and PIF4 form a functional complex to regulate large number of genes e.g. genes contributing to hypocotyl elongation. GA-mediated DELLA degradation results in activity of BZR1-PIF4 complex and regulation of its target genes. This figure was modified from Gao *et al*., 2011.

It was suggested that DELLAs more effectively target the transcription factor heterodimer, BZR1-PIF4 than BZR1 or PIF4 individually (Oh *et al.* 2012). In this system

BZR1 and PIF4 not only act synergistically on shared targets but also independently on unique target genes. Presumably there are possible additional interacting partners that influence the preference of transcription factors for targeting common genes in this model or their unique genes. This property of signal transduction pathways potentially allows the cooperative and independent actions of these two systems in different growth and developmental process. It suggested the transcription model that modulates growth in response to GA, BR and light signals.

DELLA-prefoldin interaction and its role in cell expansion

Several lines of evidence have already been discussed that showed physical interactions between DELLA proteins and transcription factors in the Arabidopsis hypocotyl. Recent studies now indicate that DELLA proteins interact with the prefoldin complex (essential proteins required for tubulin folding) in regulating epidermal cell elongation in hypocotyls.

Sambade *et al.* (2012) studied microtubule alignment in actively elongating hypocotyl epidermal cells. The lower part of the hypocotyl started to elongate by day 4 in wild type and in long hypocotyl mutants (*hy1*, *phyB-1* and overexpressed *PIF3*). In the mutants, elongation continued further into the upper parts of the hypocotyl. They compared epidermal cells isolated from the lower and upper portions of the hypocotyls in these lines. GA_3 treatment of wild type caused hypocotyl length to increase by 20% after 4 days, and they detected changes in microtubule alignment in response to GA_3, similar to those observed in dark or in long hypocotyl light mutants. They measured the polymerisation rate of microtubules with an experimental procedure that led to measurements of the speed at which asymmetric wedges of microtubules spread across the cell to form the transverse array (the phase that appears in growing cells). Their results indicated that mutants with long hypocotyls had higher rates of microtubule polymerisation than controls. This suggests that mutants that grow faster have greater rates of microtubule polymerization and of microtubule orientation, which means that microtubules transition from longitudinal to 'star' to transverse in rapidly elongating cells. These observations support the important role that microtubules organization and dynamics play in expanding cells within the hypocotyl.

Locascio *et al.* (2013) showed that GA regulates microtubule orientation through an interaction between DELLA and the prefoldin (PFD) complex, a cochaperone with 6 subunits that has a crucial role in tubulin folding. Yeast two-hybrid assays showed that GAI interacts with PFD5, part of the core α-subunits of the prefolding complex. This interaction between DELLA and PFD was also verified *in planta* using coimmunoprecipitation studies in

Nicotiana benthamiana leaves. It is known that DELLA proteins are nuclear localized, and that PFD functions in the cytosol (Hartl and Hayer-Hartl 2002). They detected the nuclear accumulation of PFD5 in the hypocotyl of wild type Arabidopsis in a DELLA-dependent manner (Locascio *et al.*, 2013). A null mutant, *pfd5*, which was complemented with PFD5-GFP under the control of *PFD5* promoter, was grown in the dark for 3 days and PFD5-GFP was detected in the cytosol, whereas in seedlings grown in PAC medium PDF5-GFP was accumulated in the nucleus. Interestingly, GA_4 application to PAC-grown seedlings restored PFD5-GFP cytosolic localization after 3hr, along with the disappearance of GFP-RGA from nuclei. These observations suggest that DELLA proteins might cause microtubular disorganisation, because PFD localization in the nucleus is RGA dependent. Given that PFD is essential for proper folding of tubulin proteins in the cytosol, a lack of PFD in the cytosol results in a changed behaviour of microtubules.

To examine this hypothesis the tubulin status of untreated and PAC-grown seedlings grown 3 days in the dark was studied. Gel filtration of the extract from seedlings showed that the α- and β-tubulin association is under GA control. In control extracts, most α- and β-tubulin was recovered in the heterodimer fraction. However, when GA synthesis was inhibited by PAC treatment, it resulted in α- and β-tubulin dissociation and they appeared in the monomer form.

In agreement with the proposed relationship between the presence of DELLA and microtubule organization further investigation involved regulation of DELLA accumulation by the circadian clock, and whether this coincides with PFD nuclear localization and microtubule orientation in the transition from dark to light. They indeed showed that microtubules are in transverse array phase during growth before dawn, and they are random longitudinal shortly after dusk in the slow growth phase. Random microtubule arrangement coincided with accumulation of GFP-RGA at the start of dusk and the nuclear accumulation of PFD6-YFP, whereas transverse organization occurred when PFD6-YFP was detected in the cytosol at the end of the night.

Expression of several TUA (α-tubulin) genes required DELLA-dependant accumulation of PFD in the nucleus. The relative transcript level of TUA genes was maximal (3-fold) before dark in the wild type, whereas in *della* and *pfd5* mutants it was 1.5-fold. It is interesting to note that in this study the maximal daily expression of TUA genes did not coincide with the period of maximal growth rate.

In animals PFD functions as a regulator of the c-Myc transcription factor (Satou *et al.* 2001; Miyazawa *et al.* 2011) . Therefore it is possible that in plant cells the PFD complex also plays a regulatory gene expression role in a DELLA-dependant manner.

1.4.Introduction to, and general aims of my Ph.D. project

Mutants have played a major role in our understanding of how GA promotes growth. Plants defective in GA biosynthesis or GA signalling were isolated in many species, including Arabidopsis, peas and rice, which provided insight into the mechanisms by which GA regulates growth. These mutants were the basis for isolating and characterizing genes involved in the GA signal transduction pathway. GA mutants have also been important in cereal breeding; the *sd1* mutant in rice and *Rht-B1b* and *Rht-D1b* in wheat were the basis for improved yield during the Green Revolution, and they have been used extensively worldwide. The *semidwarfing1* (*sd1*) gene mutation of rice is recessive, and exogenous GA can restore normal height. It encodes a defective GA 20-oxidase enzyme, an enzyme involved in the GA biosynthesis pathway. There are three different origins for *sd1* that have been used in producing high yielding cultivars in China, Japan and the USA. In one case there is a big deletion in the GA 20-oxidase gene which results in an early stop codon, and the product of this gene is probably an inactive enzyme (Ashikari *et al.* 2002; Spielmeyer *et al.* 2002). The two other alleles are single nucleotide substitutions in *sd1,* which result in a weaker semi-dwarf phenotypes, and the enzyme may still retain some activity (Monna *et al.* 2002; Spielmeyer *et al.* 2002;Hedden 2003). It was suggested that semi-dwarf *sd1* plants have a modest reduction in height possibly because of the partial functional redundancy from other members of the GA 20-oxidase gene family and of their overlapping expression patterns (Hedden, 2002).

In wheat, *Rht-B1b* and *Rht-D1b* alleles confer a partially GA-insensitive phenotype. They have single nucleotide substitutions in the N-domain of DELLA that introduce early stop codons close to the DELLA motif (Peng *et al.* 1999). It is suggested that translation of the mutated gene is reinitiated from a methionine-rich region that follows the stop codon, resulting in the formation of N-terminally truncated RHT-1 proteins lacking the DELLA domain (Peng *et al.* 1999). This protein is resistant to GA-dependant degradation since it cannot interact with the GA-GID1 complex, and it therefore functions as a constitutive repressor of growth (Pearce *et al.*, 2011). *Rht-B1c* is another allele at the *Rht-1* locus. It has a 2 Kb insertion in the gene, which causes severe dwarfism in varieties that carry this allele (Wu *et al.* 2011; Wen *et al.* 2013).The 2Kb insert is mostly spliced during RNA processing,

leaving a 90 bp in-frame insertion. Therefore the encoded protein, the RHT-B1C, has a 30 amino acid in-frame insertion which is located near the DELLA region, and which prevents interaction of DELLA with the GID1-GA complex (Pearce *et al.* 2011; Wu *et al.* 2011). It was discussed earlier that the current model of GA signalling proposes that GA mediates degradation of DELLA by the 26S proteasome. When the GA-GID1-DELLA complex is formed, it is targeted by the F-box subunit (SLY1, GID2) which recruits DELLA to be recognized by the 26S proteasome. Therefore, it appears that RHT-B1C causes severe growth suppression since it has no physical interaction with GID1.

The semi-dwarfing genes discussed above were of particular interest in terms of their practical applications in breeding before the underlying science was understood. When Peng *et al*., (1999) characterized mutants at the*Rht-1* locus, the importance of GA responses in wheat breeding was revealed. Since then there have been extensive attempts to identify new mutants that might make similar contributions in wheat breeding.

In this study, my aim is to characterize and investigate a large number of mutants in the *Della* genes of barley and wheat that have enhanced GA signalling. Analysis of a wide range of mutants might give insight into understanding the general action of DELLA, and its role in specific aspects of GA responses in barley and wheat. So, the broad aim of this project is to study overgrowth alleles to promote our scientific understanding. Part of this will also involve exploring their potential utilization in barley and wheat breeding.

CHAPTER 2

Barley overgrowth mutants: growth responses to abscisic acid (ABA)

Introduction

In the past, using "suppressor" screens has led to the isolation of useful mutants in plant systems such as Arabidopsis (Carol *et al*., 1995; Wilson and Somerville, 1995; Silverstone *et al.*, 1997; Peng *et al*., 1999). These mutants with close to wild type phenotype were isolated from dwarf parents and they were the basis of discovery of new genes involved in GA responses. In the study of barley overgrowth mutants, a suppressor screen was used to raise the opportunity of isolating novel GA response mutants in cereal. In this screen taller plants were isolated in dwarf backgrounds that were defective in GA biosynthesis (GA 3-oxidase) or in GA receptor or in DELLA function (Chandler and Harding 2013). The dwarf plants had been treated with the mutagen sodium azide and taller plants with enhanced growth were isolated in the M_2 generation and called overgrowth mutants; these plants still retained the dwarfing mutation. Further characterization of these mutants led to the identification of 13 independent overgrowth alleles, 12 of which have been characterized at the DNA sequence level. All resulted from a new mutation; 11 occurred in the *Slender 1*(*Sln1*) gene, and one was identified in the *Spindly 1* (*Spy1*) gene. Each new *Sln1* allele involved a single nucleotide substitution resulting in a single amino acid substitution in the SLN1 (DELLA) protein. All mutations occurred in the GRAS domain of DELLA (Figure 2.1) and they specifically changed highly conserved single amino acids in the LHR1 and PFYRE motifs. These motifs are conserved functional units containing amino acid residues that have undergone natural selection and maintain identity across different plant species; therefore it appears that any changes in the conserved residues are likely to affect DELLA behavior or its function. For instance, it has been suggested that LHRI is a region involved in DELLA protein binding to downstream targets, whereas PFYRE is a region of DELLA involved in GID1 binding (Hirano *et al.* 2010). Therefore, mutated conserved residues in LHR1 and PFYRE in overgrowth mutants are likely to alter DELLA function, which in turn will probably influence growth behavior of overgrowth mutants.

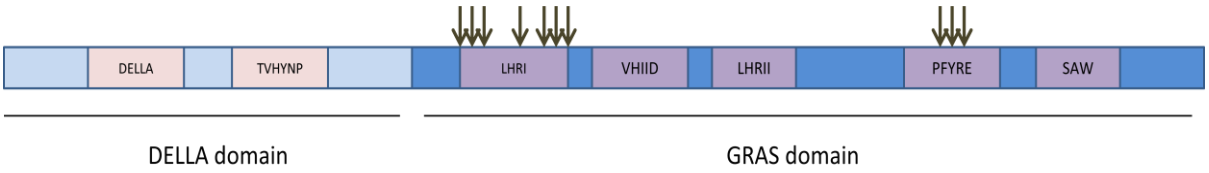

Figure 2.1. The sites of overgrowth mutations in the SLN1 protein are shown with arrows. Each arrow represents a single amino acid change of a highly conserved residue in the DELLA protein, resulting from a single nucleotide substitution in the *Sln1* gene. Note that all the mutations are in the GRAS domain, and specifically in the LHRI and PFYRE conserved motifs.

Overgrowth mutants were characterized as plants whose maximum leaf elongation rate (LER_{max}) was greater than that of their dwarf parent. LER_{max} is a robust indicator of GA response when measurements are made under standard conditions (Chandler and Robertson 1999). Leaf elongation rate is obtained from successive daily measurements of leaf one length throughout its period of growth (approximately one week). The maximum value in each set of daily increments is the LER_{max}.

Overgrowth mutants are associated with enhanced growth resulting from increased GA signalling capacity, and so they are of special interest for studying growth responses to hormones such as abscisic acid (ABA).The first evidence that suggested ABA inhibits GA signal transduction came from studies on barley aleurone layers. After seed germination, the developing embryo releases active GA to aleurone cells, inducing hydrolytic enzymes such as α-amylase. This enzyme is secreted from aleurone to the starchy endosperm to hydrolyze starch, and along with other hydrolases that degrade other components in the grain reserves; they supply nutrition to the growing seedling. This response is also seen in isolated aleurone layers treated with GA, which made the aleurone system of interest for decades to study hormone responses. ABA suppresses α-amylase production and suppresses seedling growth. Since aleurone layers do not synthesize their own bioactive GA, it was concluded that ABA inhibits α-amylase production due to interference with GA signalling (Chrispeels M.J and Varner 1967a; Chrispee M.J and Varner 1967b; Weiss and Ori 2007). The strongest evidence was provided by studying *Sln1* loss-of-function mutants. It was reported in barley *sln1a* and rice *slr1-1* (both characterized by a slender phenotype and by constitutive GA responses) that

α-amylase was produced by half grains without addition of GA_3, yet it was still reduced by ABA (Chandler 1988; Lanahan and Ho 1988;Ikeda *et al.* 2001).

Although aleurone is a powerful model system to study GA and ABA interactions, it has limitations, since it is labour intensive and involves destructive assays. Growth systems have been developed which allow non-destructive assays to be made (repetitive sampling and therefore better statistics), involving GA and ABA biosynthesis or signalling mutants. Generally ABA causes growth reductions that might be due to interfering with GA biosynthesis or GA signalling or both. Ikeda *et al* (2001) showed that application of ABA caused an approximate 20% reduction in the shoot length of both wild type and *slender* rice (*slr1-1*), and higher concentrations caused a greater reduction in shoot length, suggesting that GA signalling might be affected by ABA regardless of the fact that ABA might also act independently of GA signaling. However they did not provide any information on whether ABA interferes with GA biosynthesis. In barley, leaf elongation rates were measured with or without ABA treatment (Dewi, PhD thesis 2006), and LER_{max} of ABA-treated grains was lower than controls. LER_{max} was also determined for grains germinated in GA_3 (90 µM) with ABA at various concentrations. 90 µM GA_3 is near-saturating for GA_3responses, and would ensure wild type barley grows at the normal rate if ABA only interferes with GA biosynthesis (Chandler and Robertson 1999). However, the results showed progressive reductions in LER as ABA concentration increased, indicating that ABA was involved with the signalling pathway or it might also affect leaf elongation through an independent mechanism.

There is other evidence that suggests ABA also interferes with the GA biosynthesis pathway. The effects of endogenous ABA accumulation (induced by dehydration), and of exogenous ABA on the endogenous GA profile were analyzed in grains of Himalaya barley (Dewi, PhD thesis 2006). The endogenous content of GA_1 was 10-20% of the content of the control, and GA_{44} and GA_{20} also were at much lower levels than those of the control grains. Similar effects were observed through dehydration for 4 days. This result suggested that ABA had effects on expression or activity of GA 20-oxidase enzymes that catalyse the synthesis of GA_1 and its precursors. Moreover, most significantly for this thesis, endogenous ABA induced by dehydration gave similar effects to exogenous ABA on the contents of GA_1, GA_{44} and GA_{20}. This suggests that the growth responses of plants to exogenous ABA could be interpreted as potential responses to stress conditions. Zentella *et al*. (2007) also suggested that GA and ABA reduce and increase each other's synthetic and catabolic genes respectively in Arabidopsis. Relative mRNA levels of the GA biosynthetic gene, *GA20ox1*, were significantly reduced by ABA, and conversely, transcript levels of the GA catabolic gene

GA2ox6 were increased. Similar results were observed in plants under dehydration stress, where Arabidopsis seedlings were transferred to mannitol and the osmotic stress induced by this chemical down-regulated *GA3ox1* and up-regulated *GA2ox6* after 24 hrs stress (Claeys *et al.* 2012).

Preliminary studies on the growth responses of barley overgrowth mutants to ABA have been carried out by Chandler and Harding (unpublished data). The growth rates of Himalaya and overgrowth mutants were inhibited by ABA, but for some overgrowth mutants there were suggestions that ABA was less effective. Furthermore, there were indications of differences between overgrowth alleles in their response to ABA.

This chapter will explore in greater detail the growth of overgrowth alleles in the presence of ABA and under drought stress.

Materials and Methods

Plant materials

Barley grains used in these experiments were single and double overgrowth mutant derivatives of *Hordeum vulgare*, L. 'Himalaya' and 'Sloop' that were provided by Dr Peter M. Chandler (CSIRO Plant Industry, Canberra). The grains were mostly from glasshouse-grown plants from harvest years between 2003 and 2012. Plants were generally grown from March to July, or from August to December in compost-based soil with natural lighting and photoperiod for the 6 warmer months and with photoperiod extension to 14 h for the other 6 months of the year. Internal curtains or whitewash was used to minimize heating during the 6 warmer months. Temperature was typically maintained in the range 14°C-23°C, although extremes of approximately 10°C and 30°C were occasionally encountered. A range of barley mutants used in this study is shown in Table 2.1.

Overgrowth mutant derivatives of Himalaya

Overgrowth alleles isolated in Himalaya occurred in the *grd2b*, *gse1n* or *Sln1d* dwarfing backgrounds. All overgrowth alleles were backcrossed for two generations to the wild type. This allowed us to separate the original dwarfing mutation of GA biosynthesis and GA receptor from the new overgrowth mutation, and PCR analysis confirmed the loss of the original dwarfing mutation in these lines. Backcrossing of overgrowth mutants in the *Sln1d* background allowed the establishment of overgrowth alleles in a 'cleaner' genetic background (non-mutagenised) for more detailed analysis, although they still retain the original *Sln1d* dwarfing mutation.

Overgrowth mutant derivatives of Sloop

Single overgrowth mutants, isolated originally in the Himalaya genetic background were backcrossed to Sloop, and after three backcross generations for each allele, homozygous mutant and homozygous wild type lines were isolated (BC_3F_2) (more details are provided in Chapter 3).

Double overgrowth mutants

Overgrowth mutants occurred in two different genes (*Sln1* and *Spy1*), so it was possible to intercross some overgrowth alleles and isolate double mutants. Double overgrowth mutants

were constructed in both Himalaya and Sloop backgrounds and their genotypes were confirmed by sequencing the appropriate PCR products.

Table 2.1. List of barley mutants which were used in the experiments of this chapter

Line	Genotype	Mutation[a]		Reference
		Nucleotide	Amino acid	
Himalaya	WT	-	-	
TR100[b]	*Sln1d.9*	G1442A	R481H	Chandler and Harding, 2013
M247[b]	*spy1a*	G812A(*Spy1*)	G271D (SPY1)	-
M240[b]	*sln1m*	G680A	G227E	-
M242[b]	*sln1n*	G710A	C237Y	-
M245[b]	*sln1o*	C1454T	S485F	-
M243[b]	*sln1s*	G829A	A277T	-
M260[c]	*Slnd.9, spy1a*	See above	See above	This thesis
M250[c]	*sln1m, spy1a*	See above	See above	This thesis
M253[c]	*sln1n, spy1a*	See above	See above	This thesis
M254[c]	*sln1o, spy1a*	See above	See above	This thesis
M251[c]	*sln1s, spy1a*	See above	See above	This thesis
Sloop	WT	-	-	Commercial barley variety
Sloop M1(hulled) or M2[d] (hulless)	*spy1a*	See above	See above	This thesis
Sloop G1(hulled) or G2 [d] (hulless)	*sln1s*	See above	See above	This thesis
Sloop DOM21 (hulled)[c]	*sln1s, spy1a*	See above	See above	This thesis
Sloop DOM22 (hulless)[c]	*sln1s, spy1a*	See above	See above	This thesis

[a] Coordinates refer to the positions in the *HvSln1* coding sequence or SLN1 amino acid sequence from Himalaya starting at ATG and ending at TGA. (accession no.= AK372064) For M247, the coordinate refers to the position in the *HvSpy1* coding sequence or SPY1 amino acid sequence, starting at ATG and ending at TGA. (accession no. = AF035820)

[b] Lines established after two backcrosses to Himalaya before selecting for homozygosity of the allele shown. For all mutants except *Sln1d.9*, the original dwarfing gene has been removed through the backcrosses to Himalaya.

[C] Lines constructed from intercross between *sln1* overgrowth alleles and *spy1a*, and selecting for homozygous double mutants in the F_2 generation.

[d] Lines established from three backcrosses of overgrowth allele to Sloop, then selecting for plants homozygous for the overgrowth allele.

Grain germination

Barley grains were placed (embryo down) between two sheets of autoclaved paper (3MM, Whatman) in envelopes that were moistened with an appropriate solution (ABA or control); and all solutions buffered to pH 5.5 with potassium phosphate buffer. This "envelope" was held vertically in a Perspex frame placed in the solution, all contained within a clear plastic box (Figure 2.2). Grains were stratified at 4°C for 2 days in the dark, and then transferred to a constant 20°C growth cabinet with low intensity fluorescent lighting (95 µmol/m^2/s). The day when grains were placed at 20°C is recorded as day 0 (0 d), and shoot growth occurred throughout the next week.

Leaf elongation rate

Leaf elongation rates (LER) were measured daily from 3d to 7d of growth at 20°C. The envelope was aligned with positional markers on a clear plastic sheet. The position of each leaf tip was marked on the plastic sheet, and the envelope was returned to the growth assembly. On the following day, the envelopes were again placed on the original sheets in their original position, and the new position of each leaf tip was marked. The distance between marks was recorded and the mean length increment (of 8-10 seedlings) was determined and expressed as a rate (mm/d). This 4 d interval covers the time when leaf 1 (L1) attains its maximal rate of elongation (LER_{max}).

Embryo size determination

Grains were placed in a plastic Petri dish (90 mm diameter) with 2 layers of Whatman No.1 filter paper (70 mm diameter) and 4 mL of distilled water. The dish was covered with a lid and incubated at room temperature in the dark for 6 hours. To remove the embryo, each grain was dissected under a binocular microscope and the scutellum shield, including the embryo, was isolated using scalpel and tweezers. For each genotype, 20 grains were dissected and isolated embryos were dried at 65°C for 24 h and 48 h. The value obtained from the dry weight of 20 embryos was divided by the number of embryos to give the average embryo size for that genotype.

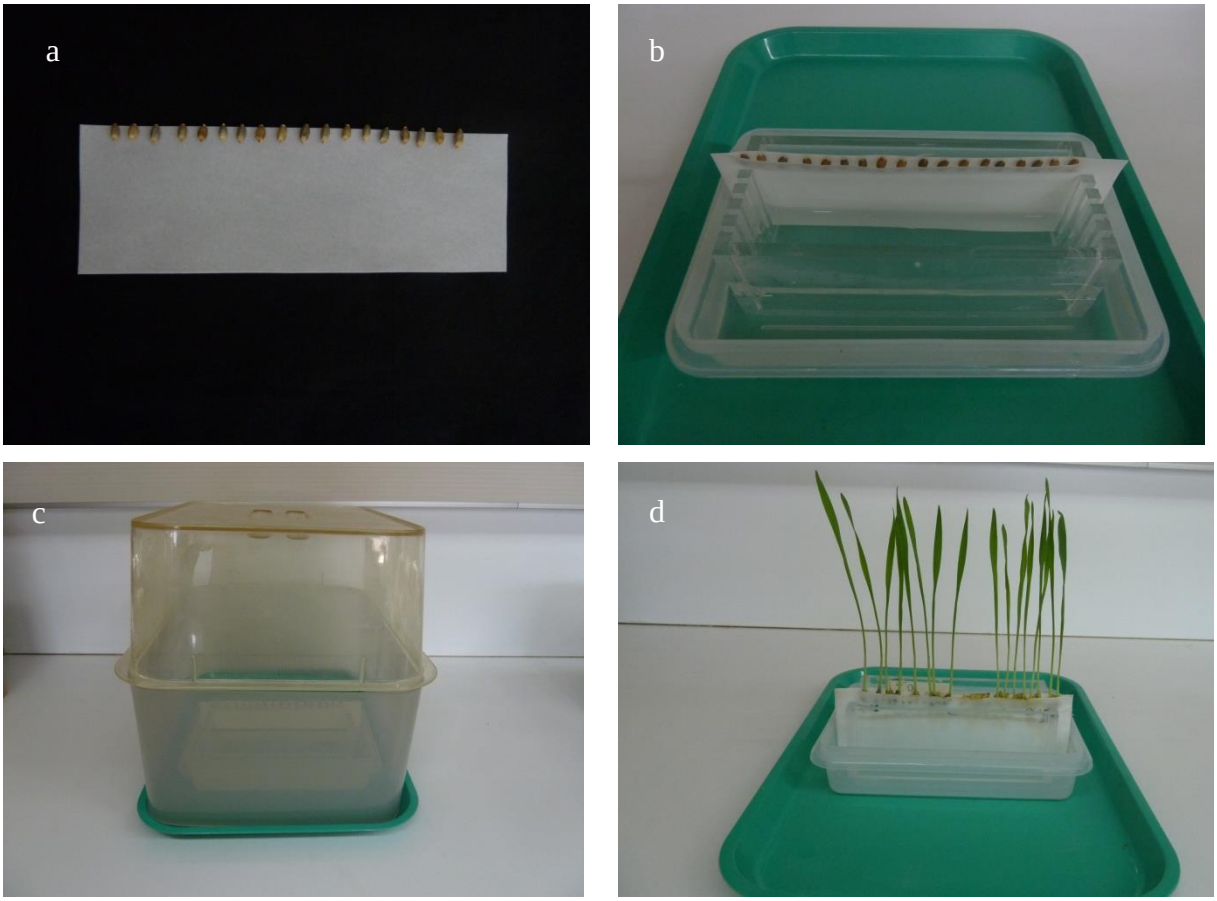

Figure 2.2. Germination using filter "envelope"

(a) Barley grains were placed (embryo down) on a piece of 3 MM Whatman paper

(b) The envelope containing barley grains was moistened with water or ABA solution for imbibition

(c) The envelope was placed within a clear plastic box

(d) Germinated grains in the envelope

ABA and water deficit stress experiments in the "cigar" system

The ABA and drought stress tests were carried out using "germination paper" (380 x 255 mm, Anchor Paper Co.) that was moistened with an appropriate solution or appropriate volume of distilled water. Eight grains of double overgrowth mutants and 8 grains of the relative wild type were placed side by side (alternately) on a line drawn 100 mm from the top of the paper (in portrait orientation), covered with another sheet of paper moistened with the same solution, and then rolled up from one side to the other to form a "cigar". They were secured loosely with a rubber band, and cigars with similar treatments were placed in a PVC cylinder (550 mm height and 90 mm diameter). The cylinders were sealed with plastic lids, then covered with black cloth and incubated at 20°C in a dark growth cabinet. To determine growth, cigars were transferred from the dark to the lab bench after 6, 10 and 12 days and shoot lengths were measured. An example of germinated grains in the cigar system is shown in Figure 2.3. Treatments included 3 µM and 6 µM ABA and 24 ml water / cigar as a saturating amount of water). Based on preliminary studies, we chose 12 ml water / cigar or 10 ml / cigar as imposing increasing degrees of water deficit.

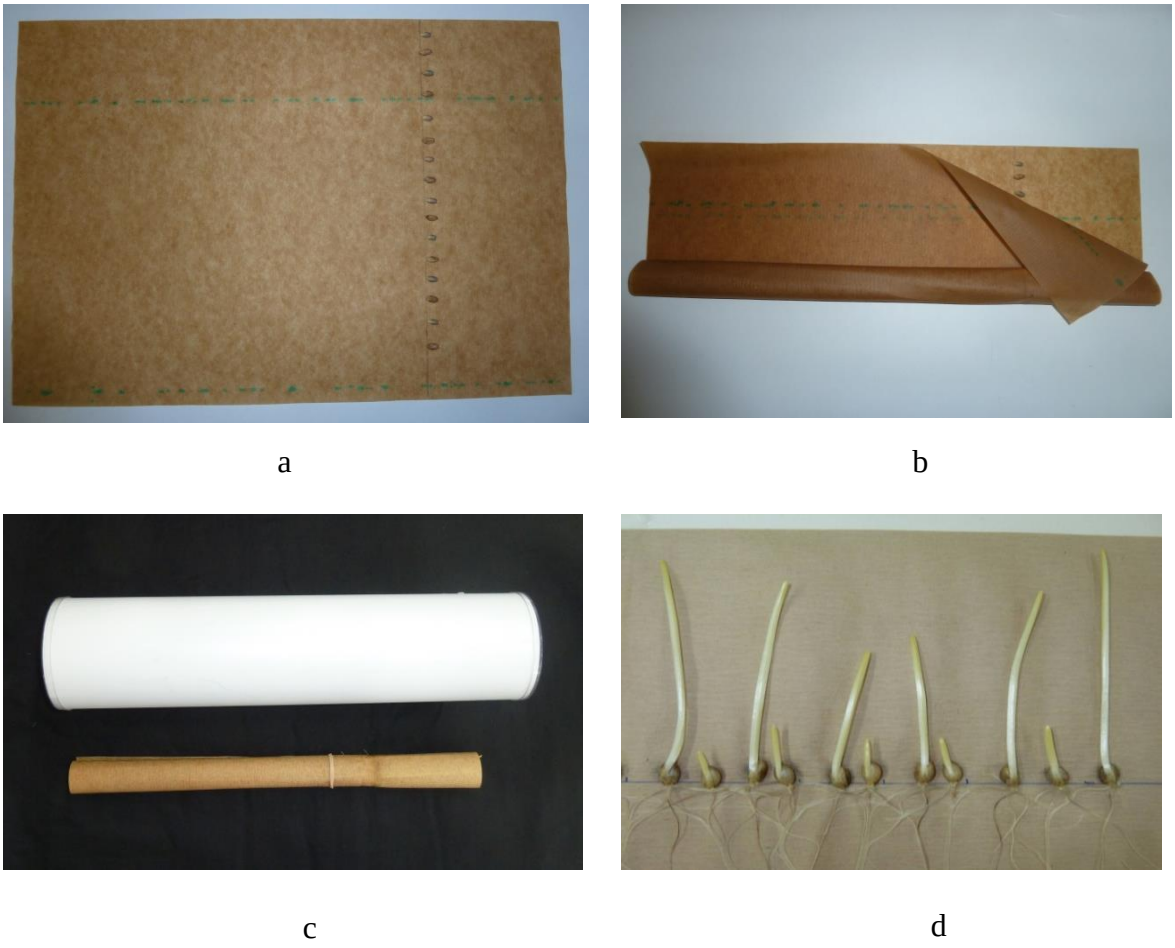

Figure 2.3. Growth response test in "cigar" system.

(a) Barley grains of control and double mutant placed side by side (alternating genotypes) on "germination paper" moistened with an appropriate solution

(b) Grains covered with another sheet of paper moistened with the same solution, and then rolled up from one side to form a "cigar".

(c) Cigar secured loosely with a rubber band, then placed in PVC cylinder

(d) Germinated grains in cigar (note the difference between control and double mutant lines in response to a treatment)

Results

The leaf elongation experiments (Materials and Methods) involve a model system, in which seedlings grow in a cabinet with constant environmental conditions on their own stored reserves (the intensity of light is well below that needed for significant photosynthesis). This system allows us to study the first leaf elongation rate during the course of growth in an appropriate solution. The plot of LER values gives a growth curve that typically has a gradual increase in growth rate, a maximum rate and then a gradual decrease because of the limited grain reserves. There are different ways to compare growth profiles: (i) LER_{max}, a single value but a robust way to compare lines with typical growth profiles; (ii) average LER gives better information when LER_{max} values are fairly similar between lines while LERs around LER_{max} have significant differences; (iii) the actual length per day can be plotted to show the accumulated length during growth.

For the present study, depending on the behavior of the growth profile, we will conduct the best method to interpret graphs and to provide the most reliable comparisons.

LERs of single overgrowth and double overgrowth mutants treated with ABA

Overgrowth mutants in Himalaya

LER of single overgrowth mutants

The leaf elongation rates (LER) of Himalaya and single overgrowth alleles with and without ABA treatment were determined from day 3 to day 7 of growth at 20°C (Figure 2.4), and the corresponding LER_{max} values are presented in Table 2.2. The growth profile of Himalaya was similar to earlier studies, in which LER increased gradually and reached a maximum at day 5-6. Overgrowth mutants had consistently higher LER values than Himalaya, with one exception; *Sln1d.9* had lower LER values than Himalaya due to the presence of the *Sln1d* dwarfing mutation in addition to the overgrowth allele *Sln1d.9* (see Discussion).

Application of 3μM ABA inhibited growth of Himalaya and overgrowth lines. Five overgrowth alleles grew faster than Himalaya and showed a consistently higher LER over the course of growth after application of ABA. This result indicates that because overgrowth mutants performed better than Himalaya in the control solution, their growth reduction in response to ABA was probably influenced by their higher growth rates. ABA caused a 36% reduction of LER_{max} for Himalaya, and the extent of reduction in growth rate of overgrowth alleles varied between 18% for *sln1n* (the least) and 41% for *sln1d.9* (the highest). Similar results obtained before that consistent with the observation that some overgrowth mutants

performed better than Himalaya in control and at the presence of ABA and *Sln1d.9* had different behavior.

Table 2.2. LER_{max} of Himalaya, single and double overgrowth mutants treated with and without 3µM ABA. Grains were placed in an envelope, imbibed in control or ABA media, stratified for 2 days at 4°C in the dark, and then grown at 20°C with constant light. Leaf elongation rates were calculated from daily leaf length measurements, and the maximum leaf elongation rate was named LER_{max}. Values are means ± SE (*n*= 8).Asterisks indicate significant difference between Himalaya and mutants (*P*< 0.001 or *P*< 0.01).ANOVA showed a significant effect of double overgrowth mutation on LER_{max} in control solution (P< 0.001). The LSD (0.05) value for LER_{max} was 4.56 mm/day.

Overgrowth alleles	**LER_{max}(mm/day)**	
	Control	**ABA 3µM (% reduction)**
Himalaya	36.6 ± 0.8	23.3 ± 0.9 (36)
spy1a	42.6 ± 1.9**	33.1 ± 0.8*** (22)
Sln1d.9	21.7 ± 0.4	12.6 ± 0.9 (41)
sln1m	56.8 ± 0.5***	39.7 ± 1.4***(30)
sln1n	48.7 ± 1.4***	39.5 ± 1.1*** (18)
sln1s	44.8 ± 1.1***	35.6 ± 1.3*** (20)
sln1o	53.6 ± 1.3***	40.7 ± 1.9*** (24)
M260 (*Sln1d.9*,*spy1a*)	39 ± 1.0	33.4 ± 0.9*** (14)
M250 (*sln1m*,*spy1a*)	48.2 ± 2.0***	47.4 ± 3.3*** (1.6)
M253 (*sln1n*, *spy1a*)	48.7 ± 1.8***	37.5 ± 2.4***(23)
M251 (*sln1s*, *spy1a*)	57.3 ± 3***	38.8 ± 1.9*** (32)
M254 (*sln1o*, *spy1a*)	56.4 ± 2.3***	48 ± 1.7*** (14)

LER of double overgrowth mutants

Overgrowth alleles were identified in the *Sln1* and *Spy1* genes, so it was possible to intercross the appropriate lines and construct double mutants (Materials and Methods). To investigate the combined effects of two overgrowth alleles on LER and its response to ABA, double mutants were grown in a control solution and in the presence of 3µM ABA (Figure 2.5). In the control solution, double overgrowth alleles generally conferred enhanced growth, greater than the effects of the single mutants, although the extent varied between different allele combinations. The LER_{max} values of double overgrowth mutants are shown in Table 2.2, and there was a significantly enhanced LER_{max} for M260 (*sln1d.9, spy1a*), M254 (*sln1o, spy1a*) and M251 (*sln1s, spy1a*) compared with the corresponding single mutants (*Sln1d.9, sln1o* and *sln1s* respectively). M253 (*sln1n, spy1a*) and M250 (*sln1m, spy1a*) did not show any significant changes.

The LER of double mutants was reduced by ABA, but all combinations of overgrowth alleles caused a significantly smaller reduction in LER_{max} compared with the effects of the single alleles. The percentage reduction in LER_{max} in the presence of ABA is shown in Table 2.2 and M250 had the lowest reduction, despite its slightly lower LER_{max} compared with *sln1m*, the single mutant (in control solution). This result indicates that M250 is almost insensitive to ABA treatment.

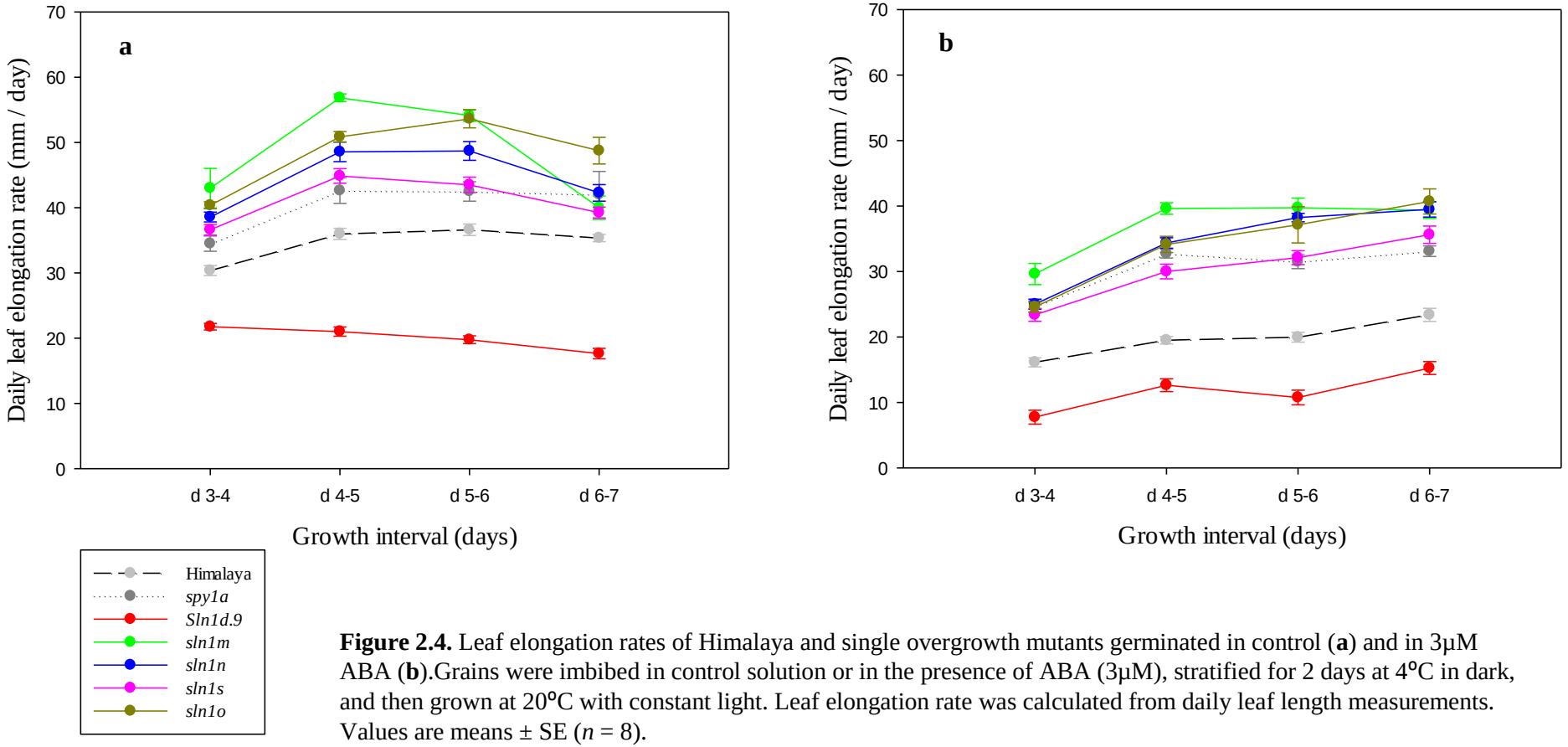

Figure 2.4. Leaf elongation rates of Himalaya and single overgrowth mutants germinated in control (**a**) and in 3µM ABA (**b**).Grains were imbibed in control solution or in the presence of ABA (3µM), stratified for 2 days at 4°C in dark, and then grown at 20°C with constant light. Leaf elongation rate was calculated from daily leaf length measurements. Values are means ± SE (n = 8).

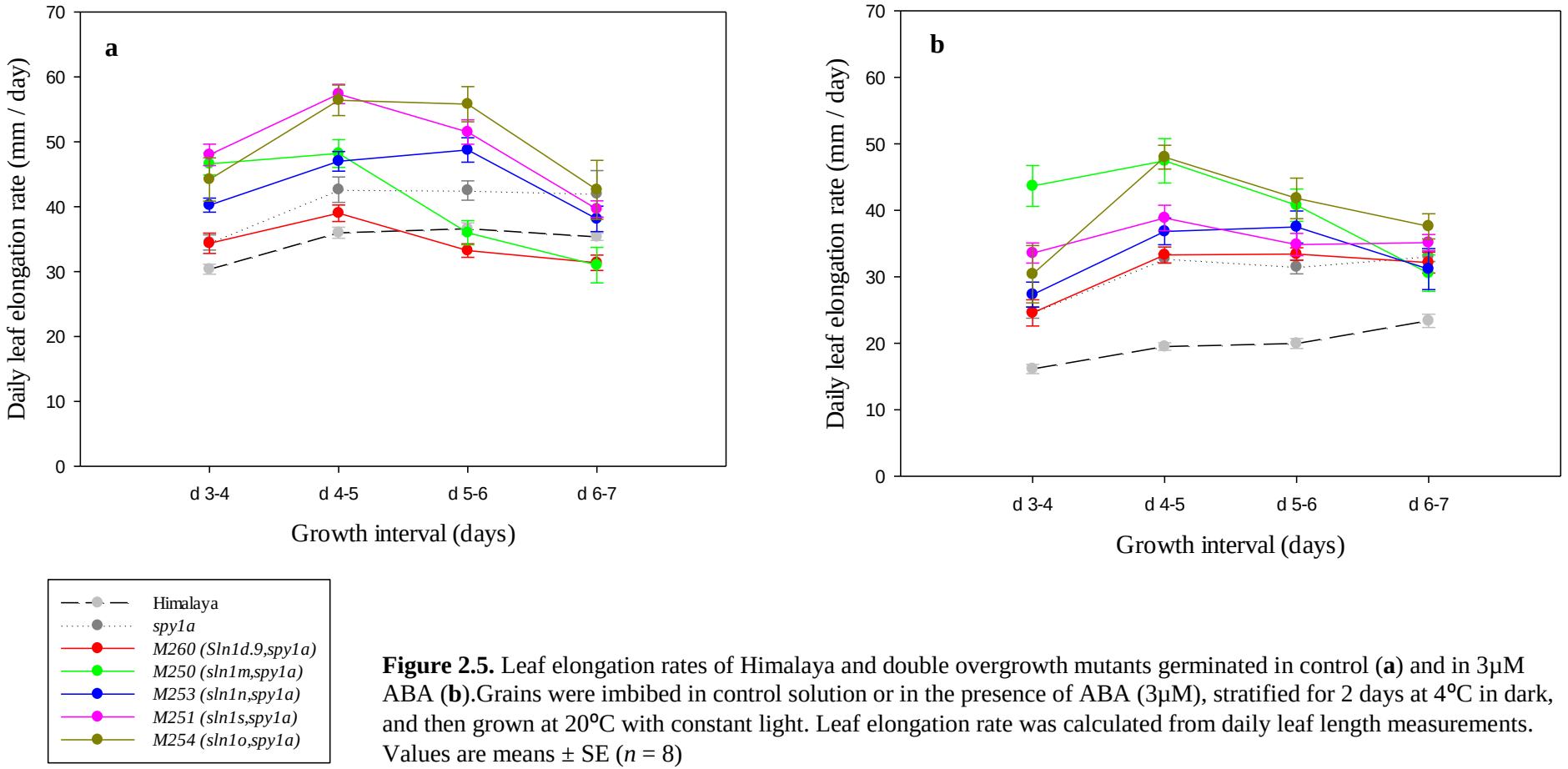

Figure 2.5. Leaf elongation rates of Himalaya and double overgrowth mutants germinated in control (**a**) and in 3µM ABA (**b**).Grains were imbibed in control solution or in the presence of ABA (3µM), stratified for 2 days at 4°C in dark, and then grown at 20°C with constant light. Leaf elongation rate was calculated from daily leaf length measurements. Values are means ± SE (n = 8)

Overgrowth mutants in Sloop

Independent experiments were carried out in the Sloop genetic background to assess the effects of overgrowth alleles on early growth rates and to evaluate their potential resistance to ABA. From previous work in Himalaya it was known that all double overgrowth mutants had some degree of sterility, although this was least for M251 (*sln1s, spy1a*) where it was possible to generate reasonable numbers of double homozygous grains. Therefore this combination of overgrowth alleles i.e. *sln1s*, *spy1a* was constructed in Sloop (The procedure is explained in Materials and Methods). The Sloop double overgrowth mutants (DOM), including DOM21 (hulled) and DOM22 (hulless) in addition to hulled and hulless*sln1s* and *spy1a* derivatives of Sloop were examined in control conditions (Figure 2.6, a & c) and in the presence of 3 µM ABA (Figure 2.6, b & d).

In the control solution (Figure 2.6a; Table 2.3) DOM21 (hulled) had significantly higher LER_{max} than the single mutants (*sln1s* and *spy1a*) and Sloop. Figure 2.6b, shows the growth profile of DOM22 (hulless) and its single mutants. Despite the greater LER_{max} of DOM22 than Sloop and *spy1a*, its LER_{max} value did not exceed that of *sln1s*. There was a similar observation in Himalaya LER experiments for M250 and M253, where the combination of *sln1m* and *sln1n* with *spy1a* did not confer greater maximum growth rate compared with their relative single mutants.

The LERs of DOM21 and DOM22 were reduced by ABA (Figure 2.6 c, d; Table 2.3), but they were greater than those of the single mutants and Sloop in general. Interestingly, DOM22 had significantly higher early LER (day3-4 and 4-5) consistent with the observation of better performance of M250 compared with *sln1m* in ABA solution, despite its unchanged LER in combination with *spy1a*. It appeared that DOM22 had a tendency for greater early growth rate (day 3-4) than DOM21, which might be due to the husk.

Table 2.3. Average LER from day3 to day 6 for Sloop and single and double mutant in Sloop background. Values are mean ± SE (n = 3, means of 8 seedlings). ANOVA showed a significant effect of the double mutant (DOM) on average LER ($P < 0.01$) and LSD (0.05) = 3.1 mm/day.

Overgrowth alleles	Average LER (d3-d6)			
	Control		ABA 3 µM	
	Hulled	Hulless	Hulled	Hulless
Sloop	26.6±1.1	25.5±0.77	8.9±0.5	1.0±0.3
sln1s	28.7±1.1	32.4±1.1	14.5±1.5	7.8±1.0
spy1a	29.0±1	26.5±1.2	16.3±1.0	11.4±0.9
DOM	33.5±1.1**	29.6±1.1**	18.2±1.0**	14.8±1.2**

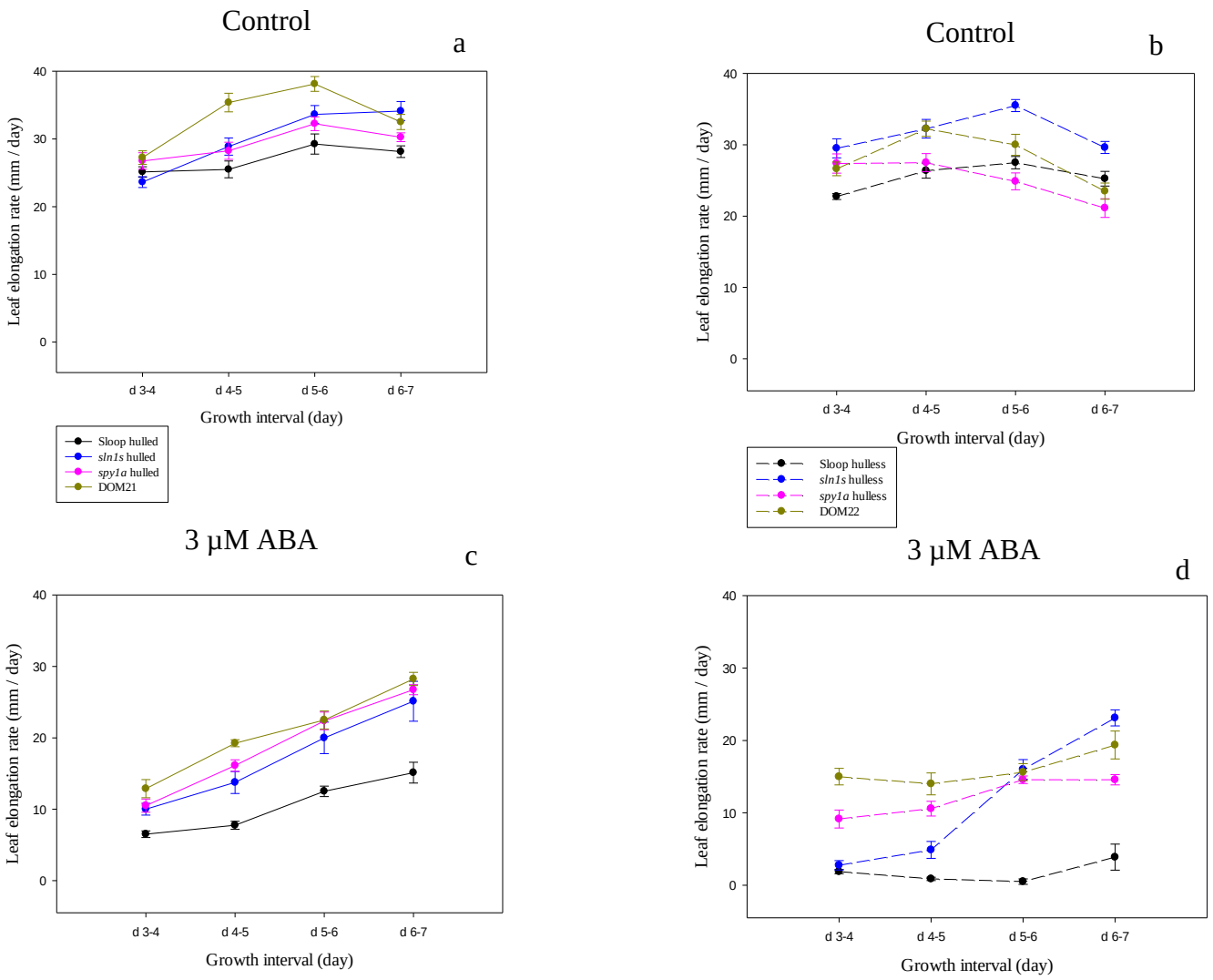

Figure 2.6. Leaf elongation rate of Sloop single and double mutants (hulled and hulless) germinated in control (a, b) and in 3µM ABA (c, d). Grains were imbibed in the control solution or in the presence of 3 µM ABA, stratified for 2 days at 4°C in dark, and then grown at 20°C with constant light. Leaf elongation rate was calculated from daily length measurements. Values are means ± SE (n = 8).)

Grain size and embryo size effects on LER

The experiments described above showed that most overgrowth mutants grew faster than Himalaya in control and ABA solutions. The possible mechanisms that might explain better performance of overgrowth mutants could be (i) grain size effects, or (ii) decreased sensitivity to ABA. The larger grain size of overgrowth mutants over Himalaya was reported before (Chandler and Harding 2013). We also observed that overgrowth mutants and double mutants had significantly larger grains than Himalaya (Table 2.4). For instance *sln1s* has grains about 9% larger than Himalaya and the difference is even more in M251 with grains up to 22% larger; in Table 2.4 (below) the difference was 14% (56.01 mg compared with 48.98 mg; $P<0.001$). The larger grains of double overgrowth mutants (*sln1s*, *spy1a*) were also observed in the Sloop genetic background, which had 7% larger grain than their relative single mutant (data not shown). An example of the grain size of Himalaya and overgrowth mutants is shown in Figure 2.7.

If grain size affects growth rate it could result from (i) larger grain structures including embryo size, that will influence initial growth rates, and/or (ii) more grain reserves in larger grains. To investigate these possibilities the grain weight and embryo weight were determined for Himalaya and M251 (Material and Methods).

Table 2.4. Overgrowth lines, average thousand grain weights and percentage increased thousand grain weights. ANOVA showed significant effect of overgrowth mutation on thousand grain weight ($P< 0.001$). The LSD (0.05) values for thousand grain weights was 3.107 g. Asterisks indicate significant difference between Himalaya and overgrowth mutants. (*** = $P< 0.001$, and ** =$P<0.01$; n = 3)

Lines	**TGW (g)**	**% increased TGW**
Himalaya	56.83 ± 0.8	-
sln1m	67.08 ± 1.03	18***
sln1n	61.83 ± 0.23	9**
sln1s	61.72 ± 0.7	9**
sln1o	64.57 ± 0.6	9***
spy1a	63.75 ± 1.18	14***
M251 (*sln1s, spy1a*)	69.3 ± 1.43	22***

Figure 2.7. Grains of Himalaya (left) and M251 (right). Same number of grains of both genotypes are shown to represent the difference in grain size between wild type and double overgrowth mutant.

Grain weights

Grain weights of Himalaya and M251 (300 grains each) were measured individually and the populations were divided into three sub-populations with equal grain numbers representing small, medium and large grains. The average grain weight for each sub-population is presented in Table 2.5. For Himalaya, grain weights ranged from 38 mg/grain (small) to 59 mg/grain (large). M251 had larger grains than Himalaya in all classes with weight increases of 24%, 14% and 9% respectively for the small, medium and large sub-populations relative to similar grain size classes of Himalaya. Grain size differences were highly significant. Importantly, this was also the case when the seeds were not grouped into size classes (P<0.001). Since endosperm reserves make up most of the grain (90%) it is clear that larger grains could potentially provide more of the reserves required for growth.

Embryo size

Embryos of different grain size sub-populations were isolated as explained (Material and Methods) and their fresh and dry weights determined (Table 2.6). M251 had larger embryos than Himalaya, and the difference for all classes of grain was 34% on average, even greater than the average differences in grain size (15%). This result suggested that embryo size might also be effective in faster initial growth of overgrowth alleles. Next, the performance of different classes of grain size for both Himalaya and M251 were examined in control and ABA solution.

LER of grains with different size

Leaf elongation for each class of grain size of Himalaya and M251 was investigated with or without 3μM ABA and results are shown in Figure 2.8. In control solution, both lines had an average LER (d3-4 to d6-7) that increased with grain size, and within a genotype there was a significant difference of grain size on LER. The average LER of M251 was higher than Himalaya; however large Himalaya appeared to have average LER and LER_{max} similar to small M251, consistent with the similar grain weights of these two classes. Despite the small differences between Himalaya and M251, when the actual lengths per day were plotted (Figure 2.9) M251 showed better performance than Himalaya for each class of grain size, and the enhanced growth of M251 was primarily due to the better early growth (day 3-4) which was consistently higher than Himalaya.

In ABA solution, the main effect of grain size was seen in the LER_{max} , which increased gradually as the grain size shifted from smaller to bigger size for both Himalaya and M251. There was a slightly higher LER_{max} for M251 compared with Himalaya, and LER_{max} of large Himalaya was fairly similar to that of small M251. Although the LER_{max} did not represent the significant differences between these two lines, the plot of actual length per day (Figure 2.9) showed that M251 performed much better than Himalaya in the presence of ABA. The great differences between Himalaya and M251were caused by the better growth at early stages (day 3-4 to 4-5) that was closely related to the better performance of M251. This result showed that the advantage of M251 was in their early LER that was on average 70% larger than Himalaya, and the effect was independent of the grain size class.

Table 2.5. Average grain weights (mg/grain) of small, medium and large sub-populations. 300 grains each of Himalaya and of M251 were weighed individually and divided into three equal sub-populations. Values are the average grain weights (mg/grain) ± SE, *n* = 100 of each sub-population. Asterisks indicate *P*< 0.001.

Grain size classes	Average Grain weight (mg/grain)	% increased grain size over Himalaya
Himalaya Overall	48.98 ± 0.53	
Small	38.76 ± 0.43	
Medium	49 ± 0.28	
Large	59.06 ± 0.39	
M251 Overall	56.01 ± 0.43	14***
Small	48.14 ± 0.41	24***
Medium	55.78 ± 0.16	14***
Large	64.12 ± 0.43	9***

Table 2.6. Average embryo weights of different classes of grain size. Twenty grains of small, medium and large grains were imbibed in water for 6 h at room temperature, then under a binocular microscope scutellum with the embryo attached was dissected from each grain, then incubated at 65°C for 48 h. Values are means divided by number of embryos (*n* = 20).

Grain size classes	Embryo wet weight (mg / embryo)	Embryo dry weight (mg / embryo)	% Increase in embryo size relative to Himalaya (DW)
Him			
Small	3.03	1.40	
Medium	3.21	1.64	
Large	3.93	2.10	
M251			
Small	3.30	1.94	38.5
Medium	3.16	2.31	40.8
Large	5.10	2.64	25.7

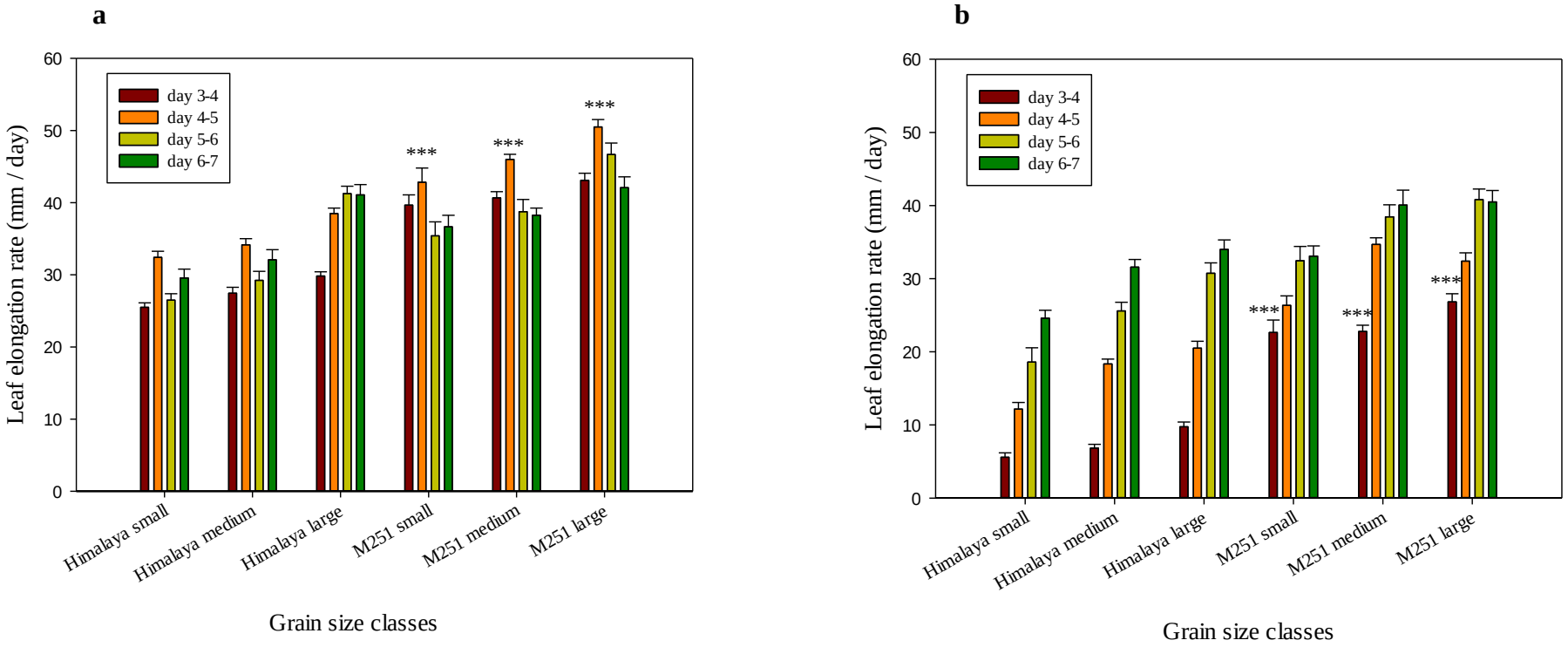

Figure 2.8. Leaf elongation rates (LER) of different classes of grain size germinated in control (a) or in 3 µM ABA (b) solution. Grains were imbibed in the presence of ABA (3µM) or in control medium, stratified for 2 days at 4°C in dark, and then grown at 20°C with constant light. Leaf elongation rate was calculated from daily leaf length measurement. Values are means ± SE (n = 8). ANOVA showed significant effect of overgrowth mutation on LER for different classes of grain size (P<0.001). The LSD (0.05) for LER_{max} was 3.19 mm/day in control solution and the LSD (0.05) for LER in day 3-4 was 4.11 mm/day in ABA treatment.

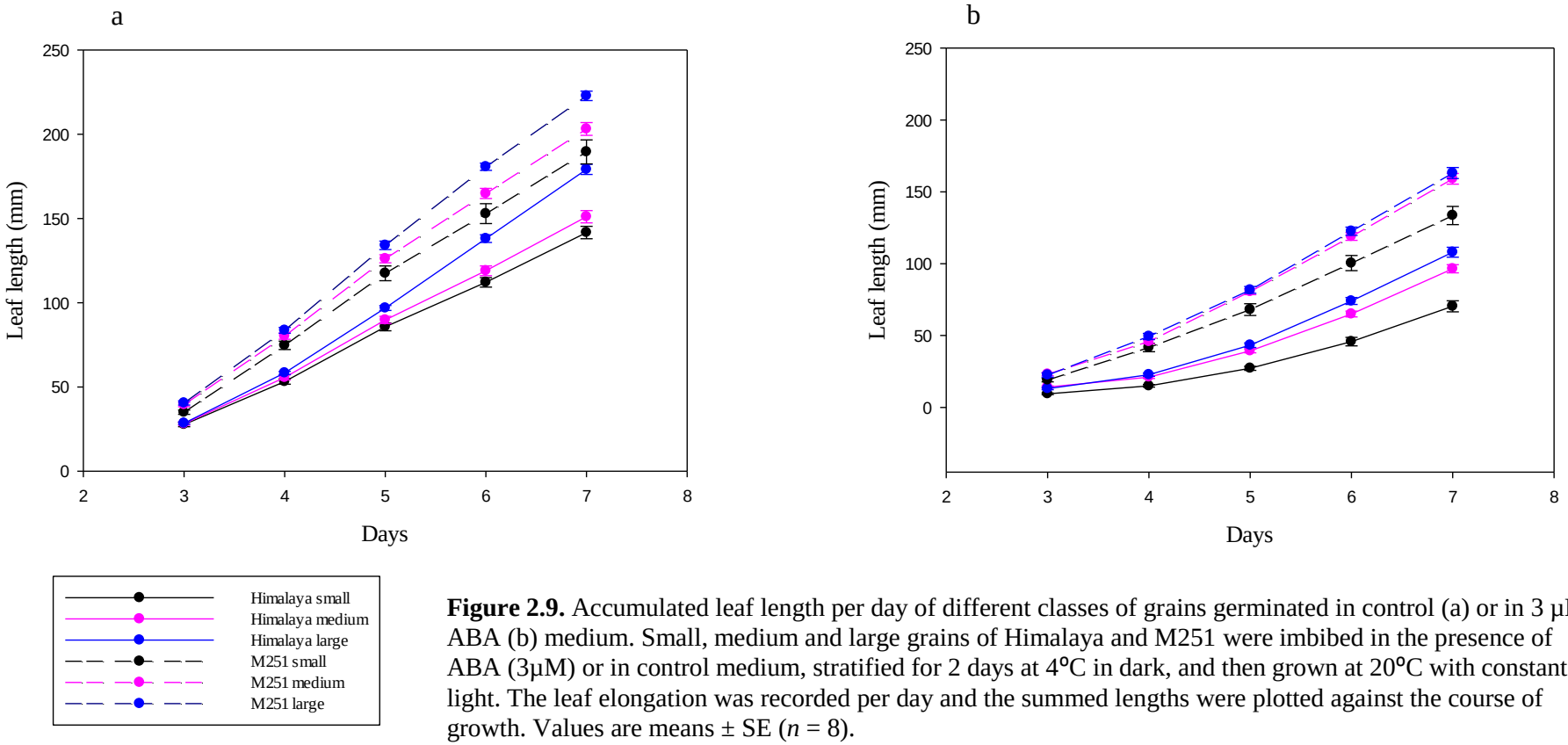

Figure 2.9. Accumulated leaf length per day of different classes of grains germinated in control (a) or in 3 µM ABA (b) medium. Small, medium and large grains of Himalaya and M251 were imbibed in the presence of ABA (3µM) or in control medium, stratified for 2 days at 4°C in dark, and then grown at 20°C with constant light. The leaf elongation was recorded per day and the summed lengths were plotted against the course of growth. Values are means ± SE (n = 8).

ABA and water deficit responses in the cigar system

The observations that double mutants had a significant degree of resistance to ABA suggested that they might also show tolerance to water deficiency. To investigate this, a series of experiments was carried out using germination paper 'cigars'. These allowed us to test growth responses to ABA and water deficit under very similar conditions. The experiments involved Himalaya, M251, Sloop and DOM22 treated with a range (3µM, 6µM and 9µM) of ABA concentrations or different degrees of reduced water availability (10ml, 12ml and 24ml water per cigar, see Materials and Methods). The lengths of coleoptiles and leaf one were measured after 6, 10 and 12 days incubation in the dark at 20°C.

ABA responses of Himalaya and M251

After 6 days of incubation (Figure 2.10a) coleoptiles were still growing (L1 enclosed) and the extent of growth declined as the concentration of ABA increased. In general M251 grew better than Himalaya especially at the higher concentrations of ABA. After 10 days incubation (Figure 2.10 b, c) the coleoptiles had reached their final lengths except for Himalaya at 9µM ABA which was still only 70% grown. Leaf one had emerged through the coleoptile in all cases except for Himalaya at 9µM ABA. By day 12 (Figure 2.10 d, e) coleoptiles had finished growing, and there was no significant difference in coleoptile length between control and ABA treatments or between Himalaya and M251. However, the leaves of M251 were longer than those of Himalaya at high concentrations of ABA, but not at the low concentration. These results indicate that the effects observed were due to higher growth rates of M251 in the presence of ABA, rather than greater extents of growth.

ABA responses in Sloop and DOM22

Results of ABA responses of Sloop and DOM22 are shown in Figure 2.11 (a - e).Sloop and DOM22 showed very similar responses to those shown by Himalaya and M251 to different concentrations of ABA for all incubation times. DOM22 had better growth than Sloop in the presence of ABA, especially at the higher concentration. The differences between extents of growth generally (Figure 2.10 vs Figure 2.11) might be due to their different genetic background.

Water deficit responses of Himalaya and M251

After 6 days of incubation (Figure 2.12 a), coleoptiles were still growing and leaf one had not yet emerged. Growth of both genotypes was progressively restricted by water deficit, with no difference between genotypes. After 10 days incubation (Figure 2.12 b, c), coleoptiles were fully grown in 24 ml and 12 ml treatments, but not fully grown in the 10 ml treatment. Leaf one had emerged in all cases except for Himalaya at 10 ml. As water availability declined, growth was more inhibited, and both lines were affected to a similar extent. After 12 days incubation (Figure 2.12 d, e), coleoptiles finished growth except for Himalaya and M251 at 10ml. Leaf one was growing in all cases except for the 10ml treatment for Himalaya and M251, where it remained enclosed in the coleoptiles. Overall, responses of Himalaya and M251 to limited water were broadly similar.

Water deficit response in Sloop and DOM22

Responses of Sloop and DOM22 to water deficit are shown in Figure 2.13 (a - e), and again very similar responses were observed for Sloop and DOM22 compared with Himalaya and M251.

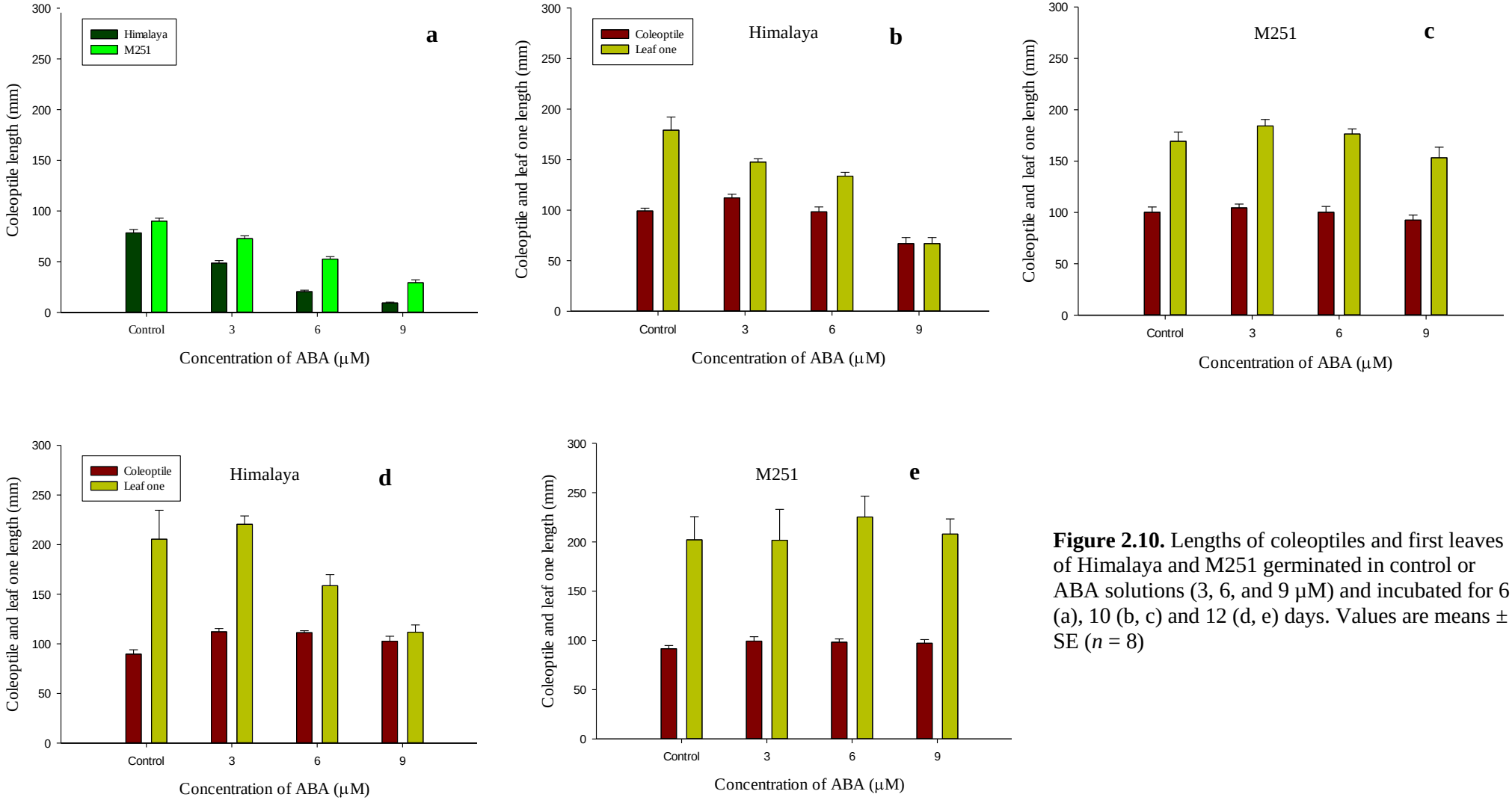

Figure 2.10. Lengths of coleoptiles and first leaves of Himalaya and M251 germinated in control or ABA solutions (3, 6, and 9 µM) and incubated for 6 (a), 10 (b, c) and 12 (d, e) days. Values are means ± SE (*n* = 8)

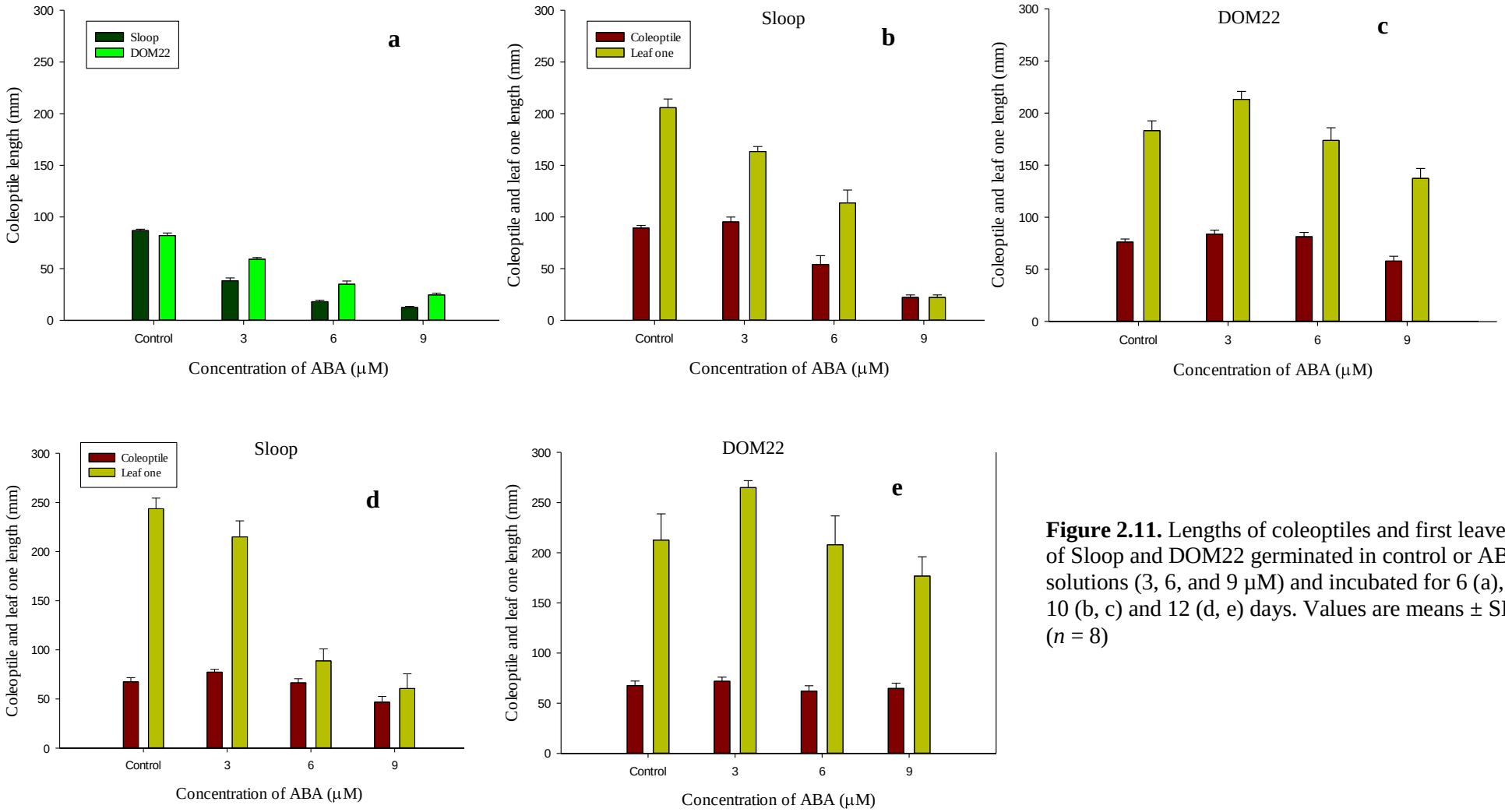

Figure 2.11. Lengths of coleoptiles and first leaves of Sloop and DOM22 germinated in control or ABA solutions (3, 6, and 9 µM) and incubated for 6 (a), 10 (b, c) and 12 (d, e) days. Values are means ± SE (n = 8)

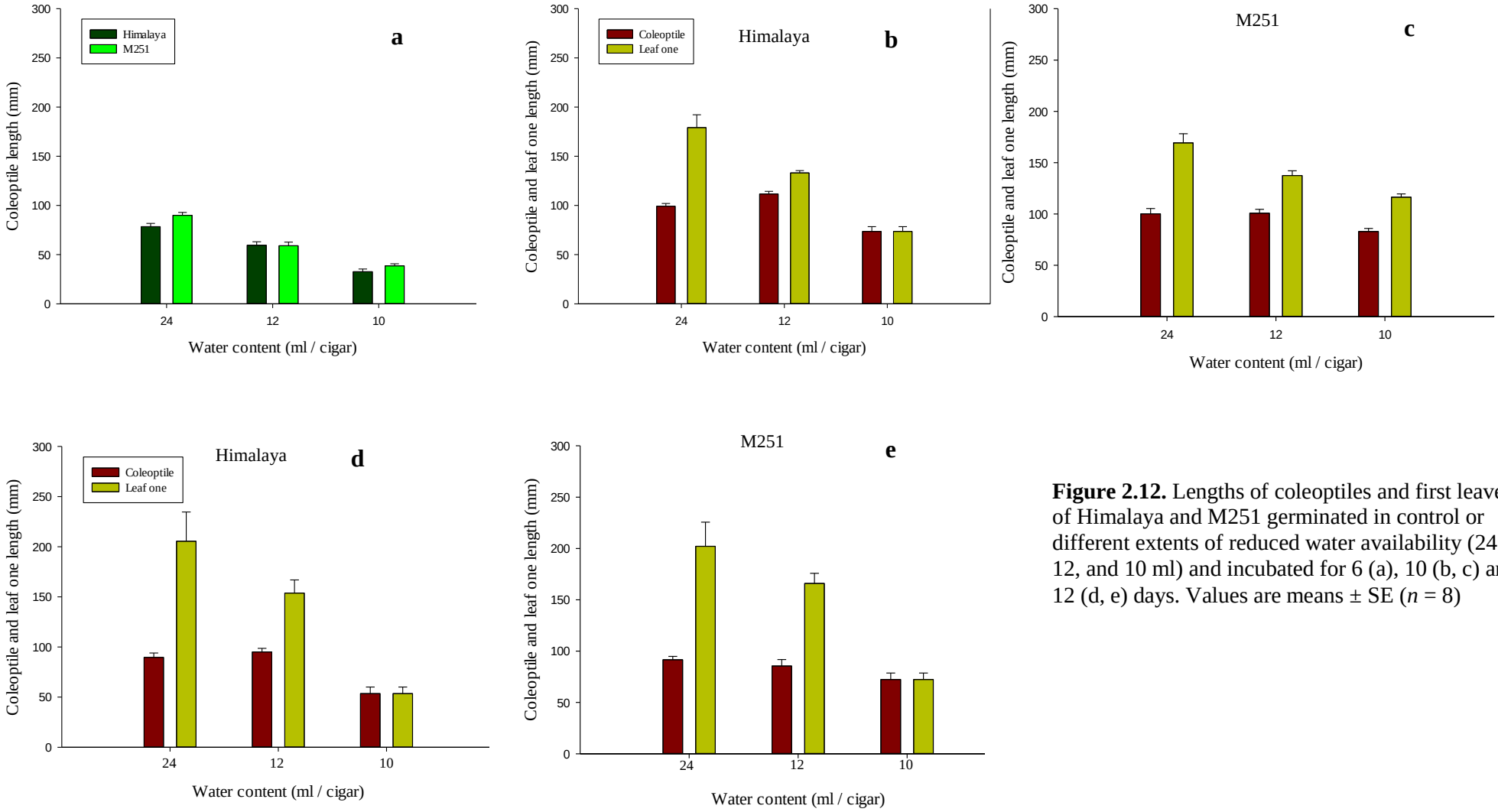

Figure 2.12. Lengths of coleoptiles and first leaves of Himalaya and M251 germinated in control or different extents of reduced water availability (24, 12, and 10 ml) and incubated for 6 (a), 10 (b, c) and 12 (d, e) days. Values are means ± SE (n = 8)

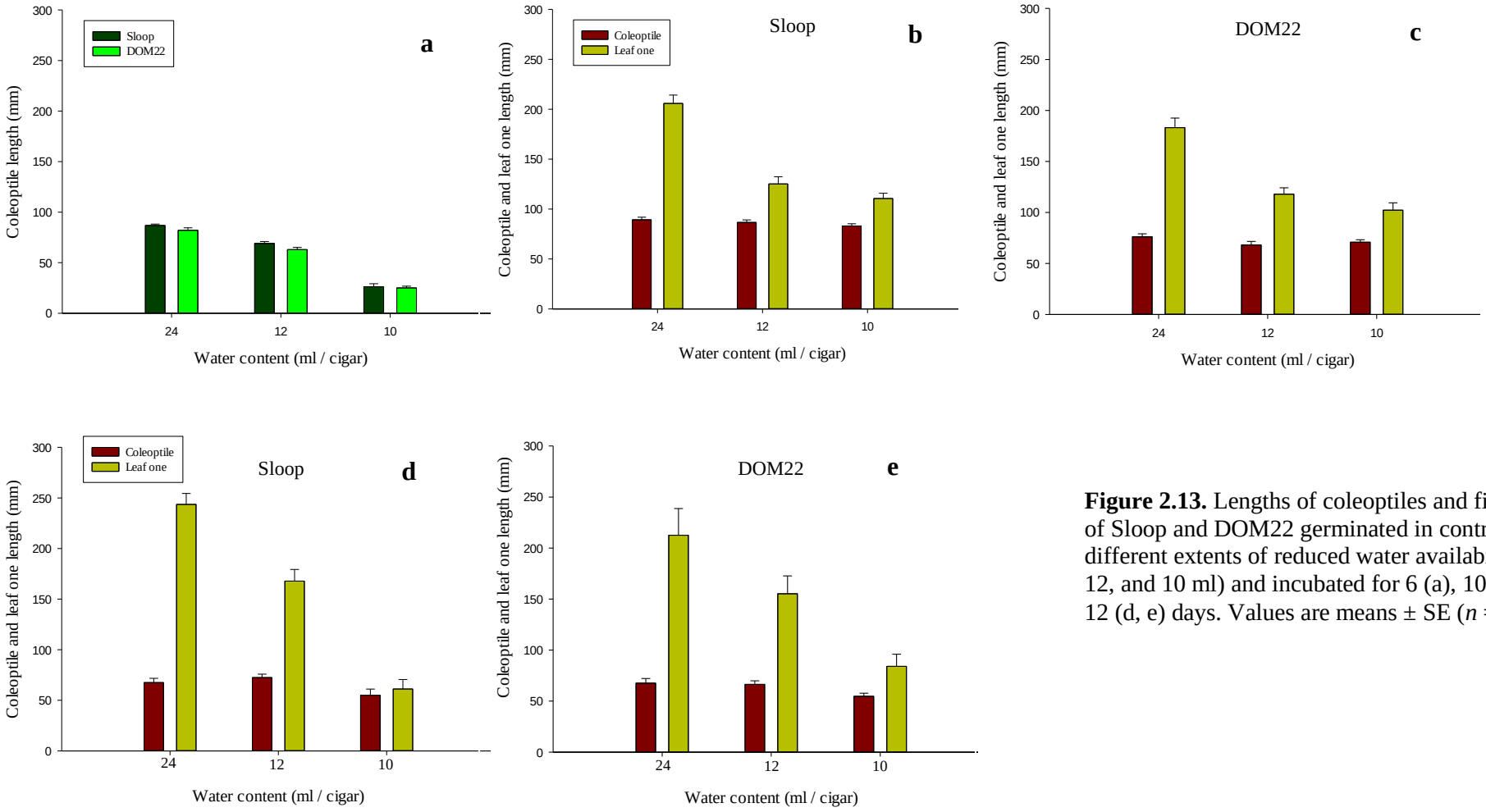

Figure 2.13. Lengths of coleoptiles and first leaves of Sloop and DOM22 germinated in control or different extents of reduced water availability (24, 12, and 10 ml) and incubated for 6 (a), 10 (b, c) and 12 (d, e) days. Values are means ± SE (n = 8)

Discussion

The results of leaf elongation experiments showed that many overgrowth alleles caused growth to occur at faster rates than Himalaya in control solution. *Sln1d.9* is an important exception that will be discussed later. In ABA solution, despite the obvious inhibitory effects of ABA on growth, overgrowth mutants still grew faster than the wild type. The simplest explanation for this observation is that overgrowth mutants confer enhanced growth relative to the wild type and this will occur even in the presence of a growth inhibitor such as ABA. What happens in a line with two overgrowth alleles combined? Will their growth rate increase more than single alleles, and consequently grow even faster in the presence of ABA? We observed enhanced growth of some double mutants over the wild type in control solution, and they grew even faster in the presence of ABA compared with their relative single mutants. For instance, *sln1s* and *sln1o* in combination with *spy1a* had a 27% and 5% increase in their LER_{max}, respectively on control solution. With ABA treatment they grew faster than the single mutants (*sln1s* and *sln1o*) treated with ABA and had 8% and 17% increases in maximum growth rate (however, the extent of growth did not show the additive effects of overgrowth alleles). There were other observations that showed certain double overgrowth allele combinations such as M250 and M253 had no significant change in their LER_{max} in control solution compared with their single mutants in control solution. *sln1m* is an extreme overgrowth allele that already has a high degree of growth, and the combination with *spy1a* did not make a substantial difference, whereas partial alleles still had the capacity to grow faster and show the effects of *spy1a*. For instance, when *spy1a* is present in the weaker overgrowth allele background i.e.*Sln1d.*9, the growth rate was enhanced in this double mutant (M260); in other words, the LER_{max} of the double mutants in both control and ABA solutions increased about 2-fold. However, *sln1n* was a moderate overgrowth allele that had no changes in combination with *spy1a*, so the saturated GA signalling might not explain unchanged LER_{max} of *sln1m* and *sln1n* in combination with *spy1a*. In ABA solution, M250 had a highly significant enhanced growth (19%) while M253 responded to ABA in a similar way to the single mutant (*sln1n*) with the same treatment.

Some double overgrowth allele combinations showed a high degree of sterility, probably associated with pollen formation. It is known that excessive GA signalling has negative effects on fertility, and complete loss-of-function DELLA *sln1c* (barley) and *slr1-1* (rice) mutants are male sterile (Lanahan and Ho, 1988; Ikeda *et al*., 2001). The extent of sterility in overgrowth allele combinations was not related to the severity of the overgrowth alleles; M260 (*Sln1d.9*, *spy1a*) with a weak overgrowth allele at *Sln1* showed severe sterility,

very similar to M250 (*sln1m, spy1a*) carrying one of the strongest *Sln1* overgrowth alleles; whereas, M251, a moderate overgrowth allele had less sterility with reasonable grain set. The different behavior of double mutants suggests that different mechanisms are involved in the enhanced GA signalling and DELLA function in early growth versus pollen development, and this might be due to the different protein partners that interact with DELLA in each developmental stage.

Thinking of possible mechanisms that might be involved in the enhanced growth of overgrowth alleles led us to consider the different grain sizes of overgrowth alleles and the wild type. The larger grain size of single and double overgrowth mutants compared with WT grains, suggested that enhanced growth might be due to larger grain structures (such as embryo) and/or more available reserves (such as starch). Grain populations for both Himalaya and M251 were divided into three sub-populations including small, medium and large grains and further analysis was conducted on these different classes of grain size. Results of LER experiments showed that within genotypes, there was a significantly higher average LER as the grain size increased, and the double mutant had higher LER for all classes of grain size relative to the wild type. Large Himalaya grains and small M251 grains had very similar grain weights and embryo size, and this was reflected in a similar LER_{max}. This gave the impression that grain size could be the main factor behind better growth, and those Himalaya grains with a similar grain size to M251 performed as well as the double mutant. However, a closer look at leaf elongation rates showed that early growth (day 3-4) was independent of grain size for both wild type and double mutant. Especially in ABA solution, the largest difference between Himalaya and M251 was related to the growth rate in day 3-4 (about 3 times greater than Himalaya). This difference is also reflected in the accumulated leaf length per day of both genotypes (Figure 2.9 b), where graphs of M251 were separated from Himalaya largely in day 3-4 (the angle between the graphs at each time point and horizontal line is larger at this time). So, it appears that the main advantage of M251 in growing faster than Himalaya is due to the much greater initial growth, and this in turn provides for an even greater growth of M251 over Himalaya.

One of the mechanisms by which ABA antagonizes GA is interfering with GA synthesis and up-regulating GA catabolism (Zentella *et al.* 2007; Claeys *et al.* 2012). This suggests a second possible mechanism by which overgrowth alleles perform better in the presence of ABA, namely a reduced sensitivity of overgrowth alleles to low GA content. GA_3 dose response curves of overgrowth mutants showed that overgrowth alleles confer enhanced growth rates across all concentrations of GA_3; however their 50% maximal response ($[H]_{50}$) to

GA_3 occurred between 0.01-1µM which was the same as previously found for wild type and GA deficient mutants (Chandler and Robertson 1999; Chandler and Harding 2013). It appears that overgrowth alleles are not shifted to greater sensitivity in their dose response curve to GA, so what has caused their better growth in ABA solution?

The accumulation of ABA (resulting from adverse conditions) normally results in retarding of growth and of cell division, mostly through stabilizing DELLA and influencing expression of downstream stress-induced genes (Claeys *et al.* 2012). DELLA activity occurs largely through binding to other transcription factors e.g. PIF family (see literature review), which thereby prevents them from regulating their target genes. In the case of overgrowth mutants, if ABA cannot stabilize DELLA by reducing GA-dependent degradation, then DELLA activity might be reduced. Overgrowth mutations occurred in the GRAS domain of DELLA and recently the role of other members of the GRAS family in stress signalling was shown in Arabidopsis (Cui *et al.* 2012). SCR (SCARECROW) and SHR (SHORTROOT) are GRAS type transcriptional regulators that are involved in regulating stress response genes and SCR even directly targets ABA transcription factors (Cui *et al.* 2012). It is known that the conserved functional units (motifs) in the GRAS domain are important in DELLA binding to other proteins such as GID1, GID2 or PIF (Murase *et al.* 2008; Sun 2010). The conserved amino acid residues in these motifs play important roles in maintaining the function of that unit. For instance, *Slr1-d4* is a dwarf rice mutant that has a single nucleotide substitution in the *Slr1* gene resulting in substitution of Gly with Val at position 576 in the SAW sub-domain of GRAS. This caused a reduction in DELLA binding to GID1, and subsequent diminished recognition by GID2 (Hirano *et al.* 2012). The overgrowth mutations of conserved amino acid residues of LHR1 and PFYRE suggest that DELLA function might be changed due to reduced interaction with other protein partners and presumably transcription factors regulating stress induced genes.

ABA is often regarded as a drought hormone (Finkelstein *et al.* 2002; Yamaguchi-Shinozaki and Shinozaki 2006), so the better growth of overgrowth mutants in ABA suggested that they might also show a degree of resistance to reduced water availability. We conducted a series of experiments in the cigar system to assess the tolerance of overgrowth mutants to water deficit. For both Himalaya and Sloop backgrounds, we did not observe significant differences between the wild type and double overgrowth mutants in their responses to limited water in all incubation time points for 24 ml and 12 ml. However double mutants grew faster than wild type in the more severe water deficit especially by days 10 and 12, and more studies might support this observation. The possible mechanisms might involve

better remobilization of grain reserves by double mutants in the more severe water deficit. However, the cigar system has not been well explored yet, and possibly testing more severe limited water treatments (less than 10 ml) will give useful information about the performance of double mutants. We also extended the study of wild type and double mutants in Himalaya and Sloop backgrounds into a soil system (moderately dry soil with 12.5% moisture). Similar to the cigar system, there were no significant advantages for double mutants to grow better than the wild type (data not shown); however at the stage of leaf two M251 and DOM22 had longer leaf length than the wild types, but there were no differences between their shoot dry weights. This experiment was a preliminary test of overgrowth alleles in dry soil conditions, and with better design of the experiment and treatment with even less soil moisture, interesting observations might be made.

It was mentioned above that *Sln1d.9* was an exception among overgrowth alleles, and behaved differently in control conditions and in combination with *spy1a*. It had a significantly lower LER than the WT most probably due to the presence of the *Sln1d* mutation in the *Sln1* gene. Since the *Sln1d.9* mutation occurred in the *Sln1* gene, it was not easy to separate these two mutations by recombination. The enhanced GA signalling induced by the overgrowth mutation in *Sln1d.9* is likely to be limited by the *Sln1d* dwarfing mutation. This suggestion is supported by the fact that a mutation identical to *sln1s* (isolated in the GA biosynthesis dwarf background) occurred in the *Sln1d* background (*Sln1d.7*) and made it possible to study an overgrowth allele with and without the presence of the *Sln1d* dwarfing gene. The LER_{max} showed a 52% reduction when *Sln1d* was present (Chandler and Harding 2013). Interestingly, in a GA_3 dose response study, *sln1s* conferred enhanced growth rates across all concentrations of GA_3; however the presence of the *Sln1d* gene did not allow the growth rates to increase as much as *sln1s*, even at the highest concentrations of GA_3 (Chandler and Harding 2013). This result suggested that overgrowth alleles are subject to reduced GA signalling resulting from impaired DELLA protein function. It has also been shown that impaired GA biosynthesis or impaired GA receptor function also impacts on growth of overgrowth alleles (Chandler and Harding 2013).

CHAPTER 3

Barley overgrowth mutants: breeding applications

Introduction

Barley is mainly produced for malting and for stockfeed in Australia. About 60% of total barley production is for feed, and the expansion of the beef, pork and dairy industries in recent decades means an increasing demand for more feed grain in the future. However, the malting barley industry is also important in the Australian agricultural economy and varieties with high malting quality are required for that market. For feed barley, grain yield is the first important factor that breeders consider, whereas for malting barley it is both yield and malting quality that are important (Menz 2010). In cereals, the potential for large grains is one of the components influencing grain yield and since it has a strong genetic component, it is one focus of breeding.

It has been shown that the potential for larger grains in barley and wheat is under strong maternal control during the early reproductive stages (post anthesis), although the actual grain size attained will depend on growing conditions after anthesis since these affect the rate and duration of grain filling (Egli 2006; Sadras and Egli 2008). To have a better understanding of how early reproductive development can set an upper limit for grain size, we need to consider the different stages of grain development (Figure 3.1). The development of barley grain is usually divided into three stages: pre-storage (cell division or morphogenesis), storage (maturation) and desiccation (late maturation). The molecular changes during barley grain development have been studied extensively (Sreenivasulu and Schnurbusch 2012). It appears that the first step of increasing sink strength occurs at the early grain development stage (pre-storage phase). This is tightly coupled to the function of the nucellus, a tissue of maternal origin which is shown in orange in Figure 3.1. This tissue consists of three different zones reflecting cell division, cell elongation and cell degradation. The function of nucellar tissue is in remobilization of nutrients to the early endosperm during endosperm cellularization, and this presumably determines the number of nuclei and the number of primary endosperm cells, which will ultimately influence the sink strength of the developing grain.

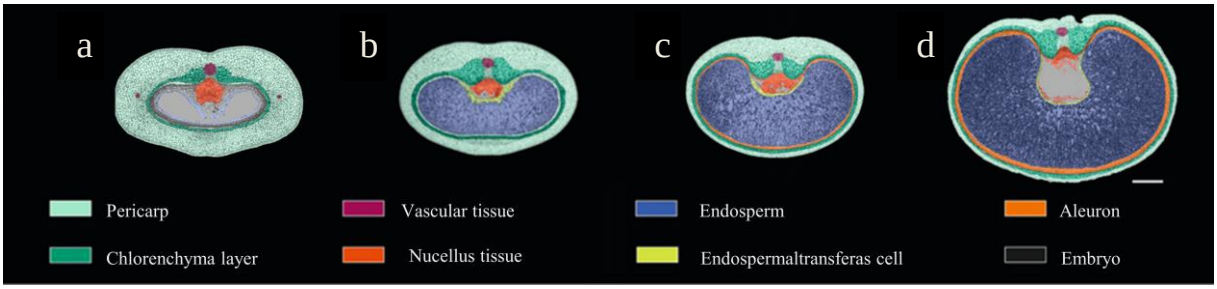

Figure 3.1. The developing barley grain. (a-d) Barley grains at different developmental stages. Colours representing individual tissues are shown at the bottom of the figure. (a) Pre-storage stage, 3 days after flowering, gibberellin biosynthesis is increased and cell wall degradation, lipid degradation, and cell differentiation occur in this stage. The white patches within the nucellar projection indicate degradation of tissue resulting in an endosperm cavity. (b - d) Storage stage, 7, 10 and 14 days after flowering, cell differentiation continues and starch accumulation, lipid biosynthesis and globulin biosynthesis occur along with increased levels of auxin and ethylene. Bar, 500 µm. Figure was modified from Sreenivasulu *et al.*, (2010).

When endosperm cellularization is completed the pre-storage phase finishes and storage product accumulation commences. This stage also determines strength of sink, which is characterized by starch accumulation and by massive remobilization and degradation processes in the pericarp. The combined analysis of transcript profiling and profiling of amino acid content highlighted the specific pathway that the nucellus and the adjacent cell row (endosperm transfer cells shown in Figure 3.1 in yellow) take for mobilization and metabolism of nutrient reserves and their transfer to the endosperm (Thiel *et al.* 2008; Thiel *et al.* 2009). From the hormonal perspective, active gene expression related to GA synthesis and GA signalling suggested a role for GA in the establishment and differentiation gradient of the nucellus, thereby regulating sink strength (Thiel *et al.* 2008). However, these results need to be further investigated by direct measurements of hormones and the levels of enzymes regulating GA biosynthesis or catabolism in the target tissue. Mutants provide promising material to explore changes in GA content relative to the wild type. For instance, *grd1*, a GA-deficient mutant, had a major reduction in total grain GAs (GA_1 and GA_4) in developing grains when compared with the tall parent. Associated with the reduction in GA, the final grain size was reduced by 20% (Chandler 2000).

Given that different studies provided evidence of GA biosynthesis and function in grain development and final grain size, should we expect larger grains in mutants with

enhanced GA signalling? Larger grains have been reported for overgrowth mutants; for instance *sln1m* produced grains 40% larger than its dwarf parent. After backcrossing of *sln1m* to Himalaya, and loss of the dwarfing gene, the grain size of *sln1m* in a tall background was increased by about 20% compared with the wild type (Chandler and Harding 2013). Larger grains were also described as a characteristic of single and double overgrowth mutants in the previous Chapter. It was shown that a combination of overgrowth alleles (double mutants) led to significantly larger grains than the single mutants; for instance *sln1s* and *spy1a* had grains 10% and 18% larger than Himalaya respectively, whereas for M251 (*sln1s, spy1a*) it was 30%.

Since overgrowth alleles conferred increased grain size in a Himalaya background, they might also lead to larger grains in commercial varieties, and be potentially useful in barley breeding. Himalaya is not a commercial variety, and is likely to be a poor donor of traits for use in breeding. Therefore it was necessary to introgress overgrowth alleles into a commercial variety that has been successfully used in barley breeding, and assess their properties in that background. If overgrowth alleles provide larger grains in the new commercial background, it becomes useful as a potential donor in breeding programs.

In this Chapter I will discuss the performance of overgrowth alleles in the commercial barley variety, Sloop. This variety was chosen to assess overgrowth alleles because it has been a good malting variety in Australia, and it has also been a parent in the development of new malting varieties. If overgrowth alleles improve grain size in Sloop, breeders will be able to use these lines as suitable trait donors in breeding programs. Moreover, overgrowth alleles improve grain size by the action of a single gene and molecular markers are available to confirm the presence of the overgrowth allele in a breeding program, which enormously reduces the time required for phenotypic screening.

Materials and Methods

Plant materials

Barley grains used in these experiments were overgrowth mutant derivatives of *Hordeum vulgare*, L. 'Sloop' that were provided by Dr Peter M. Chandler (CSIRO Plant Industry, Canberra). Eight barley overgrowth alleles (Table 3.1) were backcrossed to Sloop for three generations and BC_3F_2 grains were the starting material in my study. The grains were from glasshouse-grown plants from harvest years 2010 and 2011. Plants were grown in similar conditions in the glasshouse to those described in Chapter 2. The Sloop overgrowth lines used in this study are shown in Table 3.1.

Field grown plant materials

Yanco Agricultural Experimental Station (Yanco, NSW). Grains were sown in May 2013 and harvested in November 2013. In this trial grains of hulled and hulless sister-lines were sown in 10 m^2 plots, which accommodate about 200 plants per square meter. This is a standard plant density for optimal agronomic performance. Each line was assigned randomly (using DiGGer software) in the field. Sister-lines were studied under two different watering regimes, irrigated and dependent on natural rain (rainfed). In some cases there were insufficient grains to allow a rainfed plot, and no data is presented for these lines. The 2013 season had adequate rain, and rainfed plants were comparable to irrigated plants in both plant height and grain yield.

Small field (Library birdcage) on CSIRO Black Mountain site. Grains were sown in a single row for each line (20 grains with 4 cm space between) in September 2013, and harvested in December 2013. Irrigation was applied as required.

Overgrowth and wild type sister-lines

Sister-lines were isolated in the BC_3F_2 generation from a common (heterozygous) BC_3F_1 parent and are homozygous for either the overgrowth allele or the wild type *Sln1* or *Spy1* locus (Table 3.1). They share about 91% of the Sloop genome and 3% of the Himalaya genome after three generations of backcrossing, and the remaining 6% of loci are heterozygous. Independent backcross streams will differ as to which genes appear in each category (i.e. 'Sloop', 'Himalaya', 'heterozygous'). This makes a wild type sister-line the best

material to assess performance of its relative overgrowth mutant sister-line, since they differ principally in having or lacking the overgrowth allele.

Plants homozygous for the overgrowth allele or for the wild type allele were identified by sequencing PCR products amplified using molecular markers specific for *Sln1* and *Spy1* genes. Selected plants were then transplanted to pots, with three individual plants per 20 cm pot for each genotype.

Himalaya and Sloop differ in being either 6-rowed or 2-rowed, and in having either hulless or hulled grains respectively. A decision was made to work only with pure-breeding 2-rowed derivatives. For 6 of the eight alleles a hulled and a hulless line were selected. In the 2011 and 2012 glasshouse experiments there was a mixture of hulled (majority) and hulless (minority) plants, due to segregation at the *nud* locus. Pure lines were then established for field trials.

Table 3.1. List of Sloop overgrowth sister-lines.

Allele	**Line**	**Genotype**
WT	Sloop	*WT*
Sln1d.8	Slp A1, Slp A2 [a]	*WT*
	Slp B1, Slp B2 [a]	*mutant*
sln1m	Slp C1, Slp C2 [a]	*WT*
	Slp D1, Slp D2 [a]	*mutant*
sln1n	Slp E1, Slp E2 [a]	*WT*
	Slp F1, Slp F2 [a]	*mutant*
sln1s	Slp G1, Slp G2 [a]	*WT*
	Slp H1, Slp H2 [a]	*mutant*
sln1o	Slp J1, Slp J2 [a]	*WT*
	Slp K1, Slp K2 [a]	*mutant*
spy1a	Slp L1, Slp L2 [a]	*WT*
	Slp M1, Slp M2 [a]	*mutant*
Sln1d.9	Slp N1, Slp N2 [a]	*WT*
	Slp P1, Slp P2 [a]	*mutant*
Sln1d.7	Slp R1, Slp R2 [a]	*WT*
	Slp T1, Slp T2 [a]	*mutant*

[a] Overgrowth mutants and their wild type sister-lines are homozygous stocks derived from BC_3F_1 plants. X'1' corresponds to hulled, and X'2' corresponds to hulless derivatives for all sister lines.

DNA extraction

Leaves from young seedlings were harvested and freezed-dried in deep-well microtiter plates. The samples were ground by adding 5-mm stainless steel beads to the wells and shaking the plates in a vibration mill (Qiagen, Hilden, Germany) for 3 min at a frequency of 23 s^{-1}. The ground material was incubated for 1 h at 65°C with 375 µl of 0.1 MTris-HCl (pH 8.0), ethylene - diaminetetraacetic acid (pH 8.0) and 1.25% SDS. 187 µl of 6 M ammonium acetate was added to the samples, which were then incubated for 15 min at 4°C and centrifuged (30 min at 2,095x g). DNA in the supernatants was then precipitated (220 µl isopropanol, 5 min room temperature, 30 min centrifugation at 2,095x g). The pellets were washed with 70%

ethanol, briefly air-dried and dissolved in 225 µl distilled water overnight at 4°C. The plates were then centrifuged (2,095xg) and 150 µl of the solution transferred to fresh plates.

PCR Primers

PCR primers used in this study are listed in Table 3.2.

Table 3.2. Primers used in PCR assays to amplify *Sln1* and *Spy1* containing overgrowth alleles

Primer name	Gene name	Sequence (5'→3')	Reference
SLNF2	*Sln1*	TCGTCTTCGTCCTCCTCG	Chandler and Harding, 2013
SLNF3		CATCCGCGTCGACTTCC	
SLNF4*		GCGGATACTTCGATCTCCC	
SLNR2		ATTACCTCGGGCTCCTCG	
SLNR5		TTACAGCGTTCAAAACTCGC	
SNLR9*		TAGGGGCAGGACTCGTAGAA	
SLNR12*		CCTGCTTGATGCCGAAGT	
SPYFWD8	*Spy1*	TTACAAGAATCGGGGAGAGC	
SPYREV9		TGCAAGTATGGCCTTCTCAA	
HvSPYP3*		GCAATAGCACTAACCGAC	Robertson *et al*., 1998

* Primers also used in sequencing reaction.

PCR analysis

The PCR conditions were as follows (20 µl final volume): 10 µl Hotstar master mix (Qiagen), 4µl of 4X Q solution (Qiagen), 50-100 ng template DNA, 1 µl of 20 µM forward and reverse primers, 2 µl milli q H_2O.

Amplification was carried out on a thermal cycler running the following program: 95 °C for 15 min, then 5 cycles of 95 °C for 30 sec, 58 °C for 30 sec, 72 °C for 1 min, followed by 30 cycles of 95 °C for 30 sec, 58 °C for 30 sec, 72 °C for 1 min, followed by 72 °C for 10 min and 25 °C for 5 min.

The PCR product of each sample was fractionated on 1% agarose gels made from 1x TAE [20 mM Tris pH 7.5, 10 mM acetic acid, 0.5 mM Na_2EDTA] for 0.5 h at 50 mA and 80 V, stained with ethidium bromide, and then photographed.

Sequencing

PCR products for sequencing were purified using Exosap-IT (Affymetrix) treatment and incubating at 37 °C for 30 minutes followed by 10 minutes at 95 °C to stop the reaction. An aliquot of the purified product was added to 3.2 µl sequencing buffer, 1 µl Big dye V3.1, primer forward or reverse (primers are showed in Table 3.2), and water to 20 µl. Sequencing reactions were carried out using the following program: pre-heat step at 94 °C for 5 min, then 30 cycles of 96 °C for 10 sec, 50 °C for 5 sec, 60 °C for 4 min, followed by 60 °C for 5 min and 25 °C for 5 min. The product of each sequencing reaction was added to 3 µl of 3M sodium acetate (pH 4.6-5.2) and 40 µl of 100% cold ethanol, incubated at room temperature for 15 min, then centrifuged for 30 min at 3000 xg at 4°C. The supernatant was removed and 70 µl of 70% ethanol was added to each sample, and samples were centrifuged for 15 min at 1650 xg at 4 °C. Supernatants were removed and pellets were dried.

Sequencing analysis

Nucleotide sequences were determined using an automated sequencing system (3730xl DNA Analyzer, Life Technologies, Inc., Carlsbad, CA, USA). Analysis of the nucleotide sequences was performed using Finch tv.exe and a web based sequence analysis program.

Statistical analysis

To conduct the best comparison between overgrowth and wild type sister-lines, for each allele the mean of three offspring (BC_3F_3) per BC_3F_2 parent were calculated, which provided better estimates of the per-parent averages. The parental averages were then compared (mutant allele versus wild type) using Mixed Modeling and one-way analysis of variance (ANOVA) method by means of GenStat 16th Edition, statistical package.

Results

Growth and head characteristics of sister-lines

The construction of sister lines homozygous for the alleles of interest is described in Materials and Methods. Each pair of sister lines shares a common parent (BC_3F_1) which makes the wild type sister line the most suitable control line to compare with overgrowth mutants. Sister-lines were allowed to self, generating BC_3F_3 plants (BC_3F_4 grains) which were used to study vegetative, head and grain characteristics in two glasshouse experiments (sister-lines were placed next to each other in both glass house studies to minimize spatial effects).

First glasshouse study (August to October, 2011)

In the first GH experiment sister-lines were studied from early stages of growth. Generally overgrowth mutants grew faster than wild type sister lines and had longer second leaf sheaths (Figure 3.2a). However, two of the overgrowth alleles, *Sln1d.9* and *Sln1d.7*, behaved differently to the rest of the overgrowth alleles, and their second leaf sheaths were shorter than their relative wild type. Overgrowth sister-lines were monitored throughout growth and mutants in general had morphology close to the wild type sister-lines and to Sloop. At maturity, there was no significant difference between stem lengths of most sister-lines relative to wild type, even though at early stages growth was stimulated by most overgrowth alleles. In contrast, *Sln1d.9* and *Sln1d.7* clearly act as semi-dwarfing alleles, as plants at maturity had shorter stem lengths than the relative wild type (Figure 3.2b).

Plants were then monitored during their reproductive growth. Sister-lines were similar for traits such as anthesis date, but they differed in head and grain characteristics (Figure 3.2c and Table 3.3). Among the overgrowth alleles, certain alleles (*sln1m*, *sln1n*, *sln1s*, *sln1o* and *spy1a*) had large effects on overall head length, rachis internode length and grain size. The average percentage increases in rachis internode length and in grain size were about 42% and 15% respectively. There was a tendency (non-significant) for a lower head number per plant for overgrowth alleles compared with the wild type, although the two semi-dwarf overgrowth alleles had the opposite effect, and produced more heads per plant (with poor grain set). This preliminary experiment showed that most overgrowth alleles conferred enhanced early growth in the Sloop background without influencing mature plant height, and more importantly, resulted in larger grains. This promising result encouraged us to study overgrowth alleles in a second glasshouse experiment conducted in a different growing season, to see if these observations were reproducible.

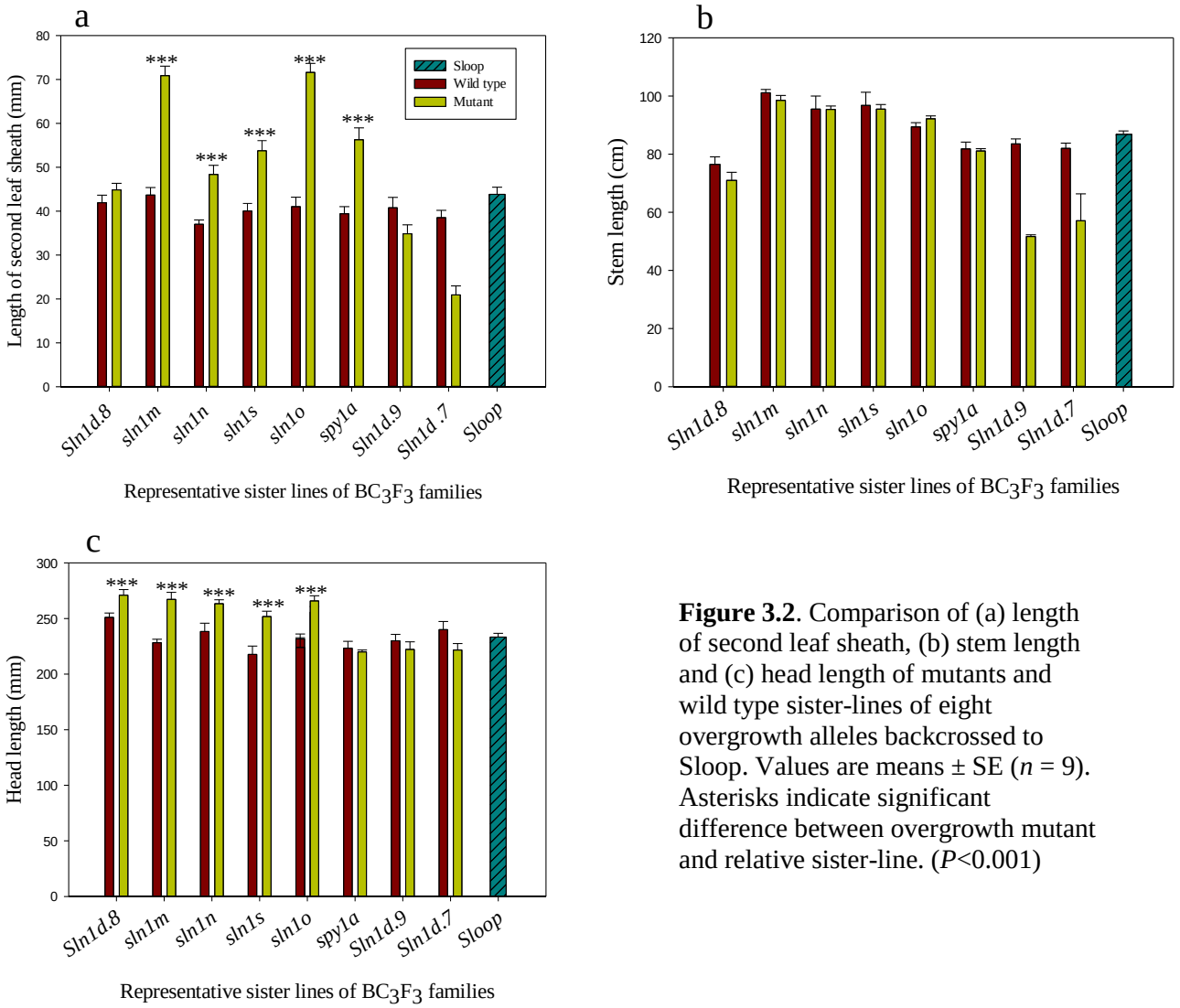

Figure 3.2. Comparison of (a) length of second leaf sheath, (b) stem length and (c) head length of mutants and wild type sister-lines of eight overgrowth alleles backcrossed to Sloop. Values are means ± SE (n = 9). Asterisks indicate significant difference between overgrowth mutant and relative sister-line. (P<0.001)

Table 3.3. Percentage increase in average rachis internode length and in thousand grain weight of selected overgrowth alleles that had enhanced early growth but no changes in final stem length. ** indicates P< 0.01

Overgrowth allele	% promotion rachis internode length	% promotion of grain size
sln1m	56.6**	16.7**
sln1n	69.2**	17.2**
sln1s	32.8**	12.4**
sln1o	40.8**	14.4**
spy1a	15.0**	13.4**

Second glasshouse study (March to May, 2012)

An independent experiment was conducted with the same sister-lines in a different growing season. Plants were monitored from early stages of growth and the results of measuring first leaf sheath lengths showed that some overgrowth alleles had longer sheaths compared to their relative wild type (Figure 3.3), which reflects faster growth in mutants based on our results from LER_{max} experiments (explained in Chapter 2). The early growth profile was consistent with the first glasshouse experiment, including *Sln1d.9* and *Sln1d.7* having shorter sheath lengths compared with the wild type sister-lines.

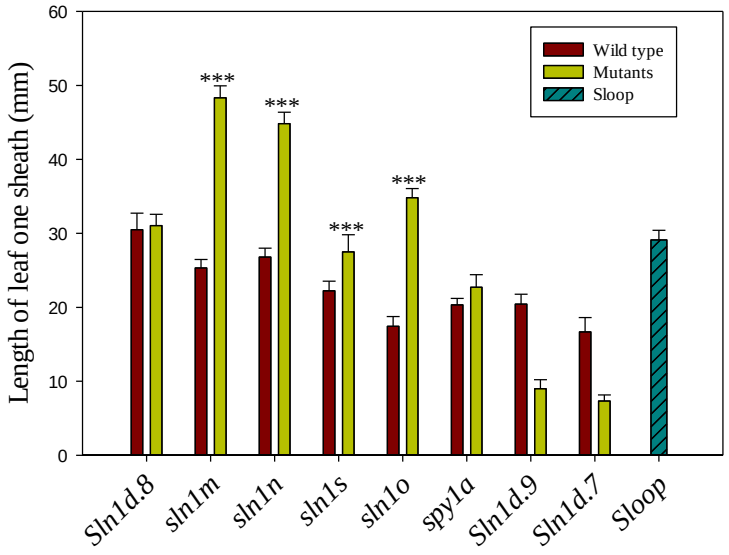

Figure 3.3. Length of first leaf sheath of mutants and wild type sister-lines of eight overgrowth alleles backcrossed to Sloop. Values are mean of three plants ± SE. Asterisks indicate significant difference between overgrowth mutant and relative sister-line. (P< 0.001)

Representative sister lines of BC_3F_3 families

Later during vegetative growth there were no obvious differences between overgrowth alleles and their wild type sister-lines, and they had close to normal appearance. Overgrowth lines also had similar anthesis date. At maturity most overgrowth lines had a similar height to their respective wild type lines, except for *Sln1d.7* and *Sln1d.9* that had a significant reduction in the mutants (Table 3.4). Consistent with the earlier study, overgrowth alleles with faster early growth had no effect on plant height at maturity and there were no significant differences between overgrowth and wild type sister-lines. Generally, growing plants in a different season (March-May) caused a reduction in mature plant height for both mutant and wild type compared with the first glasshouse study.

Head and grain characteristics were also studied in this experiment. Again, selected overgrowth alleles including *sln1m, sln1n, sln1s, sln1o* and *spy1a* resulted in significantly larger heads and larger grains compared with their relative wild types (Tables 3.4 and 3.5).

The average percentage increase in grain size for selected overgrowth alleles (*sln1m, sln1n, sln1s, sln1o* and *spy1a*) was 19% in 2012 (Table 3.5). The greater percentage increase in grain size in 2012 (19%) compared with 2011 (15%) was due in part to a very high value of *spy1a* (30.5) in 2012. This value is suspect, because it was influenced by the unexpectedly small grain in the wild type sister-line, rather than by large grains in the overgrowth line. If this value is omitted from calculation of the averages, there is a 15% increase in 2011 and 17% in 2012. A lower number (non-significant) of heads per plant was again observed in this experiment for overgrowth sister-lines with the exception for *Sln1d.9,* which produced more heads.

Table 3.4. Growth and reproductive characteristics of overgrowth allele sister-lines. Stem length, head number, head length and grain size from glasshouse studies in 2011 and in 2012 are presented. Values are pooled means of 9 representative sister-lines of each allele, with 3 replicates per sister-line.** indicates a significant difference ($P< 0.01$) between sister-lines. For statistical analysis of grain size, see Table 3.5.

Alleles	**Lines**	**Stem length (cm)**		**Head number per plant**		**Head length (mm)**		**Rachis internode length (mm)**		**Grain size (mg/grain)**	
		2011	2012	2011	2012	2011	2012	2011	2012	2011	2012
WT	Sloop	85.2	nd*	12.5	nd	229	nd	5.6	nd	54.3	nd
Sln1d.8	Slp A	76.5	66.5	11.5	11.7	245	204	7	nd	49.4	53.3
	Slp B	72.9	66.6	10.6	11.2	263**	234**	9**	nd	56.3	58.6
sln1m	Slp C	93.2	68.9	13.2	12	224	236	6	nd	54.3	55.5
	Slp D	96	77.3	10.6	9.4	258**	279**	9.4**	nd	63.4	63.5
sln1n	Slp E	95	77.2	10.3	9	235	235	6.5	nd	55.7	54.1
	Slp F	97	73	10.6	9.3	277**	275**	11**	nd	65.3	65.5
sln1s	Slp G	96	78.8	9.7	8.6	228	225	6.4	nd	57	46.6
	Slp H	93.6	83.5	9.1	8.2	258**	260**	8.5**	nd	64.1	55.9
sln1o	Slp J	90.3	81.5	11.2	9.1	230	213	5.75	nd	51.9	50.9
	Slp K	93.4	79.8	11.1	11.8	253**	251**	8.1**	nd	59.4	57.3
spy1a	Slp L	84.9	84.4	13.1	10.1	235	210	6	nd	54.4	43.3
	Slp M	79.6	79.6	9.9	7.6	229	236	6.9	nd	61.7	56.5
Sln1d.9	Slp N	85.2	71.6	10.7	9.8	234	229	6.7	nd	60.4	59.2
	Slp P	51.7	44	16.3	14.5	213	240	6.5	nd	57.1	57.8
Sln1d.7	Slp R	75.5	82.0	10.7	35.4	240	215	6.8	nd	56.0	52.8
	Slp T	43.7	49.5	12.9	19.3	225	215	5.8	nd	45.8	29.5

*nd= not determined

Table 3.5. Percentage increase in average grain size of overgrowth alleles relative to wild type sister-lines in 2012 compared with 2011. * * indicates $P < 0.01$

Overgrowth allele	**% increase in grain size**	
	2011	2012
sln1m	16.8**	14.4**
sln1n	17.2**	21.1**
sln1s	12.5**	20.0**
sln1o	14.5**	12.6**
spy1a	13.4**	30.5[1] **

[1] probably not a true indicator of increased grain size. Wild type had unexpectedly small grains, so the percentage in the overgrowth line is exaggerated.

Field trials

The results of two glasshouse experiments indicated that overgrowth alleles resulted in larger grains in the Sloop genetic background, and this effect was similar in different growing seasons. These promising results encouraged us to assess the potential of overgrowth alleles to increase grain size under field conditions. This also allowed us to study their effects on grain yield. Therefore studies of overgrowth sister-lines were continued in the field and their performance assessed under natural growing conditions. Pure breeding hulled and hulless lines were selected from the glasshouse studies and used in the field trials. Also, since the performance of *Sln1d.7* and *Sln1d.9* was not of agronomic interest, they were not included in field studies.

Field studies were carried out at the Yanco Agricultural Experimental station (Yanco, NSW) from June-December 2013. Grains were sown in 10 m^2 plots for irrigated and rainfed trials.

Canopy height, which reflects stem length, was measured for all lines at maturity and the results are shown in Figure 3.4. In the irrigated experiment (Figure 3.4a), most overgrowth mutants had heights close to wild type sister-lines, although there was a tendency for a height reduction overall. Unexpectedly *Sln1n* (E,F) showed significant reductions in both hulled and hulless overgrowth derivatives, which was not observed previously. In the rainfed experiment plant height was also measured for the available lines (some were not sown due to insufficient grains), and again for half of the overgrowth alleles there were no significant differences between mutants and wild types, whereas for others the overgrowth derivative had slightly shorter stem length. Again, the *Sln1n* mutant was reduced in height compared with the

relative wild type (E, F). Note that hulled and hulless wild types performed similarly. Plants from the rainfed experiment are comparable in height to the irrigated plots because there was sufficient natural rainfall during the growing season.

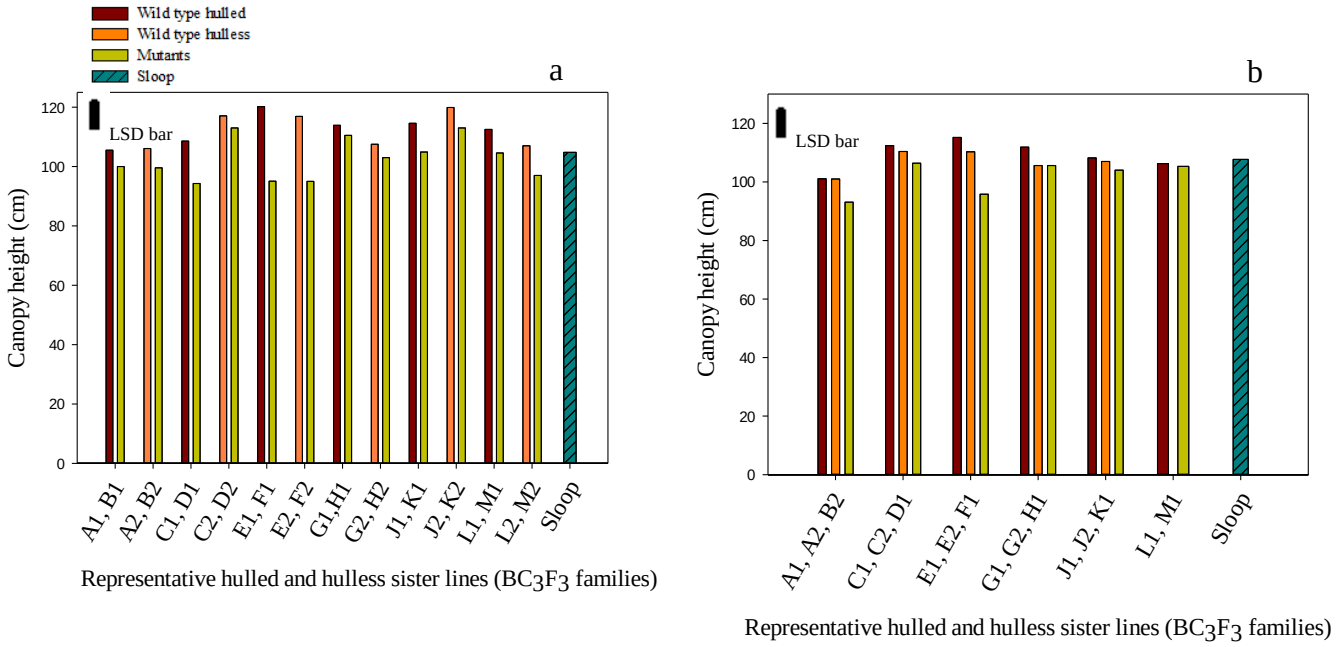

Figure 3.4. Comparison of stem lengths of overgrowth sister-lines, hulled and hulless derivatives (a) irrigated trial and (b) rainfed trial from Yanco 2013 field trial. Values are means and n = 20. The LSD (0.05) value was 8.48 cm.

These results confirmed observations from glasshouse experiments that overgrowth mutants do not increase plant height, despite the observation that they have faster early growth. The occasional observation of significant reductions in height in overgrowth mutants was inconsistent (except for E, F) between the two trials (irrigated vs rainfed), which suggests that such differences might be due to either particular growth conditions, or to chance effects when many lines are being considered.

Grain size (thousand grain weights) of overgrowth derivatives was greater than the wild types, in both irrigated and rainfed trials (Table 3.6). Average grain size (mg) for overgrowth alleles (*sln1m, sln1n, sln1s, sln1o* and *spy1a*) was 50 ± 1.3 and 48 ± 1.0 in irrigated and rainfed trials, respectively, versus the average grain size for their corresponding wild type sister-lines which was 36.0 ± 1.0 and 39 ± 1.1(LSD was 0.416 and 0.370 tonne/hectare for irrigated and rainfed, respectively). The average increase in grain size for irrigated and rainfed were 40% and 23% respectively.

The effect of overgrowth alleles on grain yield was determined from combine harvests of heads from plots, and by measuring total grain weight for each line. Yields were calculated from total grain weights divided by the plot area (g/m^2) and then values were converted to tonne/hectare. Calculated grain yields per hectare are presented in Table 3.6. Grain yields were generally lower in overgrowth mutants compared with the wild type sister-lines. For the *sln1m, sln1n, sln1s, sln1o* and *spy1a*alleles, average reductions in grain yield relative to the control lines were 24% and 22% for irrigated and rainfed respectively. Some overgrowth alleles had slightly higher grain yields in rainfed compared with irrigated plots; however the differences were insignificant and also inconsistent within a family. In both trials (irrigated and rainfed), hulless lines consistently had lower yields compared with the equivalent hulled line.

There are many factors to consider in relation to the yield reduction of overgrowth sister-lines, and these will be considered in the Discussion. Of immediate experimental interest was the observation that heads of overgrowth alleles from Yanco had occasional expression of sterility, and these results are presented in the next section.

Table 3.6. Grain yield and thousand grain weights of overgrowth sister-lines in field conditions. Plants were harvested from 10 m^2 plots from irrigated and rainfed trials and total grain weights were obtained. Grain yield per hectare was calculated from grain yield per square meter and the average grain yield was predicted based on spatial analyses. Thousand grain weight was obtained from grains that were harvested by combine harvester in irrigated and rainfed trials. ANOVA showed a significant effect of genotype on grain yield ($P< 0.001$). The LSD (0.05) values were 0.416 and 0.370 tonne/ha for irrigated and rainfed respectively.

Alleles	**Lines**	**Yield (tonne/ha)**		**TGW (g)**	
		irrigated	rainfed	irrigated	rainfed
Sln1d.8	Slp A1	5.41	5.00	-	40.95
	Slp B1	3.55	-	-	-
	Slp A2	4.57	4.13	-	40.8
	Slp B2	3.47	3.85	-	42.5
sln1m	Slp C1	5.88	5.05	37.33	39.1
	Slp D1	3.83	3.37	52.86	49.85
	Slp C2	4.3	4.33	39.9	39.35
	Slp D2	2.08	-	52.91	-
sln1n	Slp E1	4.15	4.83	32.49	40.25
	Slp F1	3.97	3.18	56.90	52
	Slp E2	4.05	3.03	40.71	41.7
	Slp F2	3.2	-	52.06	-
sln1s	Slp G1	4.93	5.15	40.40	45.05
	Slp H1	3.97	4.17	52.03	50
	Slp G2	3.31	3.13	32.26	31.8
	Slp H2	3.1	-	44.20	44.3
sln1o	Slp J1	5.77	5.43	35.36	38.15
	Slp K1	3.21	3.70	48.80	45.55
	Slp J2	3.48	3.54	33.99	40.85
	Slp K2	2.78	-	48.31	47
spy1a	Slp L1	5.66	4.77	35.08	41
	Slp M1	4.65	4.83	45.64	47.95
	Slp L2	5	-	32.96	-
	Slp M2	3.13	-	45.10	-
WT	Sloop	5.25	5.65	34.52	41

The reduced grain yield of mutants compared with the wild type sister-lines was an unexpected result. Under both glasshouse and field conditions the mutants generally produce

larger grains and in glasshouse studies there was no indication of sterility in the mutant lines. The observation of partial sterility of some overgrowth lines under field conditions is clearly relevant to reduced yield. Two approaches were used to analyze this further. The first approach involved hand harvesting heads from representative plants for each line from the Yanco trials and studying them in more detail. The second approach was growing overgrowth sister-lines in a small field plot at the Black Mountain site, which had the advantage of easier accessibility to plants for more detailed studies.

Hand harvested sister-lines from Yanco (2013)

Head and grain characteristics were studied in more detail in the irrigated trials and the results are summarized in Table 3.7. Analysis of head characteristics indicated that overgrowth alleles had a longer rachis compared with their relative wild types (Figure 3.5), with an average 20% promotion of rachis length. Grain size was also increased in mutants relative to their wild type sister-lines, although the extent varied within and between alleles. Overall there was a 30% increase in grain size for overgrowth alleles (*sln1m, sln1n, sln1s, sln1o* and *spy1a*).

Figure 3.5. Heads of *sln1n* sister-lines (E wild type, F mutant). Representative heads from hulless sister-lines that show the larger head and longer rachis internode of the *sln1n* allele. Heads were harvested from the irrigated trial, and awns have been cut short at the end of the rachis.

This study also revealed a degree of sterility in overgrowth lines which has not been observed previously in either the Himalaya background or in the Sloop glasshouse studies. The percentage of sterile splikelets was calculated from average spikelets per head and average grains per head. The results (Table 3.7) showed that overgrowth sister-lines had different degrees of sterility, and generally mutants showed more sterility than wild types. The

extent of increased sterility was neither allele specific nor related to being hulled or hulless in both mutants and wild types. This inconsistency in the expression of sterility within and between alleles suggests that external factors such as environmental conditions might interact with genotype in the expression of this characteristic.

Table 3.7. Head and grain characteristics of overgrowth sister-lines from the Yanco irrigated experiment. Rachis length and grain size are presented as percentage increase in mutants relative to the wild type sister-lines. Percentage sterility was calculated by comparing the number of spikelets in a head with the number of grains produced in that head. $n = 20$. ANOVA showed significant effects of overgrowth allele on rachis length and grain size ($P<0.001$). Asterisks indicate significant difference between overgrowth mutant and relative wild type sister-line.

Allele	Lines	% increase in rachis length	% increase in grain size	% Sterility	
				WT	Mutant
WT	Sloop	-	-	1.2	-
Sln1d.8	A1,B1	-	-	-	-
	A2,B2	25***	2.8	-	27.4
sln1m	C1,D1	32***	29.3***	3.9	10.1
	C2,D2	43***	31.8***	1.5	24.7
sln1n	E1,F1	14***	36.7***	5.2	12.1
	E2,F2	15***	30.1***	1.4	10.2
sln1s	G1,H1	24***	14.6***	2.7	9.1
	G2,H2	11***	8.7	0	4.2
sln1o	J1,K1	8***	9.6***	3.4	28.8
	J2,K2	17***	38.4***	2.1	33.6
spy1a	L1,M1	12***	0	3.9	6
	L2,M2	17***	15.9***	1.7	2.7

Sister-lines from the Black Mountain CSIRO field site (2013)

Sister-lines were sown at Black Mountain CSIRO for more detailed 'field' studies. This site was sown later than Yanco (early spring compared with late Autumn) so that all lines could be included, and Black Mountain is a cooler environment than Yanco due to its higher elevation. Hulled and hulless sister-lines were assessed in single rows of approximately 20 plants, with hulled and hulless derivatives of each allele sown side by side. Plants were analyzed for growth, head and grain characteristics (Table 3.8).

Growth was monitored throughout the growing season, and generally overgrowth mutants had faster emergence and early growth, and slightly earlier head emergence compared with the relative wild-type. These characteristics were observed in both hulled and hulless derivatives.

At maturity, stem lengths were measured for all lines and the results are presented in Table 3.8. Generally heights were similar for mutants versus wild type sister-lines for *sln1m, sln1n, sln1s, sln1o*. Consistent with the Yanco experiments, overgrowth mutants tended to have a slight reduction in height compared with the relative wild-type. However the *Sln1d.8* mutant showed a considerable reduction (about 20%) compared with the wild type, in both hulled and hulless lines. This reduction was not observed in Yanco or in glasshouse experiments which suggests that growth conditions might induce occasional allele-specific effects on stem length. Comparing hulled and hulless derivatives showed that generally there were no consistent differences between them.

We also measured mature plant dry weights for each line and the results showed that (i) overgrowth and wild type sister-lines had generally a lower dry weight than Sloop, and (ii) overgrowth mutants tended to have less biomass than the wild types.

Head and grain characteristics including average heads per plant, rachis lengths, grain size and percentage of sterility were studied in much greater detail and the results are presented in Table 3.8. Average head number per plant was lower in sister-lines compared with Sloop. There was also a slight reduction in number of heads per plant in most mutants relative to the wild type sister-line; however there were cases such as *sln1o* where mutants (either hulled or hulless) had equal or slightly higher number of heads per plant relative to wild type sister-lines. Glasshouse experiments also showed a tendency for a lower number of heads per plant in most overgrowth mutants. These observations were made in independent experiments and also in different growing conditions, which suggests that the low number of heads might be one of the factors that affected grain yield in mutants.

Overgrowth mutants generally had a longer rachis compared with the wild type, except for *spy1a* (M2) which was shorter than its relative wild type (Table 3.8).The unexpected behavior of M2 might be related to particular field conditions, since this hulless derivate had a longer rachis in the Yanco studies. Overall, overgrowth mutants (*sln1m, sln1n, sln1s, sln1o* and *spy1a*) had rachis lengths 14% longer than wild types.

Table 3.8. Growth, head and grain characteristics of Sloop overgrowth sister-lines. Stem lengths, average plant weight, average number of heads per plant, rachis lengths, grain size and percentage sterility were studied in a library birdcage experiment. Values are means $n = 20$.

Allele	Line	Stem length (cm)	Dry weight per plant at maturity(g)	Heads per plant	Rachis length (mm)	Grain size (mg/grain)	%Sterility
WT	Sloop	76.6	26.4	9	67.4	54.7	1.3
Sln1d.8	Slp A1	66.7	13.4	6.0	62.2	52.9	1.2
	Slp B1	55.2	10.2	5.7	63.3	53.1	2.1
	Slp A2	68.1	12.6	7.0	54.5	47.7	13.9
	Slp B2	52.4	10.5	6.4	62.2	50.5	13.2
sln1m	Slp C1	77.9	18.7	6.6	54.7	54.6	0.7
	Slp D1	71.1	10.3	4.2	66.9	60.2	3.4
	Slp C2	74.0	18.0	6.3	77.0	47.6	13
	Slp D2	73.0	13.8	4.9	81.1	58.6	3.7
sln1n	Slp E1	83.3	24.4	6.4	81.2	57.4	2.6
	Slp F1	79.6	22.9	6.1	91.2	66.9	0.6
	Slp E2	86.6	15.7	6.0	70.1	52.7	2.5
	Slp F2	76.1	17.7	6.2	81.7	63.0	3.6
sln1s	Slp G1	80.4	19.3	6.3	66.2	58.1	1.9
	Slp H1	73.6	14.4	4.2	75.6	64.2	2.3
	Slp G2	75.2	12.5	4.3	68.9	50.4	2.1
	Slp H2	73.9	22.4	7.2	77.5	51.6	2.2
sln1o	Slp J1	83.2	22.3	6.7	69.1	55.6	1.4
	Slp K1	81.3	22.2	7.3	83.8	57.8	1.3
	Slp J2	73.8	22.8	7.5	64.9	47.5	11.8
	Slp K2	78.3	22.2	7.9	73.9	52.9	13.7
spy1a	Slp L1	81.1	24.8	8.8	65.5	52.3	1.2
	Slp M1	70.8	16.9	4.9	70.8	62.7	1.1
	Slp L2	75.9	26.1	9.1	65.5	47.0	2.3
	Slp M2	57.9	12.5	5.6	51.8	52.0	2.4

Grain size was improved by overgrowth alleles (Table 3.8) consistent with previous studies. Excluding the *Sln1d.8* allele, there was an average 13% increase in grain size consistent with the observation of larger grains in mutants from the Yanco study. Both hulled and hulless sister-lines performed similarly, with no consistent differences.

Sterility was observed in this experiment, and the percentage increase in sterility varied between and within overgrowth alleles; it was neither allele specific nor related to being hulled or hulless. Inconsistent with the Yanco studies, in this field experiment overgrowth mutants did not show higher sterility compared with the wild types. Although the

library birdcage studies were conducted as a suitable replicate for the Yanco trial, the different temperature and field conditions, and possibly the different sowing time (Yanco in May, library birdcage in September) resulted in inconsistent sterility results between these two studies. These observations suggest that the reduced grain yield at Yanco might be influenced by the high sterility of mutants compared with wild type, but it appeared that there will be less contribution of this factor in different field conditions.

Discussion

Barley overgrowth alleles result from new mutations in the *Sln1*gene, or in one case in the *Spy1* gene, which are both negative regulators of GA signalling. Overgrowth mutants were characterised by enhanced GA signalling that improved growth rate in the early stages of growth. This characteristic was analyzed in detail in the previous Chapter. It also appeared that overgrowth alleles not only improved early growth, but they also caused larger heads and grains; for instance, it was reported by Chandler and Harding (2013) that *sln1m*, an extreme overgrowth allele with the highest growth rate, increased grain size by 40% compared with the dwarf parent. When crossed into a Himalaya background there was an increase in grain size of about 20%. This observation suggested that some overgrowth alleles might be potentially useful in barley breeding by increasing grain size.

Grain size is an important yield component, and it is also an important grain quality trait; therefore breeders have a special consideration of this trait in barley breeding programs. In addition grain size is under strong genetic control which results in a lower level of genotype-by-environment interaction for this trait than for grain yield; therefore in breeding programs selection for larger grains in early generations can be more effective than for grain yield (Tait *et al.* 2013). The importance of larger grains in barley breeding suggests that overgrowth alleles that enhance grain size might be of interest to barley breeders.

In this Chapter the potential for overgrowth alleles to increase grain size, and their effects on final grain yield were studied. Eight overgrowth alleles (*Sln1d.8, sln1m, sln1n, sln1s, sln1o, spy1a, Sln1d.7* and *Sln1d.9*) were backcrossed into a commercial variety (Sloop), to provide a better assessment of their performance in a commercial variety. After three backcrossing generations overgrowth sister-lines were isolated in the BC_3F_2 generation and grains of BC_3F_3 plants were studied in several glasshouse and field experiments. Initially all eight overgrowth alleles were studied, but field studies continued without *Sln1d.7* and *Sln1d.9*. The behavior of these two alleles was not surprising since these are the two weakest overgrowth alleles of those that were backcrossed into Sloop.

A number of independent studies showed that a particular set of overgrowth alleles (*sln1m, sln1n, sln1s, sln1o* and *spy1a*) conferred larger grains in the Sloop genetic background relative to the wild type sister-line. This study confirmed the potential of overgrowth alleles to confer increased grain size when crossed to other varieties. The percentage increase in grain size of overgrowth mutants compared with the relative wild type sister-line is summarized in Table 3.9 for a series of different investigations. These results lead us to three important conclusions. Firstly, grain size was promoted by overgrowth alleles under a wide range of

growth conditions. This indicates that the promotion of grain size was not strongly affected by seasonal and environmental factors. Secondly, the average increase in grain size was very similar for different alleles across different studies, suggesting several options for alleles to use in breeding programs. Thirdly, the two highest values for percentage increase in grain size belonged to grains from the irrigated and rainfed plots (Yanco, 2013) with 40% and 23% increases respectively. What might be responsible for the differences of magnitude across different studies? In these different growth conditions the thousand grain weights for Sloop were 54 g (GH2011), 55 g (LBC2012), 41 g (Yanco rainfed), 34.5 g (Yanco irrigated). These results showed a reduction of grain size in Sloop under true field conditions, which is not surprising. However, in the case of overgrowth sister-lines, their decrease in grain size was less in 'farm' conditions whereas wild type sister-lines had a reduction in grain size similar to Sloop. This means that in relative terms there is a larger increase of overgrowth lines under field conditions. This is a very promising result that shows the strong control of overgrowth alleles in increasing grain size.

Table 3.9. Percentage promotion of grain size (TGW) by selected overgrowth alleles in comparisons between BC3 sister lines in Sloop barley

Overgrowth allele	**GH 2011**	**GH 2012**	**LBC 2013**	**Yanco rainfed 2013**	**Yanco irrigated 2013**	**Average for allele**
sln1m	17	14	16[1]	27	38[1]	**22**
sln1n	17	21	18[1]	29	52[1]	**27**
sln1s	12	20	7[1]	25[1]	33[1]	**19**
sln1o	14	13	11[1]	17[1]	41[1]	**19**
spy1a	13	30	15[1]	17	34[1]	**22**
Average for year	**15**	**20**	**13**	**23**	**40**	

[1]Data are means of independent hulled and hulless comparisons.

The consistent and statistically significant increase observed in thousand grain weight of Sloop overgrowth derivatives at Yanco indicated that overgrowth alleles might also increase grain yield. However, the results showed an average 23% reduction of yield in overgrowth lines compared with their wild type sister-lines in irrigated and rainfed trials.

There are many factors that might have affected grain yield in overgrowth lines. One factor we considered was their higher percentage of sterility. Overgrowth lines showed a

consistently higher number of sterile spikelets per head compared with their wild type sister-lines in the Yanco study, which is clearly one factor in reducing the yield of overgrowth lines. However, an independent field study (library birdcage) did not show the same pattern of sterility as observed at Yanco, although both mutants and wild type sister-lines expressed various degrees of sterility. These observations suggested that expression of sterility is influenced by environmental conditions and timing of sowing, raising the possibility that under favorable field conditions overgrowth lines might show lower sterility; for instance in glasshouse studies there was no expression of sterility in these lines.

Studies on the basis of *Della*-induced sterility in the model species Arabidopsis were conducted in two *Della* loss-of-function mutants (*gai* and *rga*) and in two different ecotypes, *Landsberg erecta* (L*er*) and Colombia (Col-0). These studies showed that DELLA activity was very important in pollen development (Plackett *et al.* 2014). The same study also showed that there are differences between ecotypes that affect their response to GA at floral development stages. It was shown that the *rga gai* double mutant in Col-0 ecotype was completely male sterile, while in contrast the equivalent mutant in L*er* ecotype was less affected. In barley, previous studies on overgrowth alleles (Chandler and Harding 2013) showed no case of sterility in single overgrowth mutants, although double mutant combinations were frequently sterile (see Chapter 2). In the current studies, Sloop overgrowth alleles had different expression of sterility. Therefore, there might be some differences between Himalaya and Sloop in response to GA. However, Himalaya overgrowth alleles were not studied in field conditions, so we do not have equivalent data on their performance. But the importance of differences between varieties suggests that breeders, in addition to environmental conditions, should also consider the genetic background of lines using in overgrowth breeding programs to have better control of sterility.

A detailed study of sister-lines was conducted under pseudo field conditions (library birdcage) to study possible physiological differences that might account for the yield reduction of overgrowth lines. The major differences were (i) reduced biomass, (ii) reduced number of heads per plant. Final grain yield is determined by total biomass production and the proportion of biomass allocated to grains, known as harvest index (HI). It has been reported that there is a significant relationship between grain yield and biomass at anthesis time or during grain filling (Ramos *et al.* 1985). In the case of overgrowth lines, although a lower biomass may still be associated with a higher HI, this reduction would still limit grain yield. This is an area for future work, investigating HI in field conditions. A lower number of heads per plant will also affect grain yield. It was observed in glasshouse experiments that

overgrowth mutants had a tendency for lower head numbers. This reduction was also observed in the library birdcage study. Generally overgrowth mutants had less heads per plant relative to the wild type sister-lines. This also resulted in a reduction of total head weight of overgrowth mutants. These observations showed that lower number of heads per plant is likely to be one of the factors in grain yield reduction. If further investigation shows lower head number per plant in field conditions, sowing at increased densities for field plots might be an approach to increase number of heads per unit area.

The lower grain yield of hulless derivatives compared with the hulled sister-lines is probably due partially to a lower density of plants. Grains were sown at the same density in these plots, but seedling densities of hulless derivatives were often only 25 - 50% of the corresponding hulled lines. We believe this is due to mechanical damage incurred when these grains were originally harvested, because of the exposed embryo in hulless lines. However, at this stage we have no information about head number per unit area in the Yanco plots, and a lower density of plants might have resulted in increased tillering, eventually producing equivalent heads per unit area.

In conclusion, this study showed that overgrowth alleles are able to increase grain size in Sloop barley, which is an important trait in malting barley (as a trait of grain quality) and in feed barley (potentially increased yield). The relative increase in grain size was most marked under ‘farm’ conditions, when Sloop and wild type sister-lines had smaller grains. This is a very important characteristic of overgrowth alleles that farmers may prefer to see in their barley varieties. When environmental conditions are not favorable, overgrowth alleles will still produce larger grains while other lines would suffer from poor conditions, leading to an increase in screenings. Therefore even if overgrowth alleles can be made to be yield ‘neutral’, they are still of interest to breeders if they result in a reduction in screenings.

CHAPTER 4

Wheat overgrowth mutants: characteristics and potential applications in breeding

Introduction

Wheat overgrowth mutants were isolated in a suppressor screen of Maringá *Rht-B1c*,a dwarf variety (Chandler and Harding 2013). Maringá is a Brazilian bread wheat (allo-hexaploid) variety which is tall, and has wild type alleles (*Rht-A1a*, *Rht-B1a* and *Rht-D1a*) at the*Rht-1* locus. These encode DELLA proteins (orthologous to the *Sln1* gene in barley). The principal semi-dwarfing genes of the Green revolution, *Rht-B1b* and *Rht-D1b*, as well as *Rht-B1c* have been introgressed into this background to form a series of near-isogenic lines (BC7;Hoogendoorn *et al.* 1990). The*Rht-B1c*allele has a 2Kb DNA element insertion in the *Rht-B1* gene which is responsible for dwarfism in varieties that carry this allele (Figure 4.1a) (Wu *et al.* 2011; Wen *et al.* 2013).Most of the insertion is spliced from the transcript, but 90bp remains (from the 3' end of the insert, Figure 4.1b) which results in a 30 amino acid in-frame insertion in the RHT-B1C protein (Pearce *et al.* 2011; Wu *et al.* 2011). It was demonstrated in yeast two-hybrid assays that the 30 amino acid insertion prevented DELLA protein interaction with TaGID1 (Pearce *et al.* 2011). Based on the current model of GA-mediated degradation of DELLA, it is probable that the RHT-B1C protein would not be degraded by the 26S proteasome since there is no interaction between RHT-B1C and the GA-GID1 complex.

The 2 Kb insertion in the *Rht-B1c* allele also decreases the expression level of the mRNA about 3-fold relative to the wild type (*Rht-B1a*). The *Rht-B1c* dwarf mutant has wild type *Rht-A1a* and *Rht-D1a* alleles that have equal expression levels to the corresponding alleles of the wild type (Pearce *et al.* 2011). Apart from the 2 Kb insertion, these three genes (*Rht-A1a*, *Rht-B1c*, *Rht-D1a*) are closely related but not identical in sequence. There is about 4% nucleotide sequence divergence and 2% amino acid sequence difference between them.

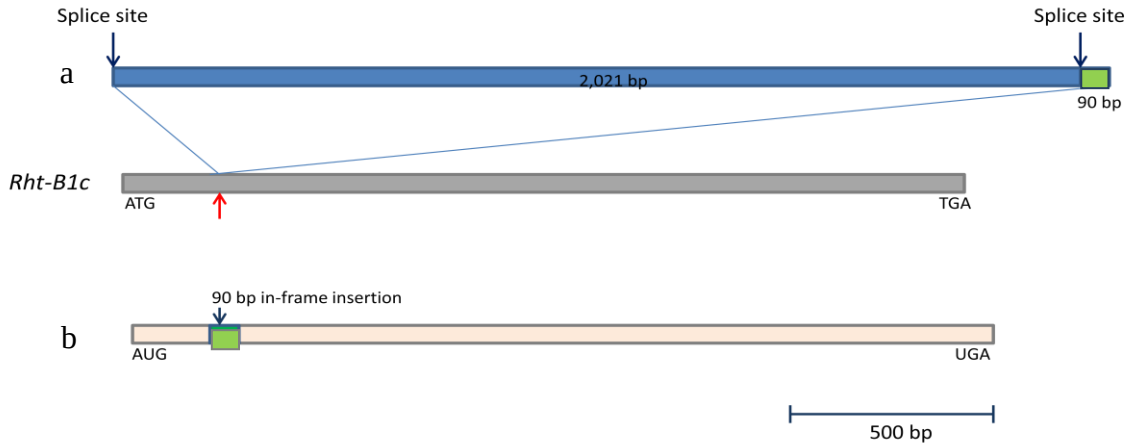

Figure 4.1. Schematic diagram of *Rht-B1c* allele and its mRNA. (a) The grey box shows the *Rht-B1c* allele from the start codon (ATG) to termination (TGA). The blue box shows the 2 Kb insertion in this allele that causes dwarfism in Maringá *Rht-B1c*. The red arrow shows the position where the DNA element was inserted in the *Rht-B1c* allele. (b) The *Rht-B1c* mRNA that contains the 90 bp insertion (shown by green box). Splicing removes most of the 2 Kb insertion and leaves 90 bp from the 3' end of the insertion.

In earlier studies, grains of Maringá *Rht-B1c* were treated with sodium azide, sown in the field, and the M_2 generation i.e.800,000 plants during the early stage of growth and 800,000 plants at maturity were screened for plants that grew faster(Chandler and Harding 2013). Approximately 300 'tall revertant' lines were isolated that had enhanced growth compared with their dwarf siblings. Further characterization of selected plants showed that about half retained the dwarfing gene whereas the other half lacked the gene (putative deletion lines, see Chapter 6). Overgrowth mutants retain the *Rht-B1* gene, and further sequencing studies classified them into 70 independent mutational events that represented 35 unique overgrowth alleles (on average, each allele was isolated in two independent events). All of the new alleles resulted from a second site mutation in the parental *Rht-B1c* allele, and most (20/35) led to single amino acid substitutions in the DELLA protein (Figure 4.2). Of 35 overgrowth alleles, five occurred at the two exon-intron junctions, and were classified as putative splice site alleles (see Chapter 5). The remaining 10 overgrowth alleles were due to early termination codons.

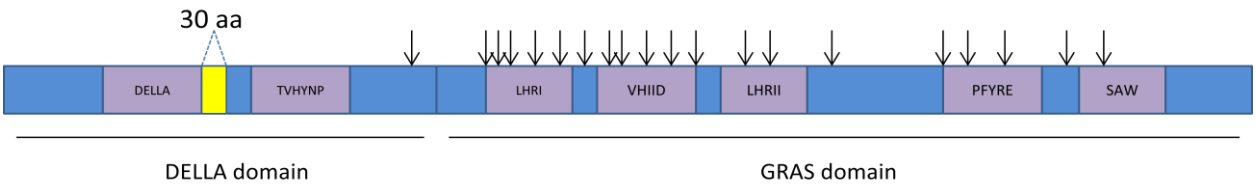

Figure 4.2. Schematic diagram of RHT-B1C protein and sites of amino acid substitutions. Conserved sequence motifs of DELLA proteins are shown in purple boxes, and yellow box shows 30 amino acid insertion in the RHT-B1C protein. Arrows show the single amino acid substitutions that resulted from single nucleotide changes in overgrowth alleles.

These new alleles result in plants with a range of heights, from slightly taller than the dwarf parent (*Rht-B1c*) to as tall as the wild type Maringá (*Rht-B1a*) (Figure 4.3). These changes in height show the critical role of particular amino acid residues in DELLA function. The large number of overgrowth alleles with mutations in the RHT-B1C protein provides interesting material for studies on the mechanism by which DELLA negatively regulates growth, which might be pursued in future work. However, the other interesting application of overgrowth alleles is studying those with semi-dwarf phenotypes for their possible application in wheat breeding studies.

The importance of semi-dwarfing alleles at the *Rht-1* locus is well-known. *Rht-B1b* and *Rht-D1b* semi-dwarfing alleles have been major factors in breeding higher yielding wheat varieties since the Green Revolution (reviewed by (Hedden 2003)). *Rht-B1b* and *Rht-D1b* are characterized by DELLA gain-of-function mutations, and result from premature stop codons in the DELLA domain due to single nucleotide substitutions. It has been suggested that these mutations stop translation, but then reinitiation occurs at a methionine-rich region downstream of the site of the mutation. This results in the production of an N-terminally truncated DELLA protein that cannot interact with the GA-GID1 complex, and so constitutively represses GA signaling (Peng *et al.* 1999; Pearce *et al.* 2011). This GA insensitivity results in reduced leaf and stem elongation, and a semi-dwarf phenotype. There are also some well-known negative traits associated with these alleles such as short coleoptiles and poor early vigor, which is a disadvantage in drier areas leading to a reduction in final yield (Richards 1992). These unfavorable characteristics have led to extensive attempts to characterize and introduce new semi-dwarfing alleles that are potentially useful for all environments.

Figure 4.3. Maringá *Rht-B1c*, *Rht-B1a* and three examples of overgrowth mutants (left to right). Each red arrow shows a different overgrowth mutant that represents a range of height in overgrowth alleles. Figure was borrowed from Chandler and Harding, 2013.

The large number of different overgrowth alleles allows us to select a group of semi-dwarf overgrowth mutants with heights ranging from about 75-90% of the tall Maringá, approximating heights of *Rht-B1b* and *Rht-D1b* isolines (lines beyond this range, either taller or shorter, are of less breeding interest). It is interesting to look at these mutants for traits of potential agronomic value. These studies might result in the characterization of overgrowth alleles potentially useful in wheat breeding.

In this Chapter I have summarized our results of characterizing overgrowth alleles for their effects on final plant height, grain yield, coleoptile length, and grain dormancy. These studies have been carried out jointly by our research team (Peter Chandler, Carol Harding, Shek Hossain and myself).

Materials and Methods

Plant materials

Wheat lines used in these experiments were overgrowth mutant derivatives of *Rht-B1c*. The grains used in the majority of these experiments are M_4 or M_5 generation from the initial isolation in the M_2 generation. In addition, there were also Maringá tall (*Rht-B1a*), dwarf (*Rht-B1c*) and semi-dwarf (*Rht-B1b*) isolines. All lines were provided by Dr Peter M. Chandler (CSIRO Plant Industry, Canberra). A list of the overgrowth alleles is presented in Table 4.1.

Table 4.1. List of wheat overgrowth alleles. In this Chapter we only studied overgrowth alleles that introduced single amino acid substitutions in the RHT-B1C protein.

Rht-B1c **allele**	**Nucleotide[1] substitution**	**Amino acid[1] substitution**		***Rht-B1c*** **allele**	**Nucleotide substitution**	**Amino acid substitution**
Rht-B1a **(tall)**	n.a.[2]	n.a.[2]		***c.17***	C3519T	S528F
Rht-B1b **(semidwarf)**	n.a.[2]	n.a.[2]		***c.18***	G3624A	G563D
Rht-B1c **(dwarf)**	n.a.[2]	n.a.[2]		***c.19***	G3697A	W587ter
c.1	G2715A	G260E		***c.20***	G3874A	W646ter
c.2	G2726A	V264M		***c.21***	G2792A	V286M
c.3	G2747A	A271T		***c.22***	CC2108TA	P58ter
c.4	G2829A	G298D		***c.23***	G3047A	D371N
c.5	G2831A	A299T		***c.24***	G2864A	A310T
c.6	G2849A	A305T		***c.25***	C3071T	Q379ter
c.7	C2865T	A310V		***c.26***	G3671A	E579K
c.8	C2966T	P344S		***c.27***	G148A	Splice
c.9	C2972T	L346F		***c.28***	G148T	Splice
c.10	G3065A	G377R		***c.29***	G147A	Splice
c.11	G3076A	W380ter		***c.30***	G2084A	Splice
c.12	C3117T	P394L		***c.31***	G2335A	W133ter
c.13	G3190A	W418ter		***c.32***	G2083A	Splice
c.14	C2447T	P171S		***c.33***	G3841A	W635ter
c.15	G3477A	R514H		***c.34***	G3290T	E452ter
c.16	C3507T	T524I		***c.35***	C2705T	Q257ter

[1]Coordinates refer to the positions in the *Rht-B1c* coding sequence or RHT-B1C amino acid sequence from Maringá *Rht-B1c*, starting at ATG and ending at TGA. The sequences are under accession no. KC43134.
[2]n.a = not applicable

Plant growth conditions

Plants studied in this Chapter were grown at the Black Mountain CSIRO site or at Yanco Agricultural Experimental station (Yanco, NSW). Growth conditions were similar to the barley studies described in Chapter 3.

Grain yield

Grain yields of overgrowth alleles were determined under 'farm' conditions where grains were sown in 10 m^2 plots in the Yanco Agricultural Experimental station (Yanco, NSW) in May 2013. Each line was assigned randomly in the field either for irrigated or rainfed trials, and grain yield was calculated from total grain weight divided by the plot area (g/m^2) and then values were converted to tonne/hectare.

Coleoptile lengths

Grains of overgrowth mutants were sown in rectangular flats (55 x 28 x 10 cm) containing soil with 25% vermiculite. There were 14 grains for each allele in each experiment. Flats were watered, covered with an inverted empty flat and then black plastic, and incubated in a growth cabinet in the dark with a temperature cycle of 12°C for 12 h and 8°C for 12 h for 20 days. Flats then were transferred to the lab and coleoptile lengths determined. This experiment was carried out 2-4 times for most overgrowth mutants.

Dormancy studies

Grain dormancy was assessed on heads harvested from plants grown in the field at Black Mountain (library birdcage). Heads that had just reached physiological maturity (loss of any green colouration) were harvested and kept in the fume hood for 48 hours for final grain drying. They were threshed by hand and stored in manilla envelopes in a laboratory environment (low humidity, 18-24°C). Dormancy tests were carried out in plastic trays (23 x 23 cm) with 4 layers of 3MM paper and sufficient water to maintain a surface gloss. Each week, one hundred grains of each line were placed in a tray (four lines per tray), embryo up, and trays were covered with lids and incubated at 20°C with constant light (95 µmol/m^2/s). The number of seeds that germinated was determined after 7 days. Dormancy assessment was based on the number of weeks of after-ripening required for grains to show 50% germination under these conditions.

In one experiment germination index was calculated, instead of percent germination. The procedure was the same as described above, but the number of seeds that germinated was determined every day. We used the following formula to calculate the germination index.

$$Germination\ Index = \frac{nG1}{1} + \frac{nG2}{2} + \frac{nG3}{3} + \cdots + \frac{nG7}{7}$$

Where nG1, 2, 3etc. represents the number of grains germinated after 1, 2, 3 etc days.

Table 4.2. Summary of 'birdcage' experiments involving wheat overgrowth allele1

Year	Missense overgrowth lines	Missense alleles represented	Data
2011	150[2]	16	Height, grain dormancy
2012	34	18	Height, grain dormancy
2013	40	20	Height, grain dormancy

[1]Plants were grown as single rows (20 plants at 4 cm spacing, 35 cm between rows) at Black Mountain, Canberra, ACT. Grains were sown in May/June, and harvested in December. Irrigation was applied as necessary.
[2] Includes many lines that were potentially sibs, and which were excluded from later experiments.

Table 4.3. Summary of field experiments involving wheat overgrowth alleles

Site[1]	Year[2]	Crop Growth[3]	Number of 10 m^2 plots (replication)				Data
			Total	Controls[4]	Overgrowth alleles	Missense alleles[5]	
Temora	2012	Dryland	112	6 (x3)	47 (x2)	32 (x2)	Height, yield
Yanco	2012	Irrigated	112	6 (x3)	47 (x2)	32 (x2)	Height
Yanco	2012	Dryland	112	6 (x3)	47 (x2)	32 (x2)	Height
Yanco	2013	Irrigated	108	6 (x3)	45 (x2)	32 (x2)	Height, yield
Yanco	2013	Dryland	108	6 (x3)	45 (x2)	32 (x2)	Height, yield

[1] Temora and Yanco are both located in southern NSW, in cereal production areas.

[2] Grains were sown in May/June, and harvested Nov/Dec.

[3] Limited irrigation was provided if necessary.

[4] Three Maringa isolines (tall, *Rht-B1b, Rht-B1c*), two commercial wheat varieties (EGA Gregory, Janz), and one dwarf barley were sown as controls and checks.

[5] The 32 overgrowth lines represent 18 out of the 20 different alleles that cause single amino acid substitutions in the DELLA protein encoded by *Rht-B1c*.

Results

Twenty overgrowth alleles that resulted in amino acid substitutions of RHT-B1C (new alleles of *Rht-B1*) were characterized for stem length, yield, coleoptile length and grain dormancy.

Stem length

The most obvious effect of overgrowth alleles was on plant height. The stem lengths of overgrowth alleles and Maringá *Rht-B1a*, *Rht-B1b* and *Rht-B1c*isolines are presented in Figure 4.4. Overgrowth alleles showed a range in height from slightly taller than the dwarf parent to as tall as the tall isoline. There is a particular interest in alleles in the range of 75-90% of *Rht-B1a* that might correspond to breeders' interests. Semi-dwarfing alleles including *c.24*, *c.17*, *c.23*, *c.26* are in this range. The heights of overgrowth alleles were obtained from several (5-6) experiments in different seasons under field conditions. There might be some changes in the relative rankings for some overgrowth alleles between seasons, but this is only a minor effect, if genuine. An indication of the variation between means, and the significance of the differences, can be seen in the height data for the Yanco 2013 experiment (Table 4.2).

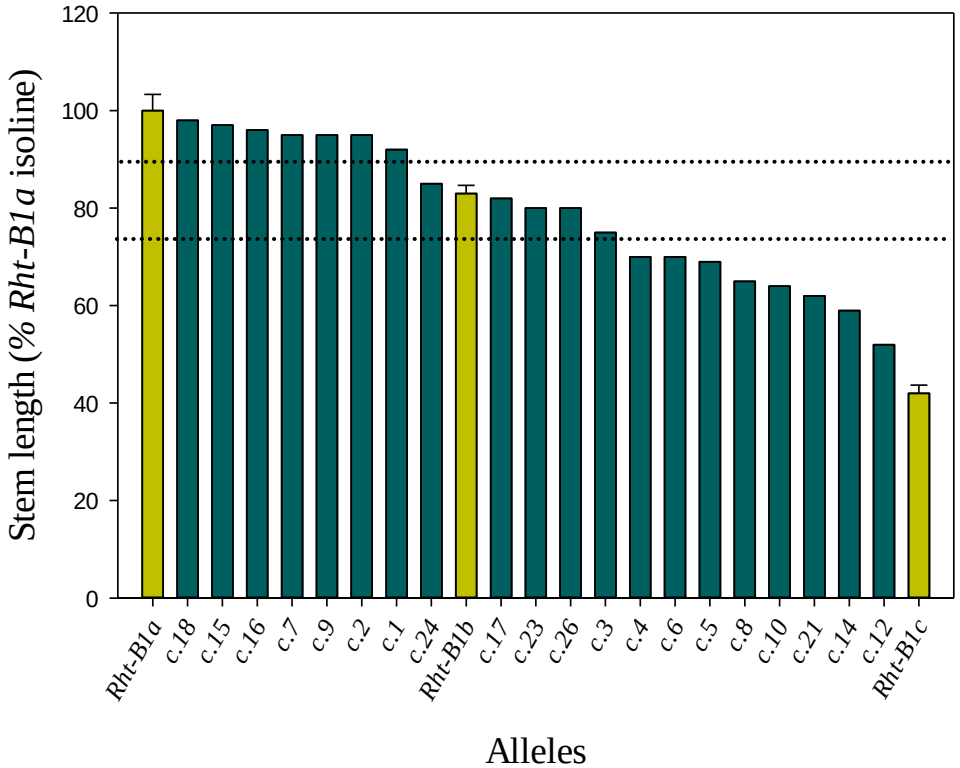

Figure 4.4. Stem lengths of overgrowth alleles in comparison to Maringá dwarf, semi-dwarf and tall isolines. Values are means from 5-6 different experiments in the field from different seasons. The standard error bars shown for the Control isolines are indicative of variation for the overgrowth alleles. Dotted lines indicate 75% and 90% height of the *Rht-B1a*isoline, and alleles with height between these two lines are assigned as semi-dwarfing alleles. In different conditions the stem length of Maringa tall ranges from 105-120 cm.

Grain yield

The results of grain yield studies are shown in Table 4.4. Overgrowth alleles and Maringá isolines were studied under standard field conditions in Yanco (see Materials and Methods). The average grain yield was predicted based on spatial analyses. The results of rainfed plots are also presented as a percentage of the *Rht-B1b* isoline (Figure 4.5).

Table 4.4. Grain yields and canopy heights of overgrowth alleles from the irrigated and rainfed trials (Yanco 2013). Plants were harvested from 10 m^2 plots from irrigated and rainfed trials and total grain weights were obtained. Grain yield per hectare was calculated from grain yield per square meter. Values are averages from replicated plots (n = 2-3). ANOVA showed a significant effect of genotype on both parameters (P< 0.001). The LSD (0.05) values for grain yield were 0.725 and 0.451 tonne/ha (irrigated and rainfed respectively), and the LSD values for stem length were 6.57 and 8.04 cm (irrigated and rainfed)

Allele	**Canopy height (cm)**		**Grain yield (Tonne/ha)**	
	irrigated	**rainfed**	**irrigated**	**rainfed**
Rht-B1a	134	144	3.62	4.01
Rht-B1b	117	120	5.32	4.97
Rht-B1c	61	62	4.14	4.60
c.1	121	133	3.76	3.98
c.2	127	135	3.85	3.68
c.3	105	102	5.11	4.88
c.4	99	94	5.73	4.71
c.5	92	91	4.70	4.70
c.6	92	94	4.26	4.32
c.7	128	132	3.61	3.62
c.8	91	85	4.49	5.16
c.9	124	120	4.93	4.44
c.14	82	78	4.65	4.59
c.15	120	134	2.88	3.81
c.16	126	127	3.06	3.83
c.17	110	107	4.65	4.78
c.18	127	131	4.58	4.06
c.21	87	84	4.67	4.81
c.23	109	108	4.98	4.75
c.24	117	114	4.97	4.76
c.26	106	108	4.53	4.62

Overgrowth alleles showed a wide range in grain yield from 72% to 104% of *Rht-B1b*, which yielded 5.0 tonne/ha (rainfed trial). Generally overgrowth alleles had grain yields less than *Rht-B1b*, the highest yielding control line. Semi-dwarfing alleles (*c.24, c.17, c.23 and c.26*) had an average grain yield 96% of *Rht-B1b*. The *c.23* and *c.24* alleles had consistent grain yields close to *Rht-B1b*, whereas *c.17* and *c.26* were slightly lower and at the borderline of significance. It suggests a comparable grain yield of these lines to the *Rht-B1b* isoline. Overgrowth alleles with stem lengths shorter than *Rht-B1b* generally had higher yields than overgrowth alleles on the taller side (4.8 ± 0.1 for shorter alleles, and 4.0 ± 0.2 for taller alleles).

The result of polynomial regression analysis for rainfed data (Figure 4.6) showed a high correlation ($R^2 = 0.81$) between canopy height and grain yield. The occasional observation of higher yield for some overgrowth alleles including *c.8* and *c.3* (irrigated data) compared with *Rht-B1b* suggests that there is the potential for comparable yields to *Rht-B1b* also for other overgrowth alleles. Most overgrowth alleles had a higher yield than the tall isoline.

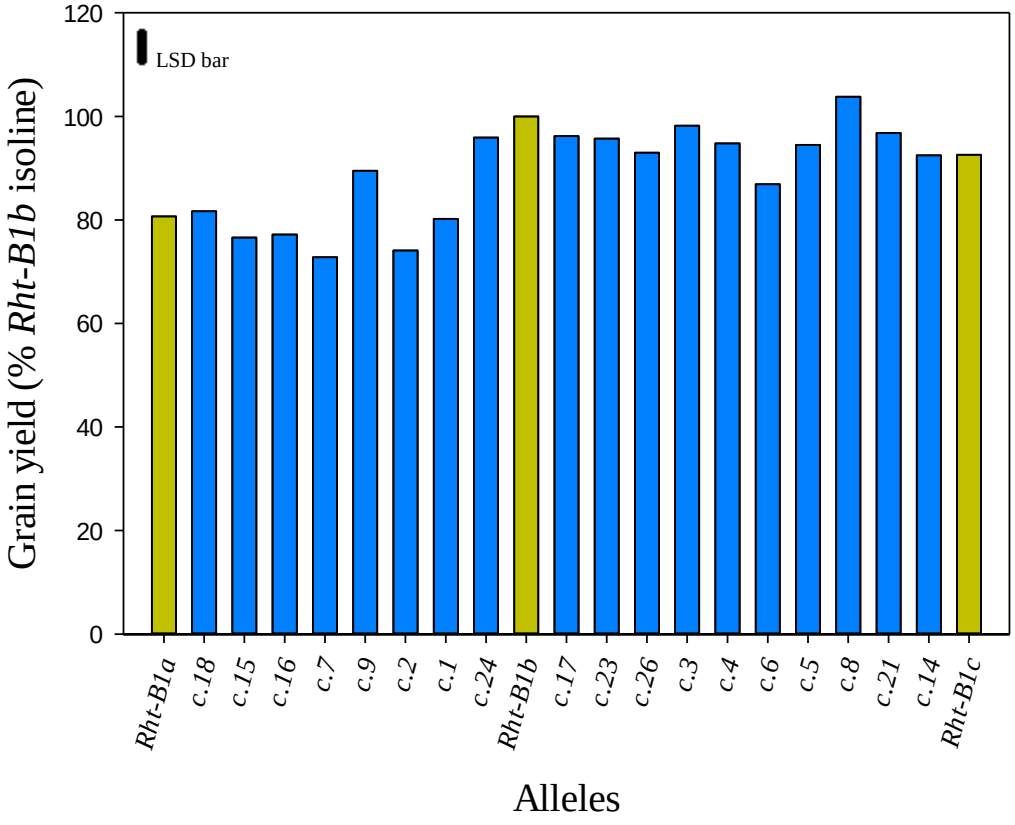

Figure 4.5. Grain yield of overgrowth alleles and Maringá dwarf, semi-dwarf and tall isolines. Grains yield of rainfed trials are presented as percentage of *Rht-B1b*. Overgrowth alleles are in order from tallest stem length to shortest (left to right).

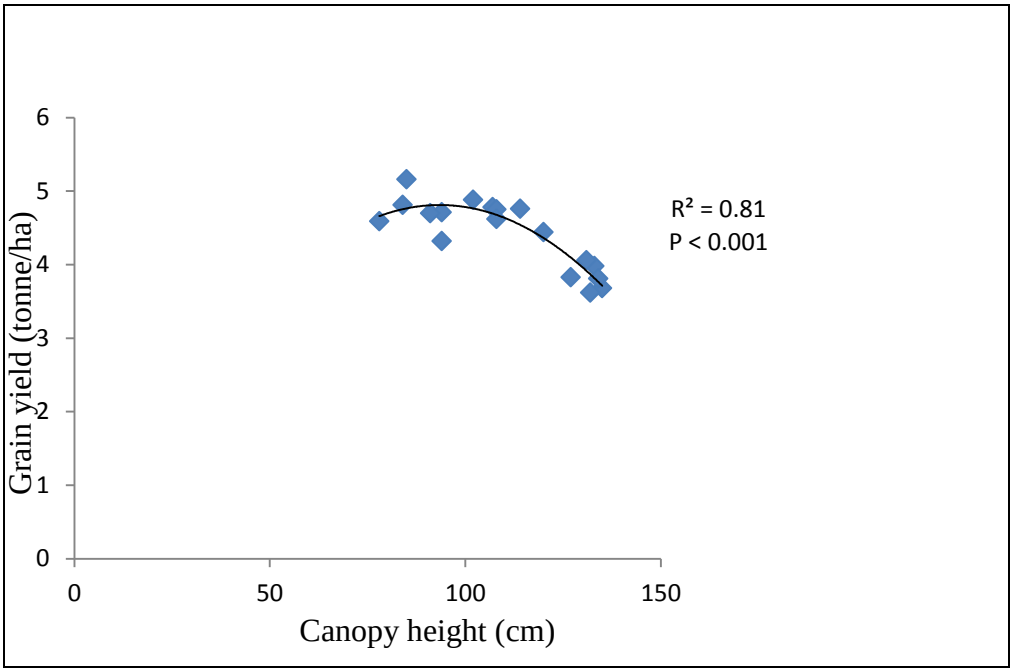

Figure 4.6. Correlation between canopy height and grain yield in rainfed trial. Second order polynomial regression shows the significant correlation between canopy height (independent variable) and grain yield (dependant variable). $R^2 = 0.81$.

Coleoptile length

The effects of overgrowth alleles on coleoptile length were also studied in several experiments and the results are presented in Figure 4.7. Alleles are ordered based on their stem length from tall to short (left to right).

The results showed that overgrowth alleles had coleoptile lengths that range between the dwarf parent and the tall isoline. Tall overgrowth alleles had longer coleoptile lengths than *Rht-B1b*, although the extent varied among different alleles. Short overgrowth alleles mostly had shorter coleoptiles than *Rht-B1b*. Some semi-dwarfing alleles had slightly longer coleoptiles, for instance *c.24*, whereas others were shorter than *Rht-B1b*. The statistical significance of the data and of the correlation between stem length and coleoptile length will be discussed in the Discussion.

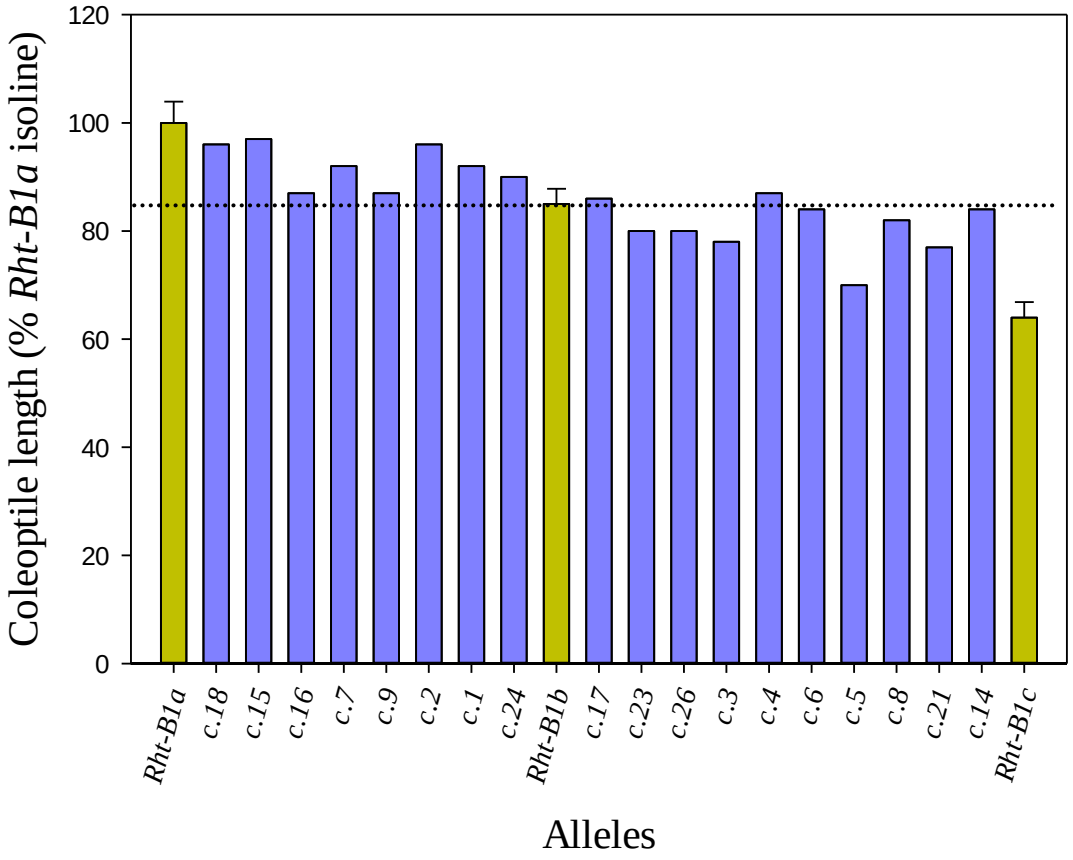

Figure 4.7. Coleoptile lengths of overgrowth alleles and Maringá dwarf, semi-dwarf and tall isolines. Results are presented as percentage of *Rht-B1a*. The standard error bars shown for the control isolines are indicative of variation for the overgrowth alleles. Dotted line indicates percentage coleoptile length for *Rht-B1b* isoline.

Grain dormancy studies

To study the effects of overgrowth alleles on grain dormancy, we took an approach that gave us robust information on germination frequency as well as how this frequency changed as a function of time of after-ripening. Aliquots of 100 grains of each line were tested each week after grain harvest, and dormancy was assessed based on the percentage of germination and the time required for dormancy to be lost.

The summary results of many dormancy experiments are shown in Table 4.5, and later in the Results an example of the data on which the summary is based will be shown (Figure 4.8). These results came from experiments in up to four different growing seasons, depending on how early an allele was first defined. Overgrowth alleles are presented in order from tall to short, and the degree of dormancy is assigned in five categories including low, medium low, medium, medium high and high (Table 4.5). Generally, tall overgrowth alleles had low to

medium low dormancy and the shorter overgrowth alleles had medium to high dormancy. These results showed an overall inverse correlation between grain dormancy and stem length; however, there were some exceptions in this ranking, which will be discussed in the Discussion.

Table 4.5. Grain dormancy of overgrowth alleles. This is a summary result of several experiments in different seasons. Overgrowth alleles are presented in order from tall to short (top to bottom). Degree of dormancy is assigned in five categories, including low, medium low, medium, medium high and high.

Allele	Degree of dormancy
Rht-B1a	low
c.18	medium low
c.15	low
c.16	low
c.7	medium low
c.9	medium low
c.2	low
c.1	low
c.24	medium
Rht-B1b	low
c.17	medium
c.23	medium
c.26	medium
c.3	medium low
c.4	medium
c.6	medium high
c.5	medium
c.8	medium
c.21	medium
c.14	medium
c.12	high
Rht-B1c	high

low

medium low

medium

medium high

high

Figure 4.8 shows an example of the results of a dormancy experiment on eight lines from the 2013 growing season. The data shown are for three semi-dwarfing overgrowth alleles (*c.23*, *c.24* and *c.26*), two other overgrowth alleles including *c.12* (dwarf) and *c.15* (tall), plus the Maringá isolines. Generally, lines with a low initial germination frequency required a longer time of after-ripening to cross the 50% line (indicating 50% germination in a week). They lost dormancy later than lines with a high initial germination frequency. *Rht-B1c*, with high dormancy, took 6 weeks of after-ripening to reach 50% germination in 7 days, whereas both *Rht-B1a* and *Rht-B1b* with very low dormancy already had 50% germination in the first week, and lost all dormancy quickly. Overgrowth alleles showed a wide range in their retention of dormancy. Consistent with the summary results (Table 4.5) c.*12* which is slightly taller than *Rht-B1c* had high dormancy similar to the dwarf parent with 50% germination after 6 weeks, while *c.15*, a tall overgrowth allele had lost about 80% of dormancy in the first two weeks similar to *Rht-B1a* and *Rht-B1b*. Semi-dwarfing alleles including *c.23*, *c.24* and *c.26* had intermediate dormancy between the tall and dwarf parents, and were markedly more dormant than *Rht-B1b*, although they are similar in height.

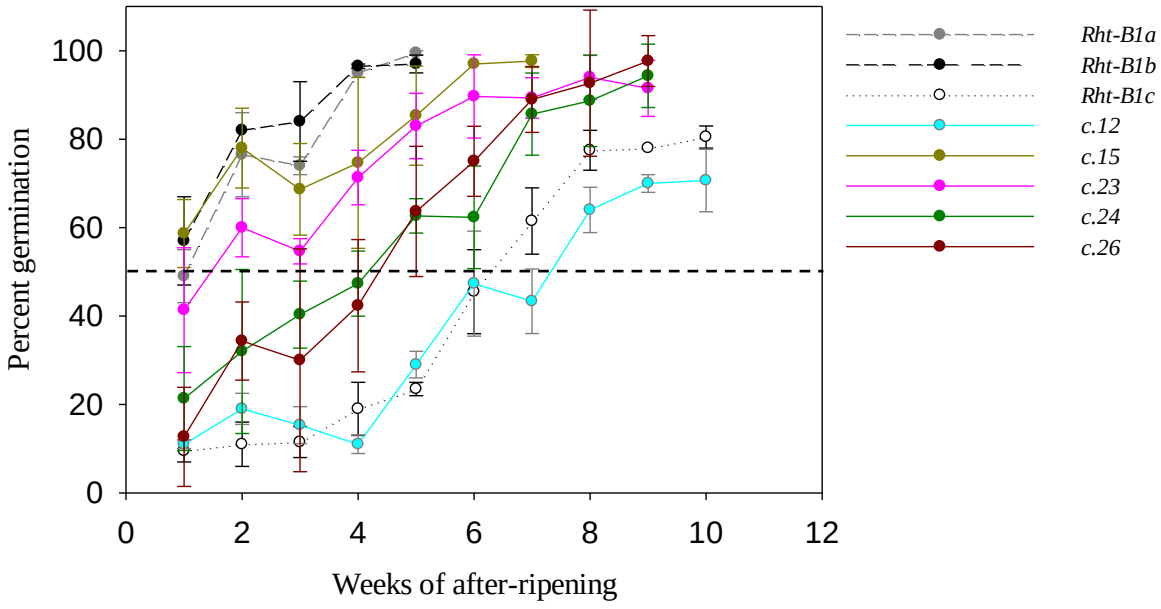

Figure 4.8. Grain dormancy of representative overgrowth alleles and Maringá dwarf, semi-dwarf and tall isolines. Values are means ± SE.

Of particular interest from a breeding perspective are semi-dwarfing alleles that retain dormancy. These might be expected to show a degree of tolerance to pre-harvest sprouting (PHS). To have a better assessment of the levels of resistance to PHS, we need to know not only the frequency of germination but also the rate at which germination occurs, especially during the early stages after imbibition. One approach to study germination rates is to calculate the germination index, which gives a weighted mean of the rate of germination (see Materials and Methods), with the emphasis placed on rapid germination.

Figure 4.9 shows the germination index of the semi-dwarfing overgrowth alleles, including *c.23*, *c.24* and *c.26* that have intermediate dormancy and good semi-dwarfing height. The pattern for germination rate was similar to what was observed in germination frequency (Figure 4.9). Lines that had moderate dormancy also had slower germination in response to available moisture, and lines with low dormancy had faster germination. Generally, semi-dwarfing alleles had moderate to low germination rates compared with *Rht-B1a* and *Rht-B1b*.

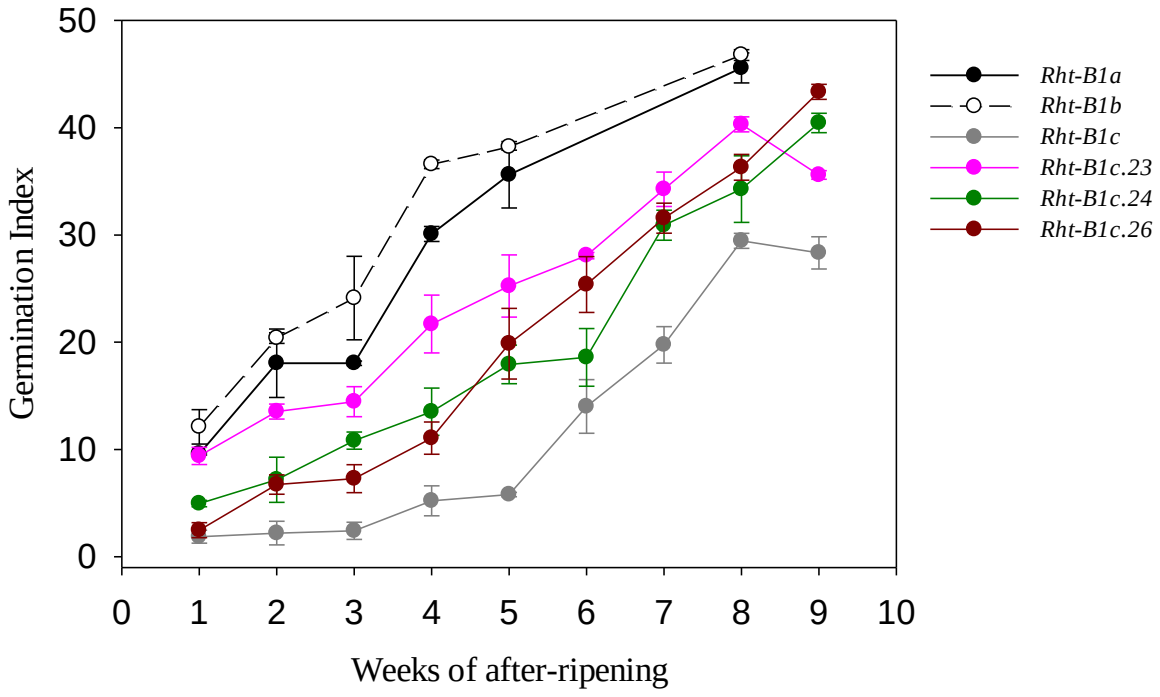

Figure 4.9. Germination index of selected semi-dwarfing alleles and Maringá dwarf, semi-dwarf and tall isolines. Values are means ± SE.

Discussion

Overgrowth mutants of wheat were isolated in a suppressor screen of dwarf Maringá *Rht-B1c*, and carry second site mutations in the *Rht-B1c* allele that are responsible for their enhanced GA signalling (Chandler and Harding 2013). In the overgrowth screen, 150 lines were originally isolated, and sequencing of the *Rht-B1c* gene eventually identified 35 different alleles in these lines. In only 70 cases we can be confident that the mutations are of independent origin, which means that on average there are two independent representatives for each allele. Of these 35 overgrowth alleles 20 result in single amino acid substitution in the RHT-B1C protein, and we have analyzed their effects on some basic traits.

This study started several years ago with more than 300 lines, and gradually the number has been reduced as alleles were identified and independent representative lines chosen. It was necessary to consider the most appropriate methodology to assess traits and handle the large number of mutants. Therefore, as experiments continued, we have conducted measurements over different growing seasons. The repetitive measurements in different seasons provide a robust estimate of traits in different overgrowth lines. Now we are focused on defining traits of particular alleles to be used in scientific investigations (Maringá backcross lines, see below) and in defining which alleles are most attractive for use in breeding.

The major focus of our phenotyping analysis is how to relate observed phenotypes as traits representing specific alleles. We are taking different approaches that allow us to confidently interpret the phenotype as a specific attribute of an allele. Firstly, the current materials are M_4 and M_5 inbred generations from the original M_2 plant. There might be some background mutations in such lines that influence the traits being measured, in addition to the effect of the overgrowth allele. Therefore, overgrowth lines are being back-crossed to the tall isoline that will allow us to eventually generate overgrowth alleles in a 'cleaner' background. Secondly, there is often more than one independent representative for each allele. This provides an internal control for most alleles, and the same behavior of two independent mutants gives us more confidence that it reflects the overgrowth allele, since the background mutations will be different. Thirdly, overgrowth alleles with potential use in breeding are being out-crossed to elite lines. We expect to see allele-specific traits being expressed after out-crossing, subject to any potential effects of the new genetic background.

The detailed phenotyping of overgrowth alleles is an important resource for studying the role of DELLA in GA responses in wheat. Since these alleles result from substitutions of highly conserved amino acid residues in RHT-B1C, these studies should show the importance

of these residues in DELLA activity. It is known from studies in Arabidopsis that the LHR1 motif is involved in interactions of DELLA with PIF4 and PIL5. DELLA interacts with these transcription factors and blocks their transcriptional activity, thereby affecting expression of their target genes, such as genes involved in hypocotyl elongation (de Lucas *et al.* 2008; Feng *et al.* 2008). Mutations in the LHR1 region in overgrowth alleles might also interfere with DELLA interaction with PIF orthologues in cereals. This suggests that mutations in other DELLA regions might also affect DELLA activities, possibly through interactions with other protein partners. These aspects of DELLA function will be discussed in the Final Discussion.

Mutants in the *Rht-1* gene were the basis for the Green Revolution in wheat. Some overgrowth alleles may therefore be potentially useful in wheat breeding; for instance, plant height is an important agronomic trait in wheat breeding, and with many overgrowth alleles there is the possibility that we might find new semi-dwarfing alleles at the *Rht-1* locus. In this study, overgrowth mutants were analyzed for traits such as stem length, yield, coleoptile length and grain dormancy that are potentially useful traits in wheat breeding.

The most obvious effect of overgrowth alleles was on plant height. Several experiments in different seasons showed very consistent results. The results indicated that different overgrowth alleles have specific effects on stem length. These provide robust evidence that different alleles affect GA signalling to different extents. We identified about 10-12 semi-dwarfing alleles potentially useful in breeding. Some were taller than *Rht-B1b*, some had similar height to the semi-dwarf isoline and some were slightly shorter. This range in height might be useful to target specific alleles to specific environments; for instance, shorter semi-dwarf alleles for cool, moist and high-input environments and taller semi-dwarf alleles for warm, dry and low-input environment (Flintham *et al.* 1997; Chandler and Harding 2013).

The grain yields of overgrowth lines were generally promising. The *Rht-B1b* isoline usually had the highest yield (grain yield was studied in two different field seasons, and two different water regimes, irrigated and rainfed trials for most alleles), but the best of the overgrowth alleles were not significantly lower than *Rht-B1b* or in some cases were only slightly lower. Grain yield integrates many aspects of plant performance, and is likely to be subject to effects of background mutations. The better assessment of grain yield will be done on backcrossed overgrowth lines, and when semi-dwarfing alleles are introduced into Australian and international varieties.

The range in height of overgrowth alleles resulted from effects of alleles on stem elongation. It was also interesting to see whether there were equivalent changes in coleoptile

length. Our data from different experiments showed that there is a general correlation between the effects of an overgrowth allele on stem length and its effects on coleoptile length. It was consistent with previous studies by Botwright *et al.* (2001) that were carried out in conditions close to field conditions. Generally, semi-dwarfing alleles had coleoptile lengths similar to that of *Rht-B1b* or in some cases slightly shorter or slightly taller, which might not be statistically significant. Further studies on backcrossed lines will provide more reliable information on coleoptile length in these lines.

The *Rht-B1c* allele confers grain dormancy in wheat (Flintham and Gale 1983), so we have investigated whether overgrowth alleles also confer dormancy. These studies involved screening overgrowth alleles and ranking them for their degree of dormancy. Overgrowth alleles showed a wide range in dormancy; alleles with higher dormancy had a lower initial frequency of germination and needed more after-ripening to lose all dormancy; lower dormancy was associated with a high initial germination frequency reaching to 100% germination in a short time. Experiments carried out in different seasons showed some changes in the absolute numbers of weeks of after-ripening required to reach 50% germination, but the relative ranking of alleles was generally maintained (data not shown).In several independent seasons, *Rht-B1b* never showed better dormancy than the tall isoline. Ranking of overgrowth alleles based on dormancy characteristics also indicated that there was an inverse correlation between dormancy and stem length. Generally, shorter alleles had higher dormancy whereas taller alleles had considerably lower dormancy. Selected semi-dwarfing alleles had a significantly lower germination frequency than *Rht-B1b,* and they needed some weeks after-ripening to lose all their dormancy, unlike the semi-dwarfing isoline. Studies of germination index (an index of speed of germination) also showed that selected semi-dwarfing alleles (*c.23, c.24* and *c.26*) had considerably lower germination rates compared with *Rht-B1b*. These results were consistent between inbred semi-dwarf lines and their equivalent backcrossed lines (already constructed for *c.23, c.24* and *c.26*), which strongly supports the effect of overgrowth alleles on dormancy.

From the breeding perspective, three semi-dwarfing overgrowth alleles (*c.23, c.24* and *c.26*) are potential candidates for use in breeding programs. They had stem lengths very close to *Rht-B1b*, relatively good yields and confer better grain dormancy than the tall or *Rht-B1b* isolines. Their germination index was also favorable, suggesting that these alleles may be useful in wheat breeding for humid areas where pre-harvest sprouting negatively impacts on yield and grain quality.

CHAPTER 5

Wheat overgrowth alleles with potential defects in splicing of the Rht-B1c transcript

Introduction

In our study of wheat overgrowth mutants, six alleles were characterized that are potentially compromised in splicing of the *Rht-B1c* transcript. Most of these mutations occurred at exon-intron junctions which made them candidates for splicing mutations. In wheat the *Rht-1* genes typically lack introns, but the *Rht-B1c* allele (parent of the overgrowth mutants) has a DNA element insertion in the *Rht-B1* gene that changes the gene structure, so that there are two exons and one intron (Figure 5.1). The inserted fragment has a length of 2,026 bp and consists of two conserved 503 bp repeat sequences that flank a 1,015 bp internal domain (Wu *et al.* 2011). Following transcription, most of the insertion is removed by splicing but a 90 bp in-frame insertion remains, located within the region encoding the N-terminal DELLA domain (Pearce *et al.* 2011).

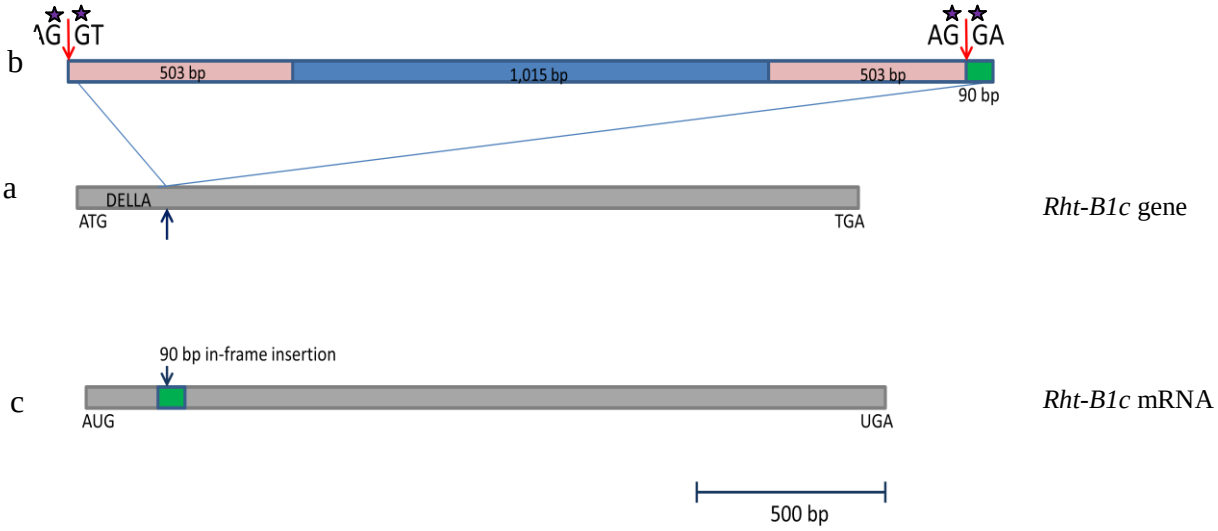

Figure 5.1. Structure of the *Rht-B1c*alelle and its mRNA. (a) The thick grey bar represents the coding sequence with the predicted start codon (ATG) and stop codon (TGA). The blue arrow shows the position (147 bp) where insertion has occurred (close to the DELLA domain). (b) The 2 Kb insert in the *Rht-B1c* allele. Red arrows show the 5' and 3' splicing sites, and stars show the 4 sites where mutations have occurred. The green box represents a 90 bp sequence that remains in the mRNA after splicing. (c) Structure of the fully spliced *Rht-B1c* mRNA. Note that most of the insertion is lost from the transcript, but 90 nucleotides remains in the mRNA.

Five of the six alleles are single nucleotide substitutions in the 5', 3' splicing sites (positions shown by stars in Figure 5.1; see Table 5.1). The one remaining allele is a di-nucleotide substitution within the 90 bp insert that results in an in-frame stop codon, but which also potentially affects splicing, based on predictions made by Exonic Splicing Enhancer (ESE) finder software (http://rulai.cshl.edu/cgi-bin/tools/ESE3). The consensus sequences of both 5' and 3' splicing sites have been determined by calculating the distribution probability of each nucleotide, and are AG|GUA and CAG|GU (GUA refers to the terminal residues of the intron at 5' splice sites and CAG refers to the terminal residues of the intron at the 3' splice site) respectively (White *et al.* 1992; Hebsgaard *et al.* 1996; Wu *et al.* 2012). The terminal G residues of the 5' and 3' ends of introns (shown above in red) play a key role in the splicing reaction; when either G is mutated, splicing to these sites is blocked (Simpson and Filipowicz 1996). It was suggested that although consensus sequences at splicing sites are important for site recognition, the individual nucleotide distribution patterns 50 nucleotides up- and down-stream of the splicing site are also important (Wu *et al.* 2012).

Splicing is a precise process that removes intronic sequences from pre-mRNA and generates an un-interrupted open reading frame (ORF) for translation (reviewed by Singh and Cooper (2012); Staiger and Brown (2013)). This is an essential process for expression of the majority of animal and plant genes. Pre-mRNA splicing machinery is a complex combination of particular sequences known as splicing codes (*cis* elements) and proteins (*trans* factors) that bind to these codes. Most introns contain conserved motifs at the intron-exon junctions that form the 5' and 3' splice sites. Splice sites are the core splicing codes that are recognized by the spliceosome. The spliceosome is composed of five small nuclear ribonucleo protein particles (snRNPs) – U1, U2, U4, U5, and U6 and over 200 additional proteins, and these particles assemble on every intron (Wahl *et al.* 2009; Will and Luehrmann 2011; Reddy *et al.* 2013). After snRNPs assembly, there are two successive transesterification reactions that join the exons (Wahl *et al.* 2009) (Figure 5.2).Other sequences within exons e.g. exonic splicing enhancers or suppressors and within introns e.g. intronic splicing enhancers or suppressors are also important for the correct recognition of exons and splicing.

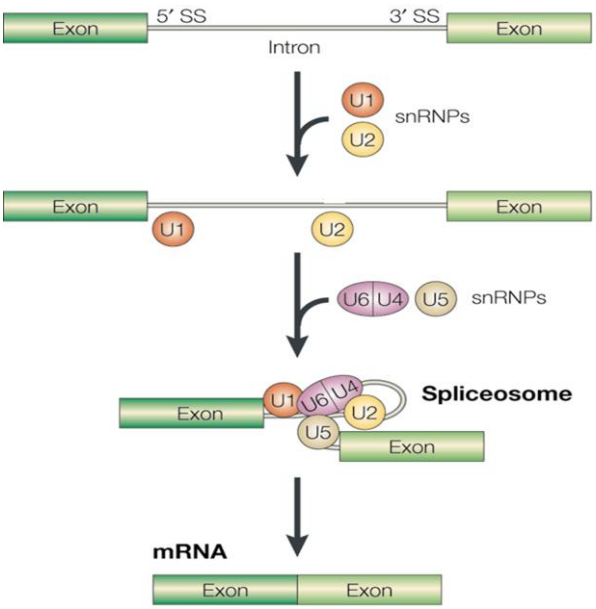

Figure 5.2. Spliceosome assembly and pre-mRNA splicing. The initial step of splice site recognition involves U1 snRNP binding to the 5' splice site (5' SS). U2 binds to the intron and a preformed complex of U4, U5 and U6 snRNPs is recruited to the intron. After major rearrangements the splicing reaction takes place.

Alternative splicing produces a spectrum of natural mRNA isoforms from a single transcript, which generates transcriptome complexity and protein diversity. This diversity gives rise to protein isoforms that have loss- or gain-of-function with altered stability (Stamm *et al.* 2005). Most alternative splicing events can be classified into four main types (Figure 5.3): (i) exon skipping, (ii) alternative 5' splice sites, (iii) alternative 3' splice sites, and (iv) intron retention (Singh and Cooper 2012; Staiger and Brown 2013). In humans the most frequent is exon skipping while alternative 3'and 5' splice sites and intron retention are less common (Kim *et al.* 2008). By contrast, in Arabidopsis and rice intron retention occurs in more than 30% of alternative events, while exon skipping is very rare (< 3%) (Ner-Gaon and Fluhr 2006).

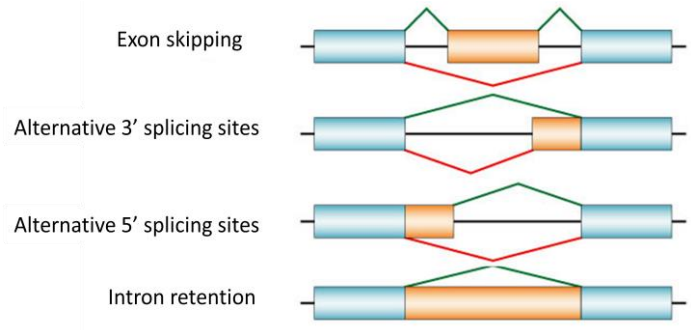

Figure 5.3. Schematic diagrams of the main types of alternative splicing. Exons and introns are shown by boxes and horizontal lines respectively. The green lines indicate the normal splicing pattern, whereas the red lines indicate the splicing pattern caused by mutation.

Around 15% of human genetic diseases are due to mutations that affect splicing (Kornblihtt *et al.* 2013). In plants, mutations in splicing events have played an important role

in varietal and crop selection (Staiger and Brown 2013). For instance, the *Waxy* (*Wx*) gene of rice (*Oryza sativa*) encodes a granule-bound starch synthase that controls grain amylose content. This gene has two exons and one intron, and the mutant form of the gene has a 5' splice site of intron 1. This splice site mutation activates a new splice site in exon 1 and reduces splicing efficiency. As a result there is a lower level of amylose which results in 'sticky' rice (Cai *et al.* 1998; Isshiki *et al.* 1998;Larkin and Park 1999).

Wheat plants that carry putative splice site overgrowth alleles of *Rht-B1c* are typically semi-dwarf in height (76-91% the height of the tall isoline). The prediction is that altered splicing of the *Rht-B1c* mRNA results in less active DELLA protein, that in turn gives rise to a taller plant. To analyze the efficiency of *Della* mRNA splicing in these mutants and the relative levels of the mRNA product, a series of experiments was conducted to assess *Rht-B1c* mRNA in these mutants.

Materials and Methods

Plant materials

Wheat grains used in these experiments were putative splice site mutant derivatives of *Rht-B1c* isolated in the screen for overgrowth mutants (Table 5.1). In addition, there were also tall and dwarf parental lines as described in Chapter 4. All lines were provided by Dr Peter M. Chandler (CSIRO Plant Industry, Canberra). Plants were grown in similar conditions in the glasshouse to those described in Chapter 2.

Table 5.1. List of wheat putative splicing site mutants used in this Chapter

Line	**Allele**	**Mutation***		**Stem length (% of *Rht-1*)**
		Nucleotide	**Amino acid**	
Rht-B1a	*WT* (tall)			100
Rht-B1c	2Kb insert in the WT (dwarf)			42
MV220	*Rht-B1c.22*	CC2108TA	P58ter	84
MV271	*Rht-B1c.27*	G148A		77
MV272	[1]	As for MV271		76
MV273	[1]	As for MV271		77
MV274	[1]	As for MV271		88
MV280	*Rht-B1c.28*	G148T		81
MV290	*Rht-B1c.29*	G147A		83
MV301	*Rht-B1c.30*	G2084A		82
MV302	[2]	As for MV301		86
MV321	*Rht-B1c.32*	G2083A		90
MV322	[3]	As for MV321		91

* Coordinates refer to the positions in the *Rht-B1c* sequence or *RHT-B1c* amino acid sequence in the Maringá genetic background starting at ATG and ending at TGA. The two splice sites are between nucleotides 147 and 148, and between 2083 and 2084. The sequences are under accession no. KC43134.
[1]Independent isolates of the *Rht-B1c.27* allele.
[2]Independent isolate of the *Rht-B1c.30* allele.
[3]Independent isolate of the *Rht-B1c.32* allele.

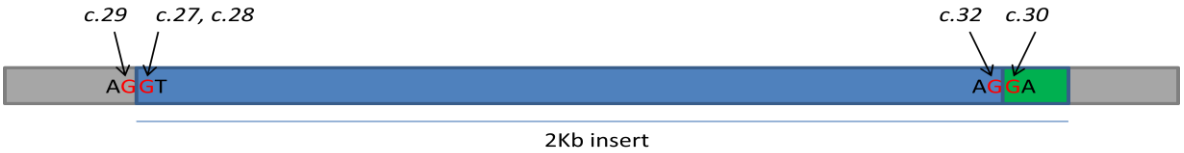

Figure 5.4. Schematic diagram of *Rht-B1c* allele and position of the splice site mutations. Blue box shows the 2Kb insertion in the *Rht-B1c* allele, and the green shows the 90 bp that remains in the mRNA while most of the insert is removed by splicing. AG/GT and AG/GA are *Rht-B1c* allele's 5' and 3'splice sites consensus sequence respectively, and nucleotides in red represent residues that are mutated in splice site alleles. Arrows indicate the residue that is mutated in each splice site allele and the nucleotide substitution is specified in Table 5.1.

RNA extraction

- *Trizol method (RNA for two step RT-PCR)*

  Total RNA was extracted using TRIzol Reagent (Invitrogen, Carlsbad, USA). 50 mg of leaf tissue of 7 day old seedlings was ground into a powder using a mortar and pestle with liquid nitrogen. Powdered material was transferred to a 2 ml tube and 1 ml TRIzol Reagent was added and incubated at room temperature for 5 min. 200 µl chloroform was added, and the sample was vortexed for 15 sec and then incubated at room temperature for 3 min. After centrifugation at 12,000 xg for 15 min at 4°C, the aqueous phase was transferred to a new 2 ml tube. RNA was precipitated by adding 500 ml isopropanol followed by incubation at room temperature for 10 min. The tube was centrifuged at 12,000 x g at 4°C for 10 min, the supernatant was removed and the pellet washed with 1 ml ethanol (75%) and centrifuged at 7,500 x g for 5 min. The pellet was dried in a fume hood and re-suspended in 200 µl RNase free water and stored at -80˚C.

- *RNA extraction for qPCR*

  Total RNA was isolated from leaf tissue of 7 day old seedlings using RNeasy Plant Mini kit (Qiagen). 1 gram tissue was ground in a 1.5 ml tube containing liquid nitrogen using a pestle. RNA extraction was carried out using RNeasy spin column and specific solutions provided by the manufacturer, and following the protocol that was recommended by this company. Extracted RNA was stored at -80°C.

RNA quantification and quality control

RNA concentrations and purity were assessed using the NanoDrop 1000, a 220-750 nm spectrophotometer (Thermo Science, USA). The ratio of the UV absorbance at 260 nm and 280 nm provides an estimate of the purity of RNA.

The quality of RNA was determined using Agilent Technologies 2100 Bioanalyzer (Agilent Technologies, USA). In this technique, there is a chip that accommodates sample wells, gel wells and a well for a size ladder (there was an interconnection between wells through micro-channels). Samples were loaded into wells and channels were filled with a sieving polymer and fluorescent dye. Dye molecules intercalated into RNA strands and the complexes were detected by laser-induced fluorescence. The software automatically compares samples with the ladder and the quality was shown in a graph that indicated 16S chloroplast rRNA and 18S and 28S ribosomal RNA peaks (Figure 5.5).

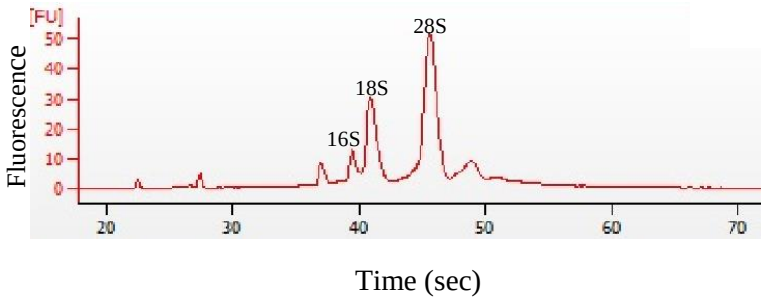

Figure 5.5. RNA quality assessed by Agilent technology. An example of a high-quality total RNA preparation showing distinct peaks for the 18S and 28 S ribosomal RNA.

cDNA synthesis

cDNA was made using the SuperScript III First-Strand Synthesis System (Invitrogen, Carlsbad USA). 2 µg RNA sample was mixed with 1µl (50 ng) random hexamer primers, 1µl of 10 mM dNTP mix, 1µl of mouse liver total RNA (Clontech, a TAKARA BIO Company), and DEPC-treated water to a volume of 10 µl. The mixture was incubated at 65°C for 5 min and snap-cooled on ice. A master mix (10 µl) containing 2 µl of 10x RT buffer, 2 µl of 0.1 M DTT, 1 µl RNAse OUT, 4 µl of 425 mM $MgCl_2$ and 1 µl (200 units) SuperScript III RT was added to each sample, and the reaction was incubated at 25°C for 10 min, 50°C for 50 min and then 85°C for 5 min. Samples were snap-cooled on ice and 1 µl RNAse H was added to each sample and incubated at 37°C for 20 min. Each cDNA sample was diluted with 179 µl nuclease free water and stored at -20°C. The final volume of each cDNA sample was 200 µl and 3 µl was used for downstream qRT-PCR or PCR reactions.

RT-PCR, qPCR and colony PCR primers

Primers used in this chapter are shown in Table 5.2.

Table 5.2. Primers used in RT-PCR, qPCR and colony PCR assays

Primer	**Gene name**	**Sequence (5'→ 3')**	**Reference**
MLR4 F	Cytochrome P_{450} (*Musmusculus*)	ACAGGCAAACCACATCGAACA	Kumala Dewi 2006(PhD thesis)
MLR4 R		GCTACGGTGTCTACCAACCAC	
RHT-D1 F	*Rht-1*	CACTACTACTCCACCATGTTCGATTCTCTG	Pearce *et al*., 2011
RHT-D1 R	As above	GCGGCAGGAGCAGCAGCC	
Rht3F3	*Rht-B1c*	GGCAACTCCACCGGACGC	
Rht3F8	As above	GATAGAGAGGCGAGGTAGGGA	
RH3F16	As above	GAACGAGGAGCCCGAGGTAATC	
Rht3F22	As above	AAGATGATGGTGTCGGGGT	
Rht3F40	As above	GGCAAGCAAAAGCTTGAGATAGAT	
Rht3R2	As above	GCTCTCGACCCAGGAGGAG	
Rht3R3	As above	GGTCGGTGGGGTTGTAGTG	
Rht3R10	As above	CACAACTCCGGCACATTCCTG	
Rht3R15	As above	ACCCCGACACCATCATCTT	
Rht3R73	As above	TAGTGCTAACAAGGTGCGGG	
M13 F		GTAAAACGACGGCCAGT	
M13 R		AACAGCTATGACCATG	

PCR analysis

PCR reactions and analysis were carried out as described in Chapter 3.

For semi-quantitative analysis, the thermo cycler conditions were adjusted to obtain just-saturating product abundance: 95°C for 15, then 5x of 61°C for 45sec, 72°C for 30sec followed by 34x 95°C for 30 sec, 61°C for 30 sec and 72°C for 30 sec with the final step of 72°C for 10 min.

Reverse transcription PCR (RT-PCR)

RT- PCR was performed using the one step RT-PCR kit (Qiagen). Per reaction there were 5 µl of 5x buffer, 1 µl dNTPs, 1 µl of 20 µM forward and reverse primer, 5 µl 5x Q solution, 1 µl enzyme mix, 50ng RNA template and 8 µl milli q H_2O.

Thermal cycle conditions were as follows: 50°C for 30 min, 95°C for 15 min then 5 cycles of 95°C for 1 min, 61°C for 1 min and 72°C for 2 min, followed by 30 cycles of 95°C for 30 sec, 61°C for 30 sec and 72°C for 90 sec, followed by 72°C for 10min. The PCR product of each sample was fractionated on 1% agarose gels as described in Chapter 3, stained with ethidium bromide and photographed.

qRT-PCR analysis

Optimizing of annealing temperature and standard curve

A temperature gradient from 58°C to 69°C was used to determine the appropriate common annealing temperature for all the primers. Dilution factor of cDNA sample was identified for determining the standard curve of every primer. Efficiency of the primers was >99%.

qRT-PCR

The qRT-PCR mixture consisted of 7 µl SsoFast EvaGreen Supermix (Bio-Rad, USA), 1 µl of each 5 µM forward and reverse primer and 3 µl cDNA. There were three biological replicates for each sample, and a no-template control was included in every run. qPCR was done in CFX96 touch ^{TM} Real-Time PCR detection system (Bio-Rad). The thermal cycling conditions for qPCR were as follows: 95°C for 3 min, followed by 39 cycles of 95°C for 10 sec, 61°C for 30 sec. A melt curve was obtained from the product at the end of the amplification by heating from 61°C to 65°C for 5 sec and 95°C for 50 sec. Data obtained through qPCR was analyzed by CFX manager software (Bio-Rad).

For each replicate a comparative quantification was estimated, based on its amplification efficiency (E), and difference between the mean Thermal cycles (C_T) value for the reference gene and for the target gene.

Relative expression = $E^{\Delta C_T}$

Where $\Delta C_T = C_T(\text{reference}) - C_T(\text{target})$

The E value was obtained by generating a standard curve. When the assay has perfect amplification efficiency (>98%) then E=2. For each sample the software generates a graph of relative quantity of the target mRNA relative to reference mRNA.

PCR product cloning

PCR products were purified prior to cloning using Qiagen PCR purification kit. 5 µl of the vacuum-dried purified PCR was cloned into the pGEM-T vector (Promega, USA) using the ligation method. After incubating samples for ligation at 4ºC overnight, transformation was carried out using theJM109 strain of *E.coli* bacterial cells. 50µl of bacterial cells was added and cells were treated with heat and cold to make them competent. After 1.5 hr incubation at 37ºC, competent cells were spread on an LB agar plate containing Amoxicillin, X-gal and IPTG. The plate was incubated at 37ºC overnight and the next day a single white colony was selected and re-streaked on a plate for another overnight incubation at 37ºC. A white colony obtained at this stage was used in the colony PCR.

Colony PCR

Following bacterial transformation and colony purification, individual white colonies were picked using a sterile toothpick and suspended in 50 µl of sterile H_2O and boiled for 10 min. Samples then were centrifuged at 16000 xg for 5 min. PCR was performed using the re-suspended colony as the template DNA. The PCR conditions were as follows (25 µl final volume): 0.25 µl Gotaq (Promega, USA), 5µl of 5x Go Green reaction buffer, 0.5 µl dNTPs, 2.5 µl colony prep, 1 µl of 20 µM forward and reverse primers, 15.75 µl milli q H_2O. Amplification was carried out on a thermal cycler running the following program: 95 ºC for 2 min, then 35 cycles of 95 ºC for 30 sec, 58 ºC for 30 sec, 72 ºC for 90 min, followed by 72 ºC for 10 min.

The PCR product of each sample was fractionated on 1% agarose gels, stained and photographed as described in Chapter 3.

RNA deep-sequencing analysis

RNA samples that passed the quality controls tests successfully were sent to the Australian Genome Research Facility (AGRF) (The Walter and Eliza Hall Institute, VIC). A high throughput technology was used to sequence all the mRNAs captured in the RNA sample. The sequences were from 200bp paired-ends and results were analyzed by a bioinformatics specialist.

Results

Semi-quantitative PCR

The analysis of splice site mutants commenced with semi-quantitative PCR studies. In these studies cDNA was synthesized from the total RNA (extracted from 7 day old seedlings that had reached the maximum leaf elongation rate) and specific primers were used to amplify *Rht-B1* sequences. In total, four regions of the gene were studied including (a) two regions from the 5' end (up-stream and adjacent to the insert), (b) across the insert, and (c) the 3' end of the gene (Figure 5.6). Tall and dwarf parents as well as putative splice site mutants were assessed in this study and the results are shown in Figure 5.6b. Analysis of *Rht-D1* gene expression was carried out as an internal control. *Rht-D1* was amplified in all lines with similar band intensity (Figure 5.6a), indicating equivalence of cDNA concentrations for all samples, and equal expression of *Rht-D1* in all lines.

At the 5' end of the *Rht-B1c* gene we examined two different amplicons. One was just up-stream from the insert and the other was from the extreme 5' region. There was similar amplification (fragments of equal intensity) for the region adjacent to the insert (Figure 5.6 d), whereas the very extreme 5' section showed less intense bands for the dwarf and its derivative mutants compared with the tall parent (Figure 5.6 c). This inconsistency was confirmed with independent PCR studies; therefore we also amplified a 3' end region of the gene as another internal control to have a better estimate of the gene amplification profile (Figure 5.6f). Interestingly, the results showed that all mutants and parents had similar levels of amplification. Therefore, three controls (two internal and one external) had uniform amplification and showed equal representation of the mRNA, while one (extreme 5' region) showed different abundance of mRNA. We concluded that there must be something specific about the extreme 5' region and, at this stage, it is hard to account for these inconsistent observations (Figure 5.6 c) and further work needs to be done.

If these mutants have splice site mutations, it is possible that the insertion region will be most affected and generate different levels of mRNA. Analysis of the cDNAs with primers that flanked the insert showed that tall and dwarf parents both amplified a single fragment (Figure 5.6 e), and the fragment was larger in the dwarf parent. This banding pattern was consistent with a 90 bp insertion in the *Rht-B1* gene of the dwarf line. Mutant lines all had the band corresponding to the *Rht-B1c* mRNA, similar to their dwarf parent, but the banding profile differed in two respects. Some mutants showed smaller bands being amplified, and these will be discussed later in the Results section (page116). Most mutants (all but *c.22*) also

showed an mRNA band that was generally less intense than in the *Rht-B1c* parent, suggesting lower levels of the *Rht-B1* mRNA in these lines. The altered profiles of bands in the insert region were confirmed with independent one step and two-step reverse transcription PCR analysis.

Since we found reductions in the intensity of the mRNA band in some of the splicing mutants, we wanted to investigate whether this corresponds to reduced input cDNA. Therefore, the insert region was also amplified using two times the amount of input cDNA and signal strength was compared with the original amount. The results (Figure 5.6g) indicate that signal strength was affected by the amount of input cDNA in most (top panel of Figure 5.6g) or in about half of the comparisons (bottom panel Figure 5.6g). The results suggest that even a relatively small (2- fold) difference in cDNA abundance can be detected by semi-quantitative PCR, although not in all cases. We tried to get a better estimate of mRNA quantity and gene expression level by turning to qPCR analysis.

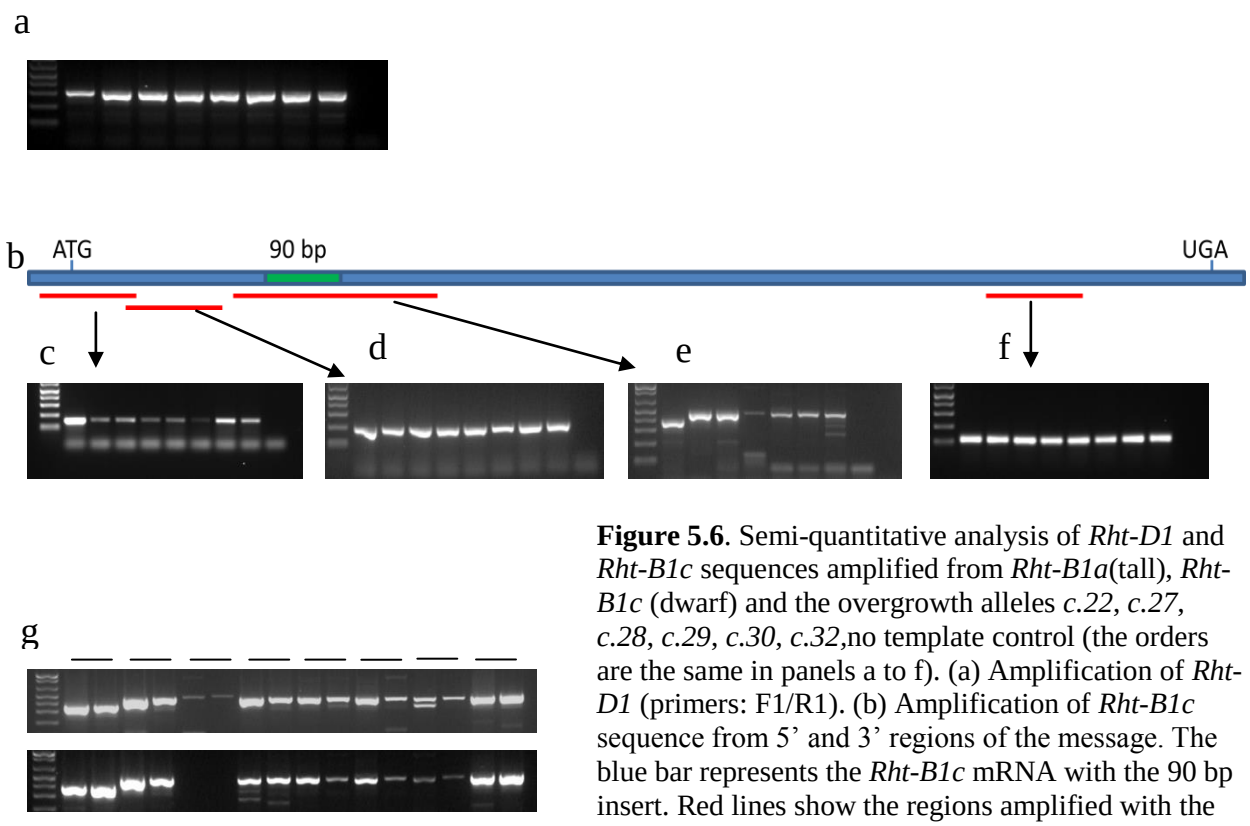

Figure 5.6. Semi-quantitative analysis of *Rht-D1* and *Rht-B1c* sequences amplified from *Rht-B1a*(tall), *Rht-B1c* (dwarf) and the overgrowth alleles *c.22*, *c.27*, *c.28*, *c.29*, *c.30*, *c.32*,no template control (the orders are the same in panels a to f). (a) Amplification of *Rht-D1* (primers: F1/R1). (b) Amplification of *Rht-B1c* sequence from 5' and 3' regions of the message. The blue bar represents the *Rht-B1c* mRNA with the 90 bp insert. Red lines show the regions amplified with the specific primers. (c,d) Amplification from the 5' end of the mRNA (primers: F8/R73, F40/R15 respectively). (e and f) Amplification across the insert and 3' end of the mRNA respectively (primers: F22/R3, F16/R10 respectively). (g) Amplification of mRNA across the insert using two different primer pairs and different amount of input cDNA. Each panel has *Rht-B1a, Rht-B1c, c.27, c.28, c.29, c.30, c.32, c.22* amplified with one specific primer pair, but with 2x and 1x amount of input cDNA. Black lines represent two gel lanes for each line, with 2x and 1x cDNA input respectively.

qPCR analysis

qPCR is a technique that is extensively used to study the expression levels of a gene. In this method the expression level of a gene is measured and normalized to a reference gene, which gives an estimate of the relative quantity of a target transcript. Ideally the reference gene should have constant expression in all tissues, and its expression should not change by any treatments under study. However, finding a suitable reference gene is a challenge in gene expression studies, particularly in systems that have not been extensively characterized; therefore we used an external gene as a reference. Prior to the synthesis of cDNA, total RNA from wheat samples was spiked with a trace amount of mouse liver total RNA. In the qPCR reaction specific primers were used to amplify a *cytochrome P450* gene present in the mouse RNA but absent from wheat RNA. Tissue samples were similar to those used for semi-quantitative PCR experiments.

It was of interest to determine whether splice site mutations in *Rht-B1c* overgrowth derivatives affected the amount of *Rht-B1c* mRNA. We first tried to amplify across the insert since the semi-quantitative results for that section suggested that there were lower amounts of mRNA for some of the mutants compared with the parent (Figure 5.6e). However, multiple attempts to amplify that particular region were unsuccessful, which led us to test the 5' and 3' ends of the mRNA. The results are shown in Figure 5.7. The left panel presents qPCR analysis of the 5' end of the gene and indicates that the abundance of the *Rht-B1c* mRNA was reduced in the dwarf parent and in most mutants compared with *Rht-B1a*. The line *c.22* (di-nucleotide substitution within the 90 bp insert) again behaved differently from the other mutants and had expression levels slightly higher than the tall parent. This amplicon is the same as Figure 5.6c (extreme 5' region) which also showed a lower amount of mRNA for the dwarf and splice alleles compared with the tall; however, there are also inconsistencies between the two experiments which cannot be easily explained.

qPCR analysis of the 3' end of the gene (Figure 5.7b) also showed that *Rht-B1c* had less mRNA (4-fold reduction) compared with*Rht-B1a*. The expression levels of the *Rht-B1c* gene were significantly reduced in all splice site mutants, to a similar extent as in *Rht-B1c.* This region was also studied by semi-quantitative PCR (Figure 5.6f). Again, in this comparison there are differences between the results of semi-quantitative PCR and qPCR which cannot be easily explained.

Although PCR analyses suggest that the amount of *Rht-B1c* mRNA is lower in some splice site mutants, the inconsistencies observed in the PCR results still need to be resolved.

These difficulties in establishing *Rht-B1c* expression levels led us to an alternative approach, investigating the structure of the *Rht-B1c* mRNA.

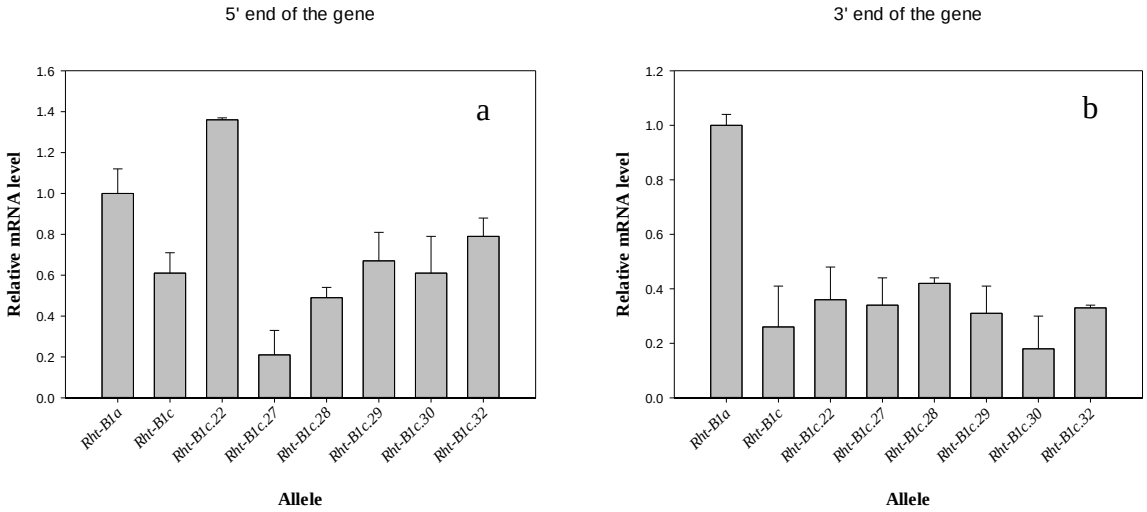

Figure 5.7. mRNA levels for *Rht-B1c* in 7 day old seedlings of *Rht-B1a, Rht-B1c* and splice site alleles, determined by qRT-PCR using genome specific primers. (a and b) relative mRNA levels for the 5' and 3' ends of the gene respectively. Values shown are means of three biological replicates, normalized against a *cytochrome P450* mRNA from mouse. Results are plotted as the ratio to the level in the *Rht-B1a* tall wild type ± SE.

Cloning and sequencing of PCR products

As mentioned above, the amplifications across the insert region (Figure 5.6 e) for splice site alleles suggested that there might be truncated *Rht-B1c* mRNAs. To analyze these mixtures in more detail the PCR products were ligated to a plasmid construct and transformed into bacterial cells. For each cDNA preparation a population containing 20 single colonies was isolated and sequenced. Ideally this number of colonies should contain a few representatives of different mRNA classes. Colony PCR was carried out for each isolated colony followed by sequencing.

In tall and dwarf parents sequencing of the single fragment showed the expected sequence of the *Rht-B1* mRNA, which in the dwarf parent contained the full length 90 bp insert. In the putative splice site mutants there were multiple fragments isolated and sequenced. Generally mRNAs of splice site alleles could be classified into four classes (Figure 5.8): (i) the full length mRNA with the 90 bp insert, (ii) mRNAs with an altered 5' splice site that retained the 90 bp insert, (iii) mRNAs with an altered 3' splice site and a

truncated 90bp insert, (iv) short length mRNAs that lacked both the 90bp insert and variable amounts of flanking sequences.

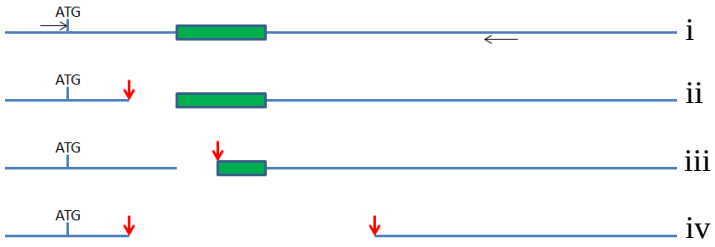

Figure 5.8. Schematic diagram of mRNAs that resulted from altered splicing events. (i) The full length message with the 90 bp insert, (ii) mRNAs with an altered 5' splice site but which retained the 90 bp insert, (iii) mRNAs with a new 3' splice site and a truncated 90bp insert (iv) short length mRNAs that lacked both the 90bp insert and flanking sequences.

Results of the colony PCR showed that most lines had mRNA isoforms that represent different classes (Table 5.3). In *Rht-B1c* the only generated sequence was the full length mRNA that contained the 90 bp insert, which suggests that this is the major functional mRNA in the dwarf parent. A similar type of mRNA (except for the di-nucleotide substitution) was also observed for *c.22*, although Figure 5.6e showed the existence of smaller fragments in this line. It appeared that smaller products of RT-PCR (in *c.22*) were not recovered in cloning and sequencing, perhaps due to the low abundance of those mRNAs.

In contrast to *Rht-B1c* and *c.22*, the rest of the splice site alleles had several representatives of different mRNA classes (Table 5.3). This result showed that full length mRNAs (column i) were poorly represented in splice mutants. However, there was much higher representation of the other classes of mRNAs (columns ii, iii and iv). These results will be described in more detail.

Alleles	Number of colonies for each class of mRNA			
	i	**ii**	**iii**	**iv**
Rht-B1c	18	-	-	-
c.22	16	-	-	-
c.27	4	2	-	10
c.28	5	-	-	12
c.29	5	-	-	14
c.30	6	-	3	9
c.32	4	-	2	10

Table 5.3. Different classes of mRNA obtained from colony PCR and sequencing studies of putative splice site alleles. There were 20 single colonies isolated for each PCR reaction (Figure 5.6e) and each colony was used as input DNA in a colony PCR reaction. PCR products were then prepared for down-stream sequencing. i, ii, iii and iv are different classes of mRNA that correspond to the classes described in Figure 5.6. Note that some colonies in each set of 20 failed to give a clear sequence.

In most cases the altered splicing results in truncated DELLA proteins where the open reading frame (ORF) is preserved. DNA sequences from colony amplification were translated (http://www.ebi.ac.uk/Tools/st/) and the results are presented in Figure 5.9. This figure contains an example of protein isoform sequences that correspond to each mRNA class (Figure 5.8). Shorter forms of DELLA (ii, iii and iv) are proteins truncated either N-terminally or/and C-terminally that retain the original ORF. These proteins might be still active, but probably with some altered features, since they have partially or totally lost some of the DELLA motifs.

There were cases of reading frame change which resulted in a different protein. For instance there was a case (Figure 5.9, last sequence) where the amino acid sequence was identical to the wild type at the beginning, but because the original mutation deleted 7 nucleotides up-stream of the insert, the amino acid sequence totally changed just before the insert towards the C-domain. This protein has an early stop codon that possibly makes it null and inactive. This is in contrast to proteins encoded by mRNAs with a preserved ORF, which might retain DELLA activity.

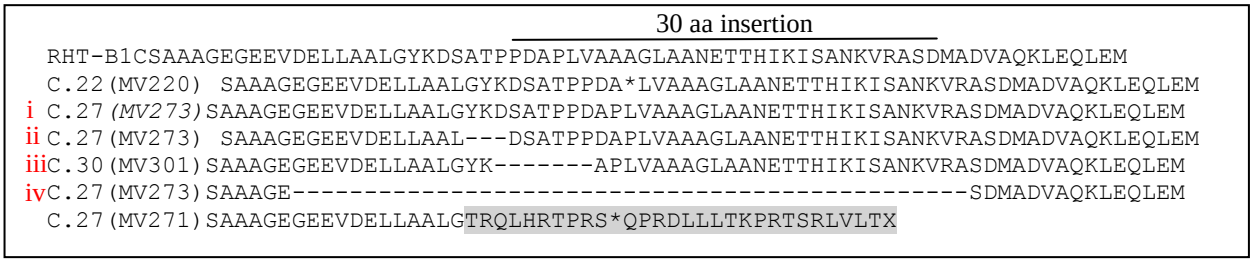

Figure 5.9. Deduced amino acid sequences from altered mRNAs of some splice mutants aligned to RHT-B1C. i, ii, ii and iv are amino acid sequences that correspond to class i, ii, iii, and iv mRNAs. Sequence of the 30 amino acid insertion is shown by a black line. Broken lines indicate absent amino acids, and asterisks shows pre-mature stop codon. The grey box represents a changed reading frame resulting from a 7 nucleotide deletion due to the new 5' splice site obtained from a particular *c.27* mRNA.

Cloning and sequencing provided strong evidence regarding the mRNA isoforms generated as a result of the altered splicing sites in mutants. However, we still do not have any firm evidence of changes in *Rht-B1* gene expression to support the results from cloning and sequencing. We expected to see less *Rht-B1c* expression in mutants compared with the dwarf parent, but PCR showed inconsistent results. Further studies on gene expression were conducted using RNA deep-sequencing high throughput technology.

RNA deep-sequencing (RNA-seq)

RNA-seq is a recently developed approach to transcriptome profiling that uses deep-sequencing technologies. This method allows the entire transcriptome to be surveyed in a very high-throughput and quantitative manner. In this technique a library of cDNA fragments with length of 30-400 bp is generated and a high-throughput sequencing technology is used to sequence each molecule. Short reads from the RNA-seq output then are mapped to the reference genome, and the alignments reveal the structure of the transcriptome. In our application we were interested in transcripts from a single gene, *Rht-B1c.*Although there is high sequence identity with *Rht-A1* and *Rht-D1*, reads from the A- and the D-genome genes were excluded using the known polymorphisms that exist between the three sequences.

Parent lines and all the splicing alleles were studied by RNA-seq technology. The alignments of observed transcripts (number of reads) of parents and splice site alleles to the full length *Rht-B1c* gene (containing the 2Kb insert) are shown in Figure 5.10. The Y axis shows the number of reads and the X axis shows the percentage along the full length Rht-B1c genomic DNA. The 2Kb insert starts at 9% along the gene length and finishes at about 46%

(shown by arrows in Figure 5.10, panel a). The results of comparing the tall and the dwarf parents suggested that *Rht-B1c* had lower abundance of *Rht-B1* mRNA (1891 reads) compared with *Rht-B1a* (6276 reads)(panel a), but significant numbers of reads were only detected in reads from the 3' end of the gene. The number of reads at the insertion region was slightly increased for *Rht-B1c,* relative to *Rht-B1a,* which might be due to one extra copy of the insertion sequence in this line. It is known from Southern blot analysis (data not shown) that there are multiple copies of the insert sequence in the whole genome of Maringá wheat.

Other panels in Figure 5.10 show the results for splice site alleles compared with*Rht-B1c*. Generally all of the mutants had higher levels of reads from within the insertion relative to the dwarf parent. Perhaps this is due to problems with splicing; however, reads from the 3' region of the mRNA were also increased. It is hard to interpret these observations since more reads suggest more mature mRNA and consequently more DELLA, which is unlikely because of the enhanced growth and tall phenotype of splice site alleles.

Higher numbers of reads in the insert region might reflect an increase in transcript number because of splicing difficulties. But a higher number of reads in the 3' end might also indicate more mRNA.

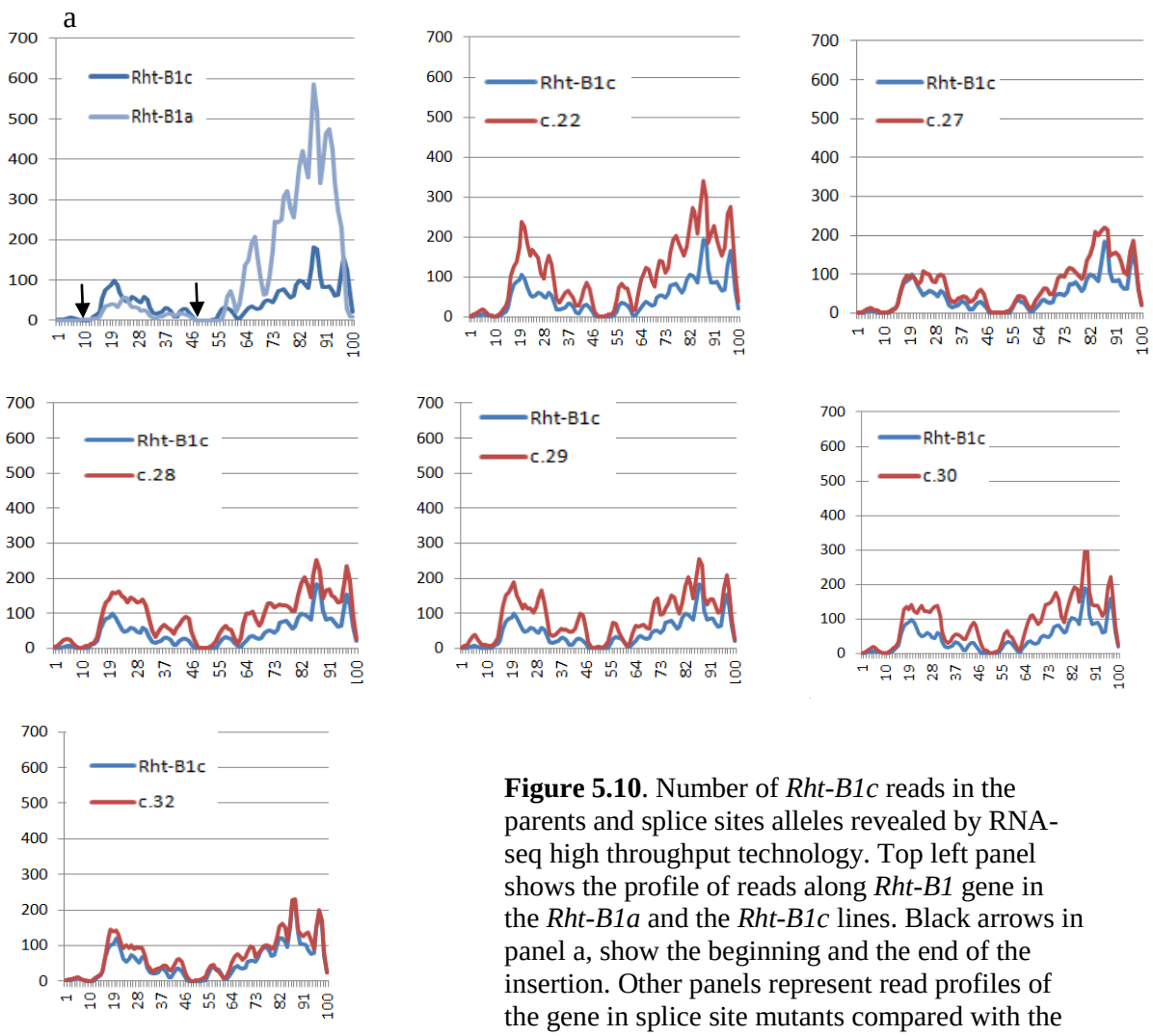

Figure 5.10. Number of *Rht-B1c* reads in the parents and splice sites alleles revealed by RNA-seq high throughput technology. Top left panel shows the profile of reads along *Rht-B1* gene in the *Rht-B1a* and the *Rht-B1c* lines. Black arrows in panel a, show the beginning and the end of the insertion. Other panels represent read profiles of the gene in splice site mutants compared with the dwarf parent.

Discussion

Putative splice site alleles, isolated in the overgrowth mutant screen, have mutations at the exon-intron junction in the *Rht-B1c* gene. *Rht-B1c* has a GT-AG type intron (GT-AG refers to the terminal residues of the intron at the 5' and 3' splice site) featuring conserved intron di-nucleotides; mutation of these nucleotides blocks the splicing event (White *et al.* 1992; Hebsgaard *et al.* 1996;Wu *et al.* 2012). Moreover, it was also shown that the first and second nucleotides of the exon are important in splicing efficiency by stabilizing the spliceosome attachment to exons (Newman and Norman 1992; Newman 1997; O'Keefe and Newman 1998; Moore 2000). *Rht-B1c* putative splice site alleles include mutations in the first nucleotides of either the intron or the exon for both the 5' and 3' splice site, and are expected to influence splicing of the *Rht-B1* transcript. In addition to these mutations, there is a di-nucleotide substitution (conferring a nearly stop codon) in the 90bp insertion that might also influence splicing events.

Rht-B1c is the dwarf parent of the putative splice site alleles and precise splicing of the ~2Kb insert in this line leaves a 90 nucleotide insertion in the mRNA. The semi-dwarf phenotype of the putative splice site alleles suggests that their increased height results either from reduced splicing efficiency of the transcript (leading to less mRNA and less DELLA protein), or from altered growth-regulating activity of the protein products. In this Chapter putative splice site alleles were studied with two aims. The first was to determine if there are changes in *Rht-B1* gene expression in the mutants, and the second was to confirm that splice site mutations do indeed affect *Rht-B1c* splicing, with this possibly accounting for the semi-dwarf phenotype of the mutants.

The expression levels of the *Rht-B1c*gene were studied in mutants and parents. We anticipated lower mRNA levels in splice site alleles compared with the dwarf parent because lower mRNA levels probably mean less DELLA protein (less growth repressor). Moreover, it is known that there is a correlation between the copy number of *Rht-1* semi-dwarfing alleles and dwarf phenotype. For instance two copies of the semi-dwarf allele (*Rht-D1b*) cause more dwarfism in *Rht-D1c* wheat plants (Pearce *et al.* 2011; Li *et al.* 2012). In another case, wheat plants that carry both *Rht-B1b* and *Rht-D1b* semi-dwarfing alleles are very dwarf, with a height close to *Rht-B1c*.

The mRNA of the *Rht-B1c* alleles of parents and mutants was studied using semi-quantitative PCR. The 5' and 3' ends were amplified as control fragments and mostly they amplified as expected with similar amplification from parents and mutants. However, one fragment behaved differently and future research could explore that region, using different

combinations of new primers to account for this unexpected result. Amplification across the insertion indicated less mRNA in most splice site mutants, and also showed some smaller fragments, possibly mRNA isoforms. This latter observation provided evidence of possible new splicing events in putative splice site mutants.

The expression levels of *Rht-B1* gene were also studied by qPCR. Amplicons from 5' and 3' ends of the gene showed a reduction in the dwarf parent relative to the tall isoline. The reduced mRNA levels of the *Rht-B1c* gene was also shown previously by Pearce *et al.* (2011) and Wu *et al.* (2011). Splice site mutants also had low expression levels of the *Rht-B1* gene similar to the dwarf parent. The results from qPCR studies were not in complete agreement with semi-quantitative studies and moreover we were not successful in amplifying across the insert to assess that amplicon with qPCR. Difficulties that we faced in interpreting qPCR data led us to using a different approach, in which a total profile of the transcripts (using the RNA-seq high throughput technique) might provide better information on expression levels of the *Rht-B1* gene.

RNA deep-sequencing provides information on transcripts based on the number of transcript reads and their alignment. Results of RNA-seq analysis showed that the dwarf parent had fewer (lower amount of *Rht-B1*mRNA) reads compared with the tall parent consistent with lower mRNA level of the dwarf parent observed in qPCR. However, the insert region had slightly more reads in the dwarf. This observation fits with the fact that *Rht-B1c* has one extra copy of the insertion. All mutants had more reads in the insertion region compared with*Rht-B1c*. This increase suggests a greater number of un-spliced transcripts in these lines, perhaps due to difficulties in splicing of the insert. RNA-seq results also showed that mutants had slightly more reads in the 3' end compared with the dwarf parent. This result can be interpreted in two different ways; it might reflect more un-spliced transcript due to splicing defects, or it could also reflect more (rather than less) mature mRNA. It was hoped to distinguish between these possibilities by studying the most diagnostic reads i.e. those that extend from the gene sequence through the 90bp insert and then continue with the gene sequence. We expected to see differences in the number of true mRNA reads between the dwarf parent and mutants that could reflect less mature mRNA in the splice site alleles. However, we did not see any cases of this read, even in *Rht-B1c*, so we could not use this approach. The other approach was to study the intron-exon transition point in parent and mutants lines. We expected to detect cases in which the splice point was shifted rather than being the same as *Rht-B1c*. These reads would reflect mRNA molecules that are isoforms of *Rht-B1c* mRNA. However, no cases were detected that clearly indicate an altered transition

point. If more time was available, we could also study *Rht-B1c* gene expression using RNA blot hybridization. If successful, this approach would provide robust evidence of the actual DELLA mRNA levels.

The strongest evidence that showed putative splice mutant alleles do affect splicing of the *Rht-B1c* transcript came from the sequences of sub-cloned fragments amplified in the semi-quantitative PCR studies. These sequences revealed that splice site alleles had different types of *Rht-B1c* mRNA. In all cases they were truncated mRNAs either from the 5' site or/and 3' site presumably due to abnormal splicing of the *Rht-B1c* gene. Further analysis of these aberrant mRNAs showed that they were potentially translated to proteins that were short forms of DELLA; however, there were also rare cases of changes in reading frame which led to a different amino acid sequence, and early stop codons.

Overall, these results are consistent with there being less mature *Rht-B1c* mRNA in splice site mutants, resulting from altered splicing events. Therefore it is likely that the semi-dwarfing phenotype of the splice site mutants is due to less functional mRNA and less DELLA protein. Another possibility is that novel mRNA isoforms might result in DELLA proteins with novel activities. It is known in Arabidopsis that DELLA interactions with partner proteins (transcription factors) such as the PIF family play an important role in hypocotyl growth. It is possible that novel DELLA proteins have lost the ability to interact with other proteins and in turn their growth repressor activity might be affected. However, truncated DELLA proteins might also be unstable, and be degraded more readily. The possibility of less DELLA protein cannot be directly tested since there is no suitable antibody available to measure the amount of the RHT-B1C protein. However, the activities of truncated DELLAs could be tested in a heterologous system- Arabidopsis- since we do not yet know which protein partners interact with wheat DELLA proteins.

CHAPTER 6

Characterization of wheat lines that are putative deletions of Rht-B1c

Introduction

It was mentioned in Chapter 4 that about one half of the taller wheat plants isolated in the dwarf suppressor screen were classified as putative deletion lines. PCR analysis with genome-specific primers suggested that they lacked the *Rht-B1* gene but retained *Rht-D1* (Figure 6.1). In the screen for overgrowth mutants, a new mutation in the *Rht-B1c*generesulted in less growth repression (i.e. taller plants), presumably by reduced activity or amount of DELLA protein(Chapter 4). A tall phenotype might also be conferred if the dwarfing gene was no longer present (i.e. the gene was deleted), removing growth repression by the *Rht-B1c* DELLA protein and allowing plants to grow faster.

Deletions have been previously described in wheat, including one arm of a chromosome or the whole chromosome and some have been extensively studied. Deletion of a whole chromosome is known as aneuploidy (Sears 1954; Sears 1966). Nullisomic-tetrasomic lines are a type of aneuploidy which lacks one chromosome pair for one genome and instead have an extra pair from either of the other two genomes; for instance nulli 4A tetra 4B lacks chromosome 4A and has 4 chromosomes of 4B. Lines with a segmental deletion of a chromosome pair have also been isolated, and these are known as ditelosomic lines, and similar to nullitetra lines they are specific to wheat. Both nullitetra and ditelosomic lines have been widely used to assign genes and molecular markers to individual chromosomes and chromosome arms. Later, following a discovery by Endo (1990), there were reports of the isolation of different size deletions in wheat. He showed that when a certain chromosome from *Aegilops cylindrical* is present in a Chinese Spring wheat background as a monosomic addition, chromosomal breaks occur in the gametes that lack the *Aegilops cylindrical* chromosome, and these generate various chromosome aberrations including deletions. The discovery of gametocidal chromosomes introduced a unique genetic system to produce even more powerful aneuploid stocks very systematically (Endo and Gill 1996). These deletion stocks had various-sized terminal deletions in individual chromosome arms. Adjacent deletion breakpoints for a given chromosome arm define a physical region on that arm called a ‘bin’. A set of lines containing deletions for each of the three genomes and

seven groups of hexaploid wheat chromosomes has been used to create a deletion map of the wheat genome.

The deletion stocks are ideally suited for mapping DNA markers to a specific chromosome region, since any missing marker can be allocated directly to the missing chromosome fragment. They have also been used to map characterized ESTs to specific chromosome regions (deletion bins), allowing construction of a cytologically- based physical map of molecular markers of wheat chromosomes (Endo and Gill 1996; Qi *et al.* 2003). In addition, the sequencing of model plant species such as rice and Brachypodium offers a potentially useful strategy for the development of high-density genetic linkage maps and gene discovery in hexaploid wheat. A gene of interest can be allocated to specific deletion bins and associated ESTs, based on synteny with other grass maps. This led to molecular cloning by comparative and wheat-based positional cloning methods (Qi *et al.* 2003). However, to construct a high resolution map we need greater marker polymorphism (low in wheat), and more characterized ESTs. Moreover, having interstitial deletion lines with deletions not involving the terminal ends of a chromosome could also provide more information of marker positions on chromosomes, which have not been isolated systematically.

If the putative *Rht-B1c* deletion lines in Maringá were genuine deletions of the gene, they would be of considerable interest. If deletions occurred as a simple event, and if they could be related to different markers on chromosome 4BS, then nested deletion lines (that all lack *Rht-B1c*and different extents of flanking DNA) would be useful material to contribute to mapping markers in wheat. In this Chapter, the aim is to confirm deletion of the *Rht-B1* gene, and to make an initial estimate of the size of the deletions.

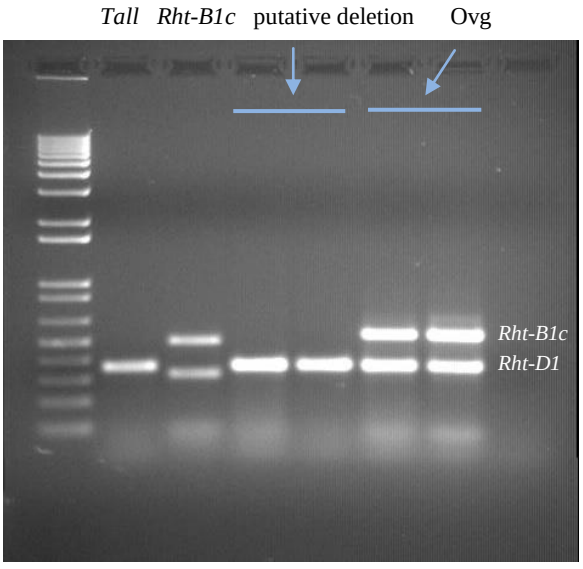

Figure 6.1. DuplexPCR of Maringá tall (*Rht-B1a*), Maringá*Rht-B1c*, two of the putative deletion lines and two of the overgrowth mutants. There is co-amplification of the *Rht-1* gene from the B- and D- genomes. Note that putative deletion lines lack the band corresponding to *Rht-B1c*. Result provided by Carol Harding.

Materials and Methods

Plant materials

The plant material for this experiment consisted of about 150 putative deletion lines isolated in the screen for wheat overgrowth mutants. In addition, there were tall and dwarf parental iso-lines as described earlier, also Maringá overgrowth lines. All lines were provided by Dr Peter M. Chandler (CSIRO Plant Industry, Canberra). Plants were grown in similar conditions to those described in previous Chapters.

DNA extraction for Southern blotting

Leaves from young seedlings were harvested and approximately 1g of leaf tissue (fresh weight) was ground with washed sand and liquid nitrogen using a mortar and pestle. The ground material was transferred to a 50 ml Falcon tube containing 4.1 ml extraction buffer (0.05 M Tris-HCl, 0.3 M EDTA , pH 8.0), 600 µl proteinase K (1 mg/ml) and 300 µl 10% SDS and incubated for 3 h at 37°C. 1 g sodium perchlorate monohydrate was added to each sample which was then centrifuged for 30 min at 4°C (5000xg). The supernatant was poured carefully into a 15 ml Falcon tube, and 9 ml ethanol sodium perchlorate ($CINaO_4$, 100% ethanol and milli q H_2O) was added to precipitate DNA, which was transferred using a long sealed glass pipette to a 1.5 ml tube containing 500 µl TE. DNA was allowed to re-suspend by incubating the sample at 4°C overnight on a shaker. The next day, 600 µl phenol: chloroform: isoamyl alcohol (25:24:1) was added to the sample which was then incubated at 4°C overnight on a shaker. Samples were centrifuged for 30 min at 16000 x g, and the aqueous phase transferred to a new 1.5 ml tube. 20 µl RNAse (1mg/ml) was added and tubes were incubated at 37°C for 1 h. 600 µl phenol: chloroform: isoamyl alcohol was added to each sample, incubated on a shaker at 4°C for 1h then centrifuged for 30 min at 16000 x g. The aqueous phase was transferred to a new 1.5 ml tube, one-tenth volume 2M of sodium acetate (pH 5.5) and two volumes of absolute ethanol were added, and then tubes were centrifuged for 2 min (at 16000 x g) to pellet the DNA. The supernatant was decanted; the pellet washed with 1 ml 70% ethanol and centrifuged for 10 min (16000 x g), DNA pellet air dried for 10 min in the fume hood. 200 µl TE was added to each sample and the tubes were incubated at 4°C for a week to re-suspend the DNA.

DNA digestion and Southern blotting

Genomic DNA was digested using restriction enzymes that do not cut the *Rht-1* coding regions from the A, B and D genomes. Each (20 µl) digestion contained 15 µg DNA, 2 µl NEBuffer 4, 2 µl NdeI (20,000 U / ml, NEW ENGLAND BioLabs Inc) and 1 µl milli q H_2O. Samples were incubated at 37°C for 3-5 h. Digested DNA was size-fractionated on 1% agarose gels made from 1 x TAE [20 mMTris pH 7.5, 10 mM acetic acid, 0.5 mM Na_2EDTA, 0.4 M NaAc] overnight at 50 mA and 40 V. The gel was stained with ethidium bromide and photographed. DNA was blotted to Hybond N^+ filter (Amersham Hybond-N^+, GE Healthcare, UK) using the capillary transfer method in 20 x SSC transfer buffer. Following overnight transfer, DNA on the air-dry filter was cross-linked using UV irradiation (Bio-Rad GS Gene linker, CA). Pre-hybridization was carried out using pre-hybridization solution (milli q H_2O, 20 X SSC, 1 M Tris, 0.5 M EDTA, 100 X Denhardts, 10% SDS) and the filter was incubated in a rotary oven at 65°C overnight. Denatured ^{32}P-labeled DNA probe was added to the hybridization solution (milli q H_2O, 50% dextran sulfate, 20 X SSC, 1M Tris, 0.5 M EDTA, 100 X Denhardts, 10 % SDS) and hybridization carried out in the rotary oven overnight at 65°C. The filter was washed once in 2 x SSC and once in 1 x SSC containing 0.1% SDS for 20 min at 65°C. The filter was then exposed to X-ray film at -80°C with an intensifying screen for visualization of radioactivity.

DNA probe

The DNA probe for Southern blot hybridization was prepared using the Amersham Megaprime DNA Labeling System (GE Healthcare, UK). A mixture of random sequence hexanucleotides was used to prime DNA synthesis on denatured template DNA (designed from the 3' un-translated region of the *Rht-B1* gene) at numerous sites along its length. The primer-template complex is a substrate for the 'Klenow' fragment of DNA polymerase I. By adding α-P32-dCTP a radiolabeled nucleotide was substituted for the non-radioactive equivalent and newly synthesized DNA formed a radioactive hybridization 'probe'. The priming reaction contained 1.5 µl template DNA, 5 µl primers, 28 µl milli q H_2O, and after denaturing DNA for 5 min, radiolabeling mixture was added containing 10µl labeling buffer, 2 µl Klenow, 4 µl α-P32-dCTP, and the mixture incubated at 37°C for 1h.

SNP chip analysis

DNA samples of all deletion lines (50 ng / µl) were sent to a commercial provider (Department of Primary Industries of Victoria) to be analyzed using the 9K and 90K wheat SNP chip arrays.

Cytogenetic analysis

Grains of selected deletion lines were sent to Dr. Peng Zhang (Plant Breeding Institute, University of Sydney, NSW Australia) to be assessed by FISH and other cytogenetic techniques.

Results

Southern blot analysis to confirm the deletion of Rht-B1c

To confirm the deletion of the *Rht-B1* gene we conducted Southern blot analysis. This is a powerful technique to analyze individual gene sequences in the whole genome. The NdeI restriction enzyme was chosen to digest the genomic DNA, since it does not cut the three *Rht-1*genes. Presumably a probe designed from the*Rht-1* gene will detect all three genomes. To construct the probe, an amplicon was designed from the 3' un-translated region (UTR) of the *Rht-B1* gene. UTRs are less conserved sequences of the gene and a probe constructed from the *Rht-B1* UTR might show preferential hybridization to the B- genome gene, but still detect the A- and D- genome genes. Figure 6.2a presents the blot analysis of the parents, Maringá tall (*Rht-B1a*) and Maringá*Rht-B1c*, and shows the organization of the *Rht-1* genes with three bands that presumably correspond to the A-, B- and D- genome genes. The *Rht-B1* gene was identified by comparing the banding pattern of the *Rht-B1a* with the *Rht-B1c* sample; a 7.5 Kb band of the tall line corresponds to a 9.5 Kb band in the dwarf. This increase in size of *Rht-B1* in the dwarf line is consistent with a 2 Kb insertion (lacking an NdeI site) into the B-genome *Della* gene that gives rise to the *Rht-B1c* allele (Wu *et al.* 2011).To identify *Rht-A1* and *Rht-D1* bands, nulli-tetrasomic lines were used including nulli4A tetra 4B and nulli4D tetra4B (these lines lacked chromosome 4A and 4D respectively, and instead had an extra 4B chromosome). Southern hybridization of nulli-tetrasomic lines with the same probe assigned the 11kb band to the *Rht-A1* gene and the 8 Kb band to *Rht-D1*gene (data not shown). Next, DNA of all the putative deletion lines was hybridized with the same probe, and representative examples are shown in Figure 6.2b.Deletion lines lacked the middle band (9.5 Kb) corresponding to *Rht-B1,* whereas the A- and D- genome bands (11 Kb and 8 Kb respectively) were retained. Of 150 putative deletion lines, 130 lines were confirmed as deletions for *Rht-B1*. Several overgrowth mutants were also tested by Southern blots and, as expected, all had a similar banding profile to *Rht-B1c* (they retain the original dwarfing gene and only have one extra new point mutation in the *Rht-B1* gene).

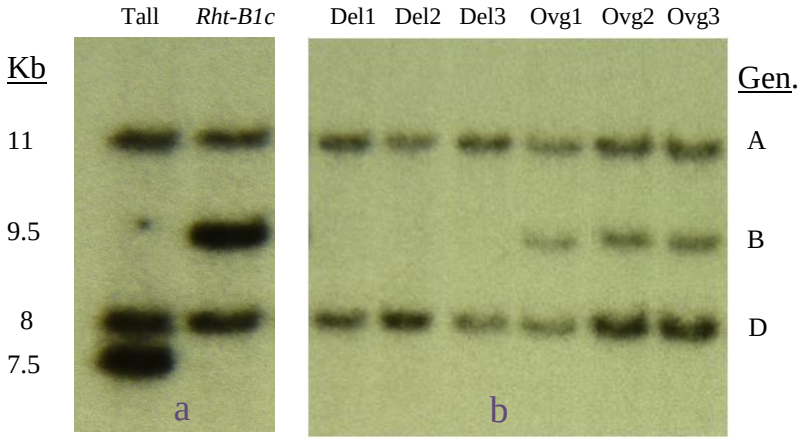

Figure 6.2. Southern blot hybridization of NdeI-digested DNA with a probe derived from the 3' un-translated region of the *Rht-B1* gene. Length of fragments (Kb) and genome assignments (Gen) are indicated. (a) Banding pattern of Maringa tall and Maringa *Rht-B1c,* (b) banding pattern of three deletion lines and three overgrowth mutants (that retain the dwarfing gene). Overgrowth mutants have a pattern similar to *Rht-B1c* (dwarf parent) and deletion lines lack the middle band corresponding to the B genome *Della* gene.

SNP chip analysis

After confirming deletion of the *Rht-B1* gene in many lines by Southern blot analysis, the next step was to define the size of the deletion. The first evidence for possible differences in the size of deletions came from phenotypic observations. Deletion lines generally had stem lengths that ranged from 85 to 100 cm (slightly shorter than Maringá tall, stem length = 110 cm). Most deletion lines were of normal appearance, but some had a very distinctive morphology with narrow leaves, a narrow stem and very poor grain set (Figure 6.3). The different phenotypes suggested two types of deletion: (i) lines with a small deletion and normal morphology, (ii) lines with large deletions which caused abnormal phenotype. To determine the size of the deletion we used a SNP chip array, a newly developed technology that used gene-associated single nucleotide polymorphisms (SNP) derived from world-wide samples of hexaploid wheat, and basically detects variation at many markers of the wheat genome(Cavanagh *et al.* 2013).

How can the SNP chip arrays be used to detect deleted markers in deletion lines? We were interested to assess the size of the deletion ideally by having patterns of markers (present or absent) based on genes around *Rht-B1c*.The SNP chip detects polymorphism through the

signals that each allele generates and the signal is generally detected from all three homeologous genes (i.e. the markers are generally not genome specific). In deletion lines we expect signals from all three genomes unless the deletion removes one of the three genomes. Therefore, the presence versus absence of markers can be calculated based on the change in signal strength for each (dose response) in a deletion line compared with the signal strength in the euploid (*Rht-B1c*).

DNA samples of *Rht-B1c* and of deletion lines were sent to DPI in Victoria (Materials and Methods) and assessed using the 9K SNP chip that was available at that time (9K SNP chip assigns 9000 markers to the whole genome). The results (not shown) were promising and showed that all deletion lines lacked markers close to *Rht-B1c* (on the basis of synteny with rice and Brachypodium). In addition, the patterns of deleted markers showed differences between lines. This initial result provided evidence at the molecular level for different sized deletions.

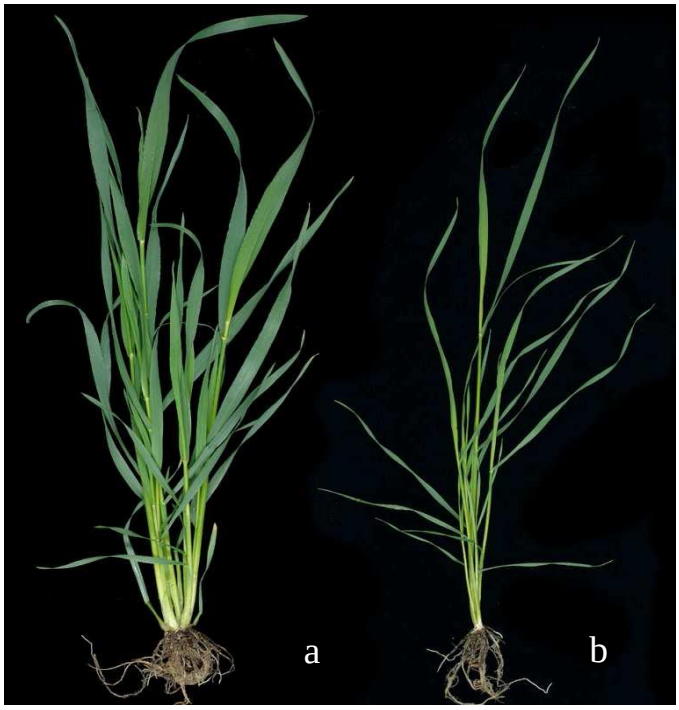

Figure 6.3. Representative wheat plants of overgrowth mutants (a) and lines with large deletion, (b).

When the 90K SNP chip became available, DNA of 60 deletion lines was sent to DPI for more detailed analysis. The 90K SNP chip assigns a total of 90,000 markers to the whole

wheat genome, and in particular 3400 markers are assigned to group 4 chromosomes. The order of these markers on chromosome 4 is unknown, but the wheat 4B genome zipper provides a notional order based on genetic mapping studies and on synteny with regions of the rice and Brachypodium genome sequences. Since wheat genome analysis is still in progress, the order of genes is likely to undergo further change. However, based on synteny, we can use particular regions of rice or Brachypodium to provide more robust information of marker order on wheat group 4 chromosomes. The results of 90K SNP array analysis are shown in Figure 6.4 and these provide insight into deletion events. In this Figure markers are presented in order from the top of the short arm of chromosome 4 (4BS) to the centromere based on the wheat 4B genome zipper and synteny with Brachypodium chromosomes 1 and 4. There was generally very good synteny for 4BS markers with Brachypodium 1g and 4g. However, there was a poor conservation of order in the distal half of the long arm (4BL) with chromosome 1 of Brachypodium. In the 'wheat markers' column of Figure 6.4 the region highlighted in red shows the position of *Rht-B1c* on chromosome 4BS. Green and blue colours show the presence and absence of markers respectively, whereas the white colour shows unassigned markers.

Markers closest to *Rht-B1c* were absent in all deletion lines, which confirms the results of Southern blot analysis and of the 9K SNP chip. All deletion lines also lacked markers on either side of *Della,* and the extent varied between lines. There were deletion lines that lacked all markers on the small arm, and others that lacked not only 4BS makers, but also all 4BL markers. Based on these observations, deletion lines were classified in three groups; (I) interstitial deletions of 4BS, ranging from small to large deletions (12 independent lines), (II) lines that have lost all 4BS markers, but retain 4BL markers (5 independent lines), (III) lines that have lost all 4BS and all 4BL markers (5 independent lines).

In terms of plant phenotypes, group I and group II were of normal morphology, including growth and head characteristics, while group III (which lacked the whole of 4B) had an abnormal phenotype noted previously (Figure 6.3) with a high number of sterile spikes (Figure 6.5), and significantly narrower peduncles compared with Maringá tall (Figure 6.6).

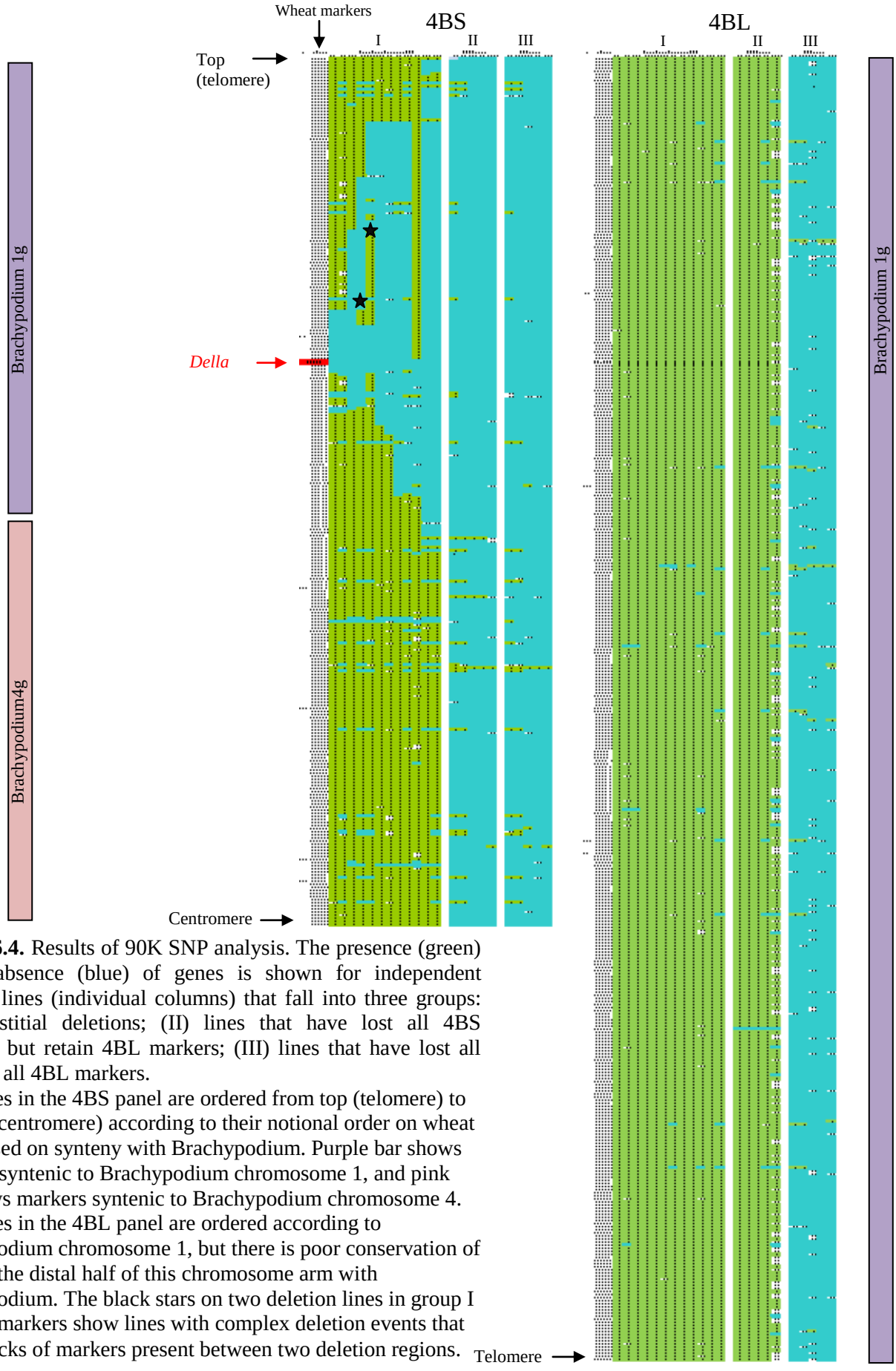

Figure 6.4. Results of 90K SNP analysis. The presence (green) or the absence (blue) of genes is shown for independent deletion lines (individual columns) that fall into three groups: (I) interstitial deletions; (II) lines that have lost all 4BS markers, but retain 4BL markers; (III) lines that have lost all 4BS and all 4BL markers.
The genes in the 4BS panel are ordered from top (telomere) to bottom (centromere) according to their notional order on wheat 4BS, based on synteny with Brachypodium. Purple bar shows markers syntenic to Brachypodium chromosome 1, and pink bar shows markers syntenic to Brachypodium chromosome 4. The genes in the 4BL panel are ordered according to Brachypodium chromosome 1, but there is poor conservation of order in the distal half of this chromosome arm with Brachypodium. The black stars on two deletion lines in group I for 4BS markers show lines with complex deletion events that have blocks of markers present between two deletion regions.

Figure 6.5. Representative heads of a 4BS deletion line (a, normal morphology), and of a 4B deletion line (b, abnormal morphology). Note poor grain set and deformed awns in 4B deletion line.

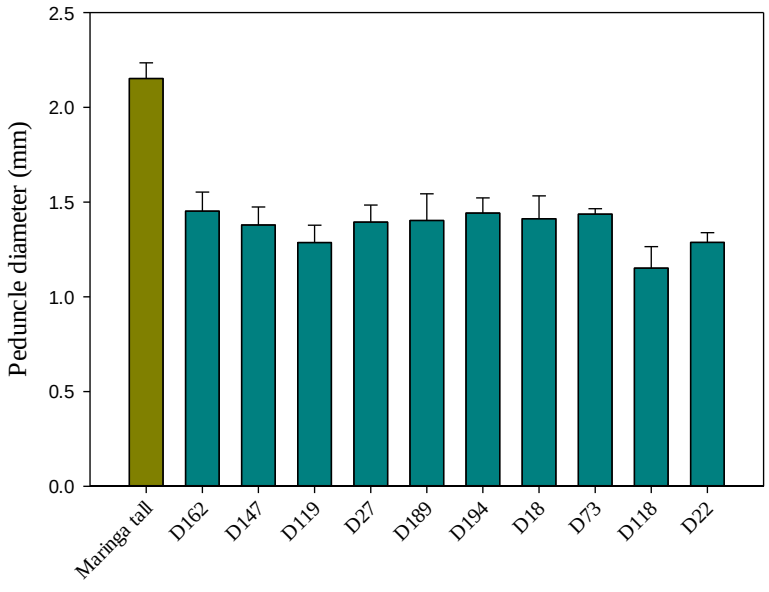

Figure 6.6. Peduncle diameter measurements of lines with large deletions compared to Maringá tall. All deletion lines showed significantly narrower peduncles compared with the tall line. Values are mean ± SE, n = 9.

Cytogenetic studies

SNP chip analysis suggested that there were lines with large deletions that lacked the short arm of chromosome 4B. It was of interest whether these might be detectable cytologically. Chromosomes are identified based on their banding patterns, chromosome size and arm ratios. Fluorescence In Situ Hybridization (FISH) analysis is a powerful tool for karyotyping to differentiate chromosomes within a genome. This procedure is important for detecting chromosomal aberrations, and for defining which chromosomes are involved in the case of aneuploidy. In this technique; genome-specific probes are used that are fluorochrome-labeled and specifically hybridize with chromosomes of one genome. Chromosomes are visualized using the fluorescence microscope.

Wheat has meta- or submetacentric chromosomes, and in theory chromosomes with one deleted arm should be distinguishable from other chromosomes; moreover, FISH should be able to detect which arm and chromosome are involved. Figure 6.7 shows FISH analysis of one of the deletion lines with all 4BS markers deleted based on SNP assays. The results clearly show a single pair of acro- or telocentric chromosomes, indicated by the arrows in Figure 6.7a,b. Chromosomes are counterstained with DAPI and fluoresce blue for FISH analysis. To detect D-genome chromosomes the pAs1 probe (red fluorescence) was used. This probe is a DNA clone from *Aegilops squarrosa* that contains D genome-specific repeated sequences (Rayburn and Gill 1986). B-genome chromosomes were detected using pHvG38 probe (green fluorescence), derived from *Hordeum vulgare* containing satellite repeats with minor sites on A- and D-genome chromosomes (Pedersen *et al.* 1996). Chromosomes visualized with these different probes revealed that chromosome 4B had a deletion of the short arm. Lines that lacked the entire chromosome 4B were also studied by cytogenetic techniques, and had a chromosome count of 40 instead of 42 in these lines (Figure 6.7 c).

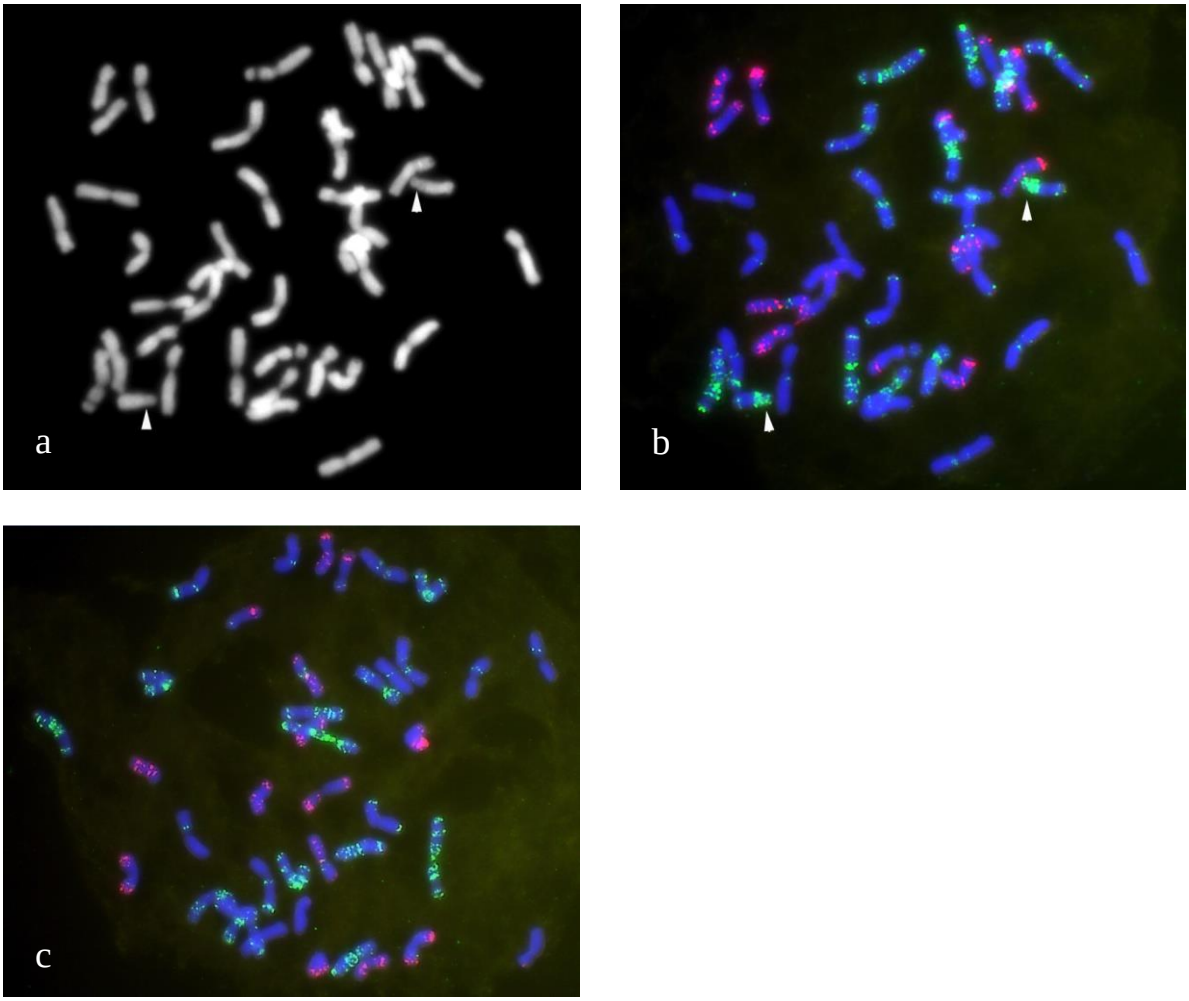

Figure 6.7. FISH on metaphase chromosomes of deletion lines belonging to group II and III. Chromosomes were counterstained with DAPI and fluoresce blue. The D-genome chromosomes were labeled by the repetitive DNA sequence probe pAs1 (red fluorescence). The barley clone pHvG38 has multiple hybridization sites (green fluorescence) on the B-genome chromosomes, and minor sites on A- and D-genome chromosomes. (a, b) show single acro- or telo-centric chromosomes of 4B in group II, that lost the whole short arm of the chromosome 4B. (c) shows a deletion line from group III that lacks chromosome 4B, the count of chromosomes is 40 instead of 42. The cytogenetic studies and images were courtesy of Dr. Peng Zhang.

Discussion

In this study, deletion of the *Rht-B1* gene in many lines was confirmed using Southern blot analysis. A newly developed technique, SNP chip array was used to define the sizes of the deletions in these lines. The results of 90K SNP chip analysis identified three classes of deletion lines;(I) interstitial deletions that lacked *Della* and various flanking regions; (II) deletion lines that lacked the short arm of chromosome 4B, but retained the long arm; and (III) deletion lines that lacked the whole chromosome 4B. The results from the SNP array provided evidence which could explain the distinctive phenotypes of some deletion lines. Lines with small deletions and lines that lacked 4BS had close to normal vegetative characteristics with fertile heads, while lines that lacked the whole 4B chromosome had narrow leaves, narrow stems and a medium to high degree of sterility. FISH analysis also confirmed SNP chip results, showing acro- or telocentric chromosomes for lines that lacked 4BS, and a chromosome count of 40 for lines that lacked the whole chromosome 4B.

Altered phenotypes due to mutation of *Della* genes were reported in other systems including Arabidopsis, rice and barley (Peng *et al.* 1997; Harberd *et al.* 1998; Chandler and Robertson 1999; Ikeda *et al.* 2001; Chandler *et al.* 2002). However, there are no reports of isolating mutants that physically lack *Della* genes in these species. In rice and barley, which have only a single *Della* gene, deletion of *Della* would presumably give rise to 'slender' plants; these are male-sterile which makes it impossible to isolate mutants with deleted *Della* gene unless it is done in family rows. In Arabidopsis there are five *Della* genes (*GAI, RGA, RGL1, RGL2, RGL3*) and it was shown that *RGA* and *GAI* are the main growth repressors. Therefore, even if a mutant with a deleted *GAI* gene was obtained, it would still be difficult to see a distinctive phenotype due to the presence of *RGA*. In wheat, the genetic buffering resulting from hoemeologous chromosomes prevents any dramatic phenotype when *Della* is deleted; for instance, the Maringá deletion lines were tall plants(not slender), with stem length slightly shorter than Maringá tall. This reduced length may reflect the fact that the smallest deletions still represent an estimated loss of at least 50 genes based on synteny with Brachypodium.

The isolation of deletion lines in Maringá has provided valuable material for wheat genetic studies, since they represent a series of nested deletion lines. The challenge in studying Maringá deletion lines was to find the best technique to assess the size of deletions most efficiently. There are only a few techniques that have been used to study deletion bins, including PCR studies using DNA markers or Southern blot analysis. Both techniques are restricted by the need to design appropriate markers from known gene sequences in a

particular chromosomal region. In wheat, both the design of primers and assigning them to specific chromosomal regions are very difficult because of three homeologous chromosomes and a low degree of marker polymorphism. However in our studies we used the wheat SNP chip arrays, a new high throughput technology that identifies thousands of markers on the wheat genome. Markers on 4BS were arranged in a notional order based on synteny with Brachypodium (wheat genome zipper). Although the long arm of chromosome 4 had poor conservation of order in the distal half, it does not affect our results since there were no interstitial deletions in the long arm.

Each class of deletion line that was defined by SNP arrays gave insight into our knowledge about deletion events. They also represent valuable material with possible applications in genetic and chromosomal studies. Class I deletion lines revealed that deletion can apparently be a simple event involving the loss of contiguous markers. However, in two cases it appears there is a complex case of deletion, with a block of markers present between two deleted regions (Figure 6.4, column 4 and 5 group I). Nested deletion lines can contribute to wheat physical mapping projects. There are 12 independent lines with different size deletions in this class. These lines can be used to order markers on chromosome 4BS based on the physical map.

We identified class II and class III deletion lines which lacked all of 4BS and the whole chromosome 4B respectively as unique examples of loss of 4BS and aneuploid lines respectively, since these have not been studied previously. An almost complete set of aneuploid lines is available in the Chinese Spring background, but it was not possible to generate stable ditelo lines of 4B, and the nulli-tetra 4B has been maintained as a heterozygote. The reason was high male sterility of those lines that lacked 4BS, making the isolation of a 4B aneuploid line impossible. A fertility gene has been mapped to the short arm of chromosome 4B, and based on 4BS deletion lines (the smallest deletion) the location of the gene on the physical map was estimated to be in the distal 16% of 4BS (Endo *et al.* 1991). Moreover, it appeared that a terminal deletion in 4BS of Chinese Spring line also interfered with centromere function and suppressed the meiotic pairing in the first metaphase between the short arms of the normal 4B and the deletion 4B chromosomes (Endo *et al.* 1991). In the Maringá background it appears that the fertility gene on 4BS does not have as extreme effect as in Chinese Spring, and nulli 4B lines still produce grains, even though the set is poor. All classes of deletion lines are stable during propagation.

Is it possible to extend this type of deletion analysis to other wheat chromosomes? This depends on whether deletions we have observed with *Rht-B1c*are specific to this gene or

not (for instance, the insertion of a transposon might result in genetic instability). If deletion is a general event, this might be very useful for mapping important genes in wheat that are still poorly known. The markers most suitable for this are those with a dominant phenotype that can also be simply screened. For instance there are other dwarfing genes that have not been characterised yet, but have a visible phenotype. If we assume that deletion is likely to affect such genes, then a systematic screen would lead to the isolation of deletion lines and of overgrowth mutants. The former could be identified by SNP chip analysis, since regions adjacent to the dwarfing gene will be likely deleted.

It is also interesting to know whether deletion was caused by the mutagen, sodium azide, or was it a spontaneous event? To test these possibilities, we are currently studying *Rht-B1c* in a different genetic background, with sodium azide or control treatments. In the M_2 generation we can assess the number of taller plants for each treatment, and assign these as overgrowth or deletion events.

Chapter 7

Final Discussion

Dwarf suppressor screens in barley and wheat resulted in the isolation of overgrowth mutants that are characterised by enhanced GA signalling. In both species, mutations of the *Della* gene (and in one case in barley of the*Spy1* gene) caused increased GA responses and resulted in plants with enhanced growth relative to the original dwarf.

The general aims in studying overgrowth alleles were described on page 24, but my research can now be described in more detail.

In barley, there were two areas of research

- Exploring novel aspects of overgrowth alleles in terms of their response to ABA
- Characterizing eight alleles backcrossed into Sloop, to investigate increased grain size and other agronomic traits.

In wheat, the research was focused in three areas

- The effects of each allele on traits such as stem length, yield,coleoptile length and dormancy
- Characterizing the expression levels of *Rht-B1* in six overgrowth mutants that were predicted to affect splicing of the insertion from this gene.
- Investigating putative deletion lines that lacked the *Rht-B1c* dwarfing gene

Overgrowth mutants in the Himalaya background were characterized for their response to ABA. It was shown that some extreme overgrowth mutants (those with highest LER_{max}), especially in combination with*spy1a* (double mutants), grew faster than wild type Himalaya in the presence of ABA. The most significant effects of mutant alleles were at the early stages of growth, when the first leaf had much faster elongation rates. The extreme overgrowth mutants had larger grains and so it was appropriate to investigate whether this was a factor in their apparent resistance to ABA. Using the double overgrowth mutant (M251), whose grains are 14% larger than Himalaya, we compared growth rates after dividing the grain populations into three weight classes, small, medium and large. These classes were identified by measuring individual grain weights in samples of Himalaya and M251 grains, and representative grains of each class were grown in the presence of ABA. Generally, larger grains had slightly faster leaf elongation during the course of growth (7 days) in both control and ABA solution. However, the most significant difference between double mutant and wild type was the early rate of leaf elongation. All grain classes of the double mutant had

consistently and significantly higher LER than Himalaya, despite the fact that grains in the smallest class of the double mutant were not as large as grains in the largest Himalaya class. This result showed that enhanced GA signalling in the double mutants promoted leaf elongation more significantly at early stages, and was presumably responsible for counteracting the effect of ABA.

Larger grains are important for barley breeding. Eight of the overgrowth alleles were backcrossed to Sloop, a commercial variety, to assess the effects of these alleles on grain size in a different background. We studied Sloop mutants and their wild type sister-lines which shared most of the recurrent parent genetic background, but differed in whether they carried the overgrowth allele. The results were very promising and grain size was promoted by a subset of five overgrowth alleles. Increased grain size was statistically significant and consistent across different trials and different growth conditions.

There are many factors that might contribute to grain size, and they often involve an increase in either photosynthesis (source strength) or in storage capacity (sink size). One important source of photosynthesis is the ear and different studies report a significant contribution (10% to 40%) of ear photosynthesis to grain mass, dependent on the environmental conditions (Araus *et al.* 1993; Maydup *et al.* 2010). Awns, as a component of the ear, are the most photosynthetically-active structure in the ear. They increase the surface area of the ear by about 36% to 59%, depending on their length, and they make a large contribution to overall source strength (Motzo and Giunta 2002). However, the increased assimilate resulting from more photosynthesis would only be used to fill grains if they have the capacity for extra storage. Sink size is under strong control of maternal tissue and it is suggested that GA might play a role during cell division and differentiation of maternal tissues in young grains prior to producing endosperm cells. It appears that overgrowth alleles have the potential for both increased source and larger sink. Our results showed significantly larger heads and longer awns for overgrowth mutants that had larger grains. Although longer awns probably increase photosynthesis of overgrowth alleles, it is also possible that the longer and more exposed rachis results in additional source strength. More study needs to be done in this area to measure the differences between awn and rachis photosynthesis in mutant versus wild type sister-lines, and to analyze the contribution of a possible increase in photosynthesis to an increase in grain mass. Advanced techniques are needed to look at GA levels and GA signalling in maternal tissues in florets after anthesis. Overgrowth alleles with larger grains will be interesting material to study the effects of increased GA signalling on sink capacity.

Overgrowth alleles had their greatest relative effect in promoting grain size under field conditions where grain size is presumably limited primarily by water deficit. It has been shown that under well-watered and terminal drought conditions awns still have high photosynthesis, but there is a reduction in grain yield in the drought condition (Hosseini *et al.* 2012). It was suggested that higher awn surface area led to higher grain yield if sink size was not a limiting factor. For instance, overgrowth alleles with a high potential for producing larger grains possibly would result in (relatively) bigger grains in adverse conditions since they have a large sink to accommodate assimilates. Moreover, grain size is a trait associated with grain quality. Future work can test the performance of overgrowth alleles in micro-malting, where they might potentially show improved malting properties. For instance, larger grains have increased levels of starch and therefore more potential extract. Moreover, enhanced GA signalling and the consequent faster germination of overgrowth mutants could increase diastatic power and reduce the time needed in steeping.

We made initial studies to identify possible factors that caused reduced grain yield in overgrowth mutants. We identified higher sterility, a slight reduction in the number of heads per plant and lower biomass as possible factors. The expression of sterility is likely related to environmental conditions which might be considered in future work with overgrowth alleles. A lower number of heads per plant can be controlled and possibly improved in future breeding programs. For instance, selection within a population may lead to isolation of overgrowth alleles with higher tiller number. Overgrowth alleles might also be crossed with appropriate varieties that have higher number of tillers. It may also be possible to increase the sowing density in plots to so that heads per unit area returns to normal values, if this is low in overgrowth lines.

In wheat, at the start of this study, there was a large (~ 300) collection of tall revertant lines under investigation. Characterization had commenced, but had not progressed very far. Twenty one different *Della* alleles had been identified by sequencing at that time, but many more were still in progress. It was not clear how many independent occurrences there might be for each allele. In addition, it appeared that many lines lacked the *Rht-B1* gene, and these were considered to be putative deletions.

Most overgrowth alleles are now in their M_4 to M_5 inbred generation (from the original M_2). The original phenotyping on earlier inbred generations is probably less reliable than the more recent phenotyping. Experimental methods have been refined, and the number of lines is now smaller. We studied the effects of each allele on stem length, coleoptile length, dormancy and grain yield. We demonstrated that overgrowth alleles have strong effects on

stem length. There was a range in height from slightly taller than the dwarf parent to as tall as the tall isoline. Further characterization showed that in most cases there was a correlation between stem length and the other traits under study. For instance stem length was generally correlated positively with coleoptile length, but inversely with grain dormancy. Grain yield tended to be highest for semi-dwarfing alleles, and lowest for tall alleles.

The study of grain dormancy has been a priority, together with the effects on stem length, and has shown that different alleles have specific effects on dormancy. It is known that the *Rht-B1c* allele is associated with high dormancy. Interestingly, shorter alleles generally had higher dormancy than taller alleles. This reflects the possibility that the mechanism by which *Rht-B1c* suppresses growth has overlap with the pathway by which this allele increases dormancy. More detailed phenotyping will be done when backcrossed lines are available to study the performance of an allele in a 'cleaner' background.

We had a particular interest in semi-dwarfing alleles, since there were several alleles with similar height to the *Rht-B1b* isoline. The grain yields of these semi-dwarfing alleles were comparable to, or slightly less than, that of *Rht-B1b*. We believe that introducing these alleles into elite lines will give grain yields comparable to existing semi-dwarfing alleles. Although these semi-dwarfing alleles did not improve coleoptile length, several showed considerable enhancement of dormancy compared to *Rht-B1a* and *Rht-B1b* isolines. These alleles have been through two back-crossing generations, and in both their effect on stem length and on grain dormancy the back-crossed lines perform the same as the original inbred lines. These alleles are candidates to be crossed to Australian and international elite lines.

During the initial characterization of overgrowth alleles it was observed that some tall revertant plants seemed to lack the *Rht-B1c* gene. This finding was unexpected although not surprising, since lack of the dwarfing gene would also result in less growth repression and subsequently plants would be taller. These lines were initially identified during PCR analysis, testing for the presence of the *Rht-B1c* allele prior to sequencing overgrowth alleles. The results showed that about half of the tall revertant lines lacked the dwarfing gene. The observation was confirmed using Southern blot analysis that indicated the presence of the A- and D-genome *Della* gene, but the absence of the B-genome gene. Deletion lines were of interest to study if they had different sized deletion events, especially if they form a collection of nested deletions. At that time, a newly developed technology, SNP chip arrays became available that allowed us to study the presence or absence of markers along chromosome 4B in the deletion lines. With this technique we showed that there was a range of different-sized deletions, from interstitial deletions (*Della* deletions within 4BS) to deletion of all markers in

the short arm, or even some that lacked markers on both arms. Collaborative studies confirmed visual changes in chromosome 4BS/4B morphology which was consistent with the SNP results. Interstitial deletions are interesting material that can contribute to wheat mapping and markers projects. They might also be useful for sequencing studies of chromosome 4BS and for precise mapping of markers on the chromosomal sequence.

The isolation of deletion lines also suggests a potentially interesting and general application for studying markers on other chromosomes. It allows us to study unknown genes that have a visible phenotype; for instance it may be possible to screen for taller plants (deletions) in a dwarf background that has an unkown dwarfing gene. This would be an effective way to map the location of markers and an unknown gene on a chromosome. This system would only work if deletions occur throughout the genome. Deletion events might be spontaneous in origin and result from the hexaploid nature of wheat, where loss of one gene is compensated by homoeologous genes. For instance, in our study most deletion lines had perfect grain set except for some that lacked the whole chromosome 4B. This suggests that even if there were small deletion events in other studies, it would be difficult to detect them. It is possible to test whether deletion lines result from mutagen treatment or whether they are spontaneous. A population of grains can be divided into two groups; one group is then mutagenized whereas the other remains untreated. These populations can be sown side by side and be analyzed for tall revertantplants.SNP chip analysis can then be used to resolve them into deletion events.

In the process of characterizing overgrowth mutants, we identified five overgrowth alleles that had mutations at the intron-exon junctions of *Rht-B1c*. We characterised the expression levels of *Rht-B1c* alleles in these mutants. Our study showed that there were reductions in the expression levels of the gene compared to the tall isoline; however the results were not easily interpretable since the dwarf parent also had lower expression of the gene. RNA deep-sequencing showed that there was an increase in transcript reads for overgrowth alleles compared to the dwarf parent both for the 5’ and 3’ region of the gene. This area of work still needs further investigation, to fully explain the overgrowth phenotype of alleles. Nevertheless, we identified novel DELLA products (derived from novel splice events) that might be unstable with no function, or they might have novel functions that influence GA responses in these alleles. It would be possible to study DELLA isoforms by constructing them and testing their activity in terms of regulation of down-stream genes.

Detailed phenotyping of barley and wheat overgrowth alleles is necessary to assess their potential contribution to science advancement. This system has provided many overgrowth

alleles in both barley and wheat with mutations in highly conserved amino acid residues (Figure 7.1). They mostly carry single amino acid substitutions in the GRAS domain of DELLA which is known to be the region responsible for growth suppression.

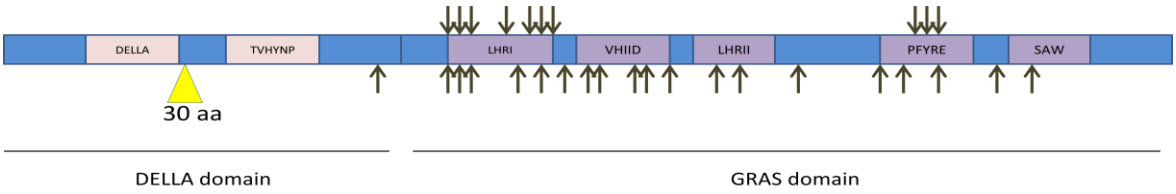

Figure 7.1. Sites of amino acid substitutions in DELLA for overgrowth mutants of barley (upper arrows) and wheat (lower arrows). Conserved sequence motifs are indicated and the yellow triangle shows the position of 30 amino acid insertion in wheat DELLA.

It is known that the conserved motifs in the N-domain (DELLA and TVHYNP) and in the C-domain (LHRI, VHIID, LHRII, PFYRE and SAW) are important in DELLA activity. These motifs are involved in DELLA binding to its partner proteins such as GID1, GID2 or transcription factors such as PIF family (Murase *et al.* 2008; Sun 2010). The conserved amino acid residues in these motifs play important roles in maintaining the function of that unit. For instance, yeast two-hybrid and yeast three-hybrid analyses of 41 mutagenized SLR1 proteins showed that not only DELLA and VHYNP are important in DELLA interaction with GID1and GID2, but some of the motifs in the GRAS domain also play an important role in keeping this interaction stable. For instance, certain amino acid residues of VHIID and LHRII are preferentially involved in binding to GID2. In addition, some residues of PFYRE and SAW make a large contribution to the stable binding of DELLA-GID1 (Hirano *et al.* 2010).

It was shown in Arabidopsis that DELLA regulates hypocotyl elongation via its direct interaction with PIF family transcription factors, mediated through the LHRI region (de Lucas *et al*., 2008). It appeared that this might be a specific function of LHRI to bind to down-stream target proteins, whereas other domain changes might affect the overall conformation of DELLA for its suppressor activity (Hirano *et al*., 2010). Many overgrowth mutations in both barley and wheat have occurred in the LHRI region, while others are distributed in other motifs. They will be interesting material to study the function of LHRI in DELLA activity since a range of phenotypes have been characterised for these alleles.

Previous studies have shown that regions important for the growth suppression activity of DELLA are scattered over the GRAS domain, and it was difficult to localize specific

regions for this DELLA function. Our understanding of DELLA motifs and their connections with DELLA activities would be improved if a crystal structure of DELLA was available. Then, we could look at the effect of each allele on DELLA conformation and its potential interaction with partner proteins. The position of amino acid substitution that we see at this stage in a linear form on a DELLA amino acid sequence might be much more interesting in the spatial form of the protein. It might group alleles based on their location on the real structure of DELLA which will lead us to better understanding of DELLA function. These alleles have the advantage of carrying mutations in conserved residues and having characterized phenotypes which allow us to study specific functions of the corresponding motifs. In addition, there are some identical mutations in both barley and wheat that would give even more information on the importance of those particular residues in DELLA activities.

In comparing barley and wheat overgrowth mutants, we have studied different aspects of GA phenotypes and DELLA responses since these two species have different ploidy levels. Barley has a single *Della* gene, while wheat has three representatives of the *Rht-1*gene. In barley, what we observe is the direct effect of changes to the *Sln1* gene, but in wheat we believe that background genes (*Rht-A1* and *Rht-D1*) influence the phenotype of *Rht-B1*o vergrowth alleles. In barley, loss-of-function DELLA mutants have obvious phenotypes, whereas in wheat, if some DELLA phenotypes were loss-of-function, they may not be obvious. There are some interesting comparisons that show the different behavior of overgrowth alleles in barley and wheat. For instance, grain size was significantly larger in many overgrowth mutants compared to the wild type in barley, whereas wheat alleles had no obvious effect on grain size. The other interesting observation was a variable degree of sterility in barley in both Himalaya (especially in double mutant combinations) and Sloop genetic backgrounds, whereas in wheat we saw no expression of sterility.

The first explanation that we have for the different DELLA phenotypes is that the existence of homoeologous genes in wheat masks the expression of overgrowth phenotypes through redundancy. We can also suggest another explanation for some differences in the behavior of overgrowth alleles in the two species. The presence of the dwarfing mutation in the *Della* sequence might influence the expression of a second site overgrowth mutation. In barley, it was possible to separate overgrowth alleles of the *Della* gene into those that also carried the *Sln1d* mutation, and those that occurred in a wild type *Sln1* gene. Interestingly, the latter group showed the most extreme overgrowth phenotypes in terms of having the highest leaf elongation rates and larger grains. Overgrowth mutants recovered from the gain-of-

function DELLA background never showed very high leaf elongation rates or consistently larger grains. The presence of the *Sln1d* dwarfing mutation in these overgrowth alleles might influence DELLA behavior. In wheat, all of the overgrowth alleles were recovered in the *Rht-B1c* dwarfing gene. Therefore all alleles still carry the dwarfing mutation, and it is possible that this effectively restricts the phenotypes of wheat overgrowth alleles.

There are some approaches that would allow us to investigate these issues further. It should be possible to examine the expression of overgrowth alleles in wheat in a background that lacks functional DELLA proteins encoded by the A- and the D- genomes. TILLING (Targeting Induced Local Lesions IN Genome) is one approach to isolating loss-of-function genome-specific alleles, and these could be combined together in the presence of a B-genome overgrowth allele. The other approach is to use transformation to look at particular overgrowth mutations, either of barley or wheat, without the dwarfing mutation, and in a background that lacks the A- and D-genome DELLA activity. This would allow alleles that produce larger grains in barley to be studied in wheat, and resolve whether it is genome redundancy or the presence of a dwarfing mutation in an overgrowth allele that affects phenotypes.

References

Achard P, Genschik P (2009) Releasing the brakes of plant growth: how GAs shutdown DELLA proteins. Journal of Experimental Botany 60(4):1085-1092 doi:10.1093/jxb/ern301

Achard P, Liao L, Jiang C, et al. (2007) DELLAs contribute to plant photomorphogenesis. Plant Physiology 143(3):1163-1172 doi:10.1104/pp.106.092254

Alabadi D, Gil J, Blazquez MA, Garcia-Martinez JL (2004) Gibberellins repress photomorphogenesis in darkness. Plant Physiology 134(3):1050-1057 doi:DOI 10.1104/pp.103.035451

Appleford NEJ, Lenton JR (1991) Gibberellins and Leaf Expansion in near-Isogenic Wheat Lines Containing Rht1 and Rht3 Dwarfing Alleles. Planta 183(2):229-236

Araus JL, Brown HR, Febrero A, Bort J, Serret MD (1993) EAR PHOTOSYNTHESIS, CARBON ISOTOPE DISCRIMINATION AND THE CONTRIBUTION OF RESPIRATORY CO2 TO DIFFERENCES IN GRAIN MASS IN DURUM-WHEAT. Plant Cell and Environment 16(4):383-392 doi:10.1111/j.1365-3040.1993.tb00884.x

Ashikari M, Sasaki A, Ueguchi-Tanaka M, et al. (2002) Loss-of-function of a rice gibberellin biosynthetic gene, GA20 oxidase (GA20ox-2), led to the rice 'green revolution'. Breeding Science 52(2):143-150 doi:10.1270/jsbbs.52.143

Bai MY, Shang JX, Oh E, et al. (2012) Brassinosteroid, gibberellin and phytochrome impinge on a common transcription module in Arabidopsis. Nature Cell Biology 14(8):810-U78 doi:10.1038/ncb2546

Bolle C (2004) The role of GRAS proteins in plant signal transduction and development. Planta 218(5):683-692 doi:10.1007/s00425-004-1203-z

Botwright TL, Rebetzke GJ, Condon AG, Richards RA (2001) Influence of variety, seed position and seed source on screening for coleoptile length in bread wheat (Triticum aestivum L.). Euphytica 119(3):349-356 doi:10.1023/a:1017527911084

Cai XL, Wang ZY, Xing YY, Zhang JL, Hong MM (1998) Aberrant splicing of intron 1 leads to the heterogeneous 5 ' UTR and decreased expression of waxy gene in rice cultivars of intermediate amylose content. Plant Journal 14(4):459-465 doi:10.1046/j.1365-313X.1998.00126.x

Callis J, Vierstra RD (2000) Protein degradation in signaling. Current Opinion in Plant Biology 3(5):381-386 doi:10.1016/s1369-5266(00)00100-x

Cao D, Cheng H, Wu W, Soo HM, Peng J (2006) Gibberellin mobilizes distinct DELLA-dependent transcriptomes to regulate seed germination and floral development in Arabidopsis. Plant Physiol 142: 509-525

Carol P, Peng J, Harberd NP (1995) Isolation and preliminary characterization of *gas1-1*, a mutation causing partial suppression of the phenotype conferred by the gibberellin-insensitive (*gai*) mutation in Arabidopsis thaliana. Planta 197: 414-417

Cavanagh CR, Chao S, Wang S, et al. (2013) Genome-wide comparative diversity uncovers multiple targets of selection for improvement in hexaploid wheat landraces and cultivars. Proceedings of the National Academy of Sciences of the United States of America 110(20):8057-8062 doi:10.1073/pnas.1217133110

Chandler PM (1988) HORMONAL-REGULATION OF GENE-EXPRESSION IN THE SLENDER MUTANT OF BARLEY (HORDEUM-VULGARE-L). Planta 175(1):115-120 doi:10.1007/bf00402888

Chandler PM (2000) Gibberellins and grain development in barley. In: McManus MT, Outred HA, Pollock J (eds) Seed Symposium: Current Research on Seeds in New Zealand. Agronomy Society of New Zealand, Auckland

Chandler PM, Harding CA (2013) 'Overgrowth' mutants in barley and wheat: new alleles and phenotypes of the 'Green Revolution' Della gene. Journal of Experimental Botany 64(6):1603-1613 doi:10.1093/jxb/ert022

Chandler PM, Harding CA, Ashton AR, Mulcair MD, Dixon NE, Mander LN (2008) Characterization of gibberellin receptor mutants of barley (Hordeum vulgare L.). Mol Plant 1(2):285-294 doi:Doi 10.1093/Mp/Ssn002

Chandler PM, Marion-Poll A, Ellis M, Gubler F (2002) Mutants at the Slender1 locus of barley cv Himalaya. molecular and physiological characterization. Plant Physiology 129(1):181-190 doi:10.1104/pp.010917

Chandler PM, Robertson M (1999) Gibberellin dose-response curves and the characterization of dwarf mutants of barley. Plant Physiology 120(2):623-632 doi:10.1104/pp.120.2.623

Chiang HH, Hwang I, Goodman HM (1995) Isolation of the Arabidopsis Ga4 Locus. Plant Cell 7(2):195-201 doi:Doi 10.2307/3869995

Chrispee.Mj, Varner JE (1967a) GIBBERELLIC ACID-ENHANCED SYNTHESIS AND RELASE OF ALPHA-AMYLASE AND RIBONUCLEASE BY ISOLATED BARLEY ALEURONE LAYERS. Plant Physiology 42(3):398-& doi:10.1104/pp.42.3.398

Chrispee.Mj, Varner JE (1967b) HORMONAL CONTROL OF ENZYME SYNTHESIS - ON MODE OF ACTION OF GIBBERELLIC ACID AND ABSCISIN IN ALEURONE LAYERS OF BARLEY. Plant Physiology 42(7):1008-& doi:10.1104/pp.42.7.1008

Claeys H, Skirycz A, Maleux K, Inze D (2012) DELLA Signaling Mediates Stress-Induced Cell Differentiation in Arabidopsis Leaves through Modulation of Anaphase-Promoting Complex/Cyclosome Activity. Plant Physiology 159(2):739-+ doi:10.1104/pp.112.195032

Croker SJ, Hedden P, Lenton JR, Stoddart JL (1990) COMPARISON OF GIBBERELLINS IN NORMAL AND SLENDER BARLEY SEEDLINGS. Plant Physiology 94(1):194-200 doi:10.1104/pp.94.1.194

Cui H, Hao Y, Kong D (2012) SCARECROW Has a SHORT-ROOT-Independent Role in Modulating the Sugar Response. Plant Physiology 158(4):1769-1778 doi:10.1104/pp.111.191502

Dai C, Xue H-W (2010) Rice early flowering1, a CKI, phosphorylates DELLA protein SLR1 to negatively regulate gibberellin signalling. Embo Journal 29(11):1916-1927 doi:10.1038/emboj.2010.75

Darnell JE (1997) STATs and gene regulation. Science 277(5332):1630-1635 doi:10.1126/science.277.5332.1630

Daviere J-M, Achard P (2013) Gibberellin signaling in plants. Development 140(6):1147-1151 doi:10.1242/dev.087650

de Lucas M, Daviere J-M, Rodriguez-Falcon M, et al. (2008) A molecular framework for light and gibberellin control of cell elongation. Nature 451(7177):480-U11 doi:10.1038/nature06520

Dill A, Jung HS, Sun TP (2001) The DELLA motif is essential for gibberellin-induced degradation of RGA. Proceedings of the National Academy of Sciences of the United States of America 98(24):14162-14167 doi:10.1073/pnas.251534098

Dill A, Sun TP (2001) Synergistic derepression of gibberellin signaling by removing RGA and GAI function in Arabidopsis thaliana. Genetics 159(2):777-785

Dill A, Thomas SG, Hu JH, Steber CM, Sun TP (2004) The Arabidopsis F-box protein SLEEPY1 targets gibberellin signaling repressors for gibberellin-induced degradation. Plant Cell 16(6):1392-1405 doi:10.1105/tpc.020958

Egli DB (2006) The role of seed in the determination of yield of grain crops. Australian Journal of Agricultural Research 57(12):1237-1247 doi:10.1071/ar06133

Elliott RC, Ross JJ, Smith JL, Lester DR, Reid JB (2001) Feed-forward regulation of gibberellin deactivation in pea. Journal of Plant Growth Regulation 20(1):87-94 doi:10.1007/s003440010004

Endo TR (1990) GAMETOCIDAL CHROMOSOMES AND THEIR INDUCTION OF CHROMOSOME MUTATIONS IN WHEAT. Japanese Journal of Genetics 65(3):135-152 doi:10.1266/jjg.65.135

Endo TR, Gill BS (1996) The deletion stocks of common wheat. Journal of Heredity 87(4):295-307

Endo TR, Mukai Y, Yamamoto M, Gill BS (1991) PHYSICAL MAPPING OF A MALE-FERTILITY GENE OF COMMON WHEAT. Japanese Journal of Genetics 66(3):291-295 doi:10.1266/jjg.66.291

Evans MMS, Poethig RS (1995) GIBBERELLINS PROMOTE VEGETATIVE PHASE-CHANGE AND REPRODUCTIVE MATURITY IN MAIZE. Plant Physiology 108(2):475-487 doi:10.1104/pp.108.2.475

Feng S, Martinez C, Gusmaroli G, et al. (2008) Coordinated regulation of Arabidopsis thaliana development by light and gibberellins. Nature 451(7177):475-U9 doi:10.1038/nature06448

Finkelstein RR, Gampala SSL, Rock CD (2002) Abscisic acid signaling in seeds and seedlings. Plant Cell 14:S15-S45 doi:10.1105/tpc.010441

Fleet CM, Sun TP (2005) A DELLAcate balance: the role of gibberellin in plant morphogenesis. Current Opinion in Plant Biology 8(1):77-85 doi:10.1016/j.pbi.2004.11.015

Flintham JE, Borner A, Worland AJ, Gale MD (1997) Optimizing wheat grain yield: Effects of Rht (gibberellin-insensitive) dwarfing genes. Journal of Agricultural Science 128:11-25 doi:10.1017/s0021859696003942

Flintham JE, Gale MD (1983) THE TOM THUMB DWARFING GENE RHT3 IN WHEAT .2. EFFECTS ON HEIGHT, YIELD AND GRAIN QUALITY. Theoretical and Applied Genetics 66(3-4):249-256

Fu XD, Richards DE, Ait-Ali T, et al. (2002) Gibberellin-mediated proteasome-dependent degradation of the barley DELLA protein SLN1 repressor. Plant Cell 14(12):3191-3200 doi:10.1105/tpc.006197

Gendreau E, Traas J, Desnos T, Grandjean O, Caboche M, Hofte H (1997) Cellular basis of hypocotyl growth in Arabidopsis thaliana. Plant Physiology 114(1):295-305 doi:10.1104/pp.114.1.295

Gilroy S, Jones RL (1994) PERCEPTION OF GIBBERELLIN AND ABSCISIC-ACID AT THE EXTERNAL FACE OF THE PLASMA-MEMBRANE OF BARLEY (HORDEUM-VULGARE L) ALEURONE PROTOPLASTS. Plant Physiology 104(4):1185-1192

Griffiths J, Murase K, Rieu I, et al. (2006) Genetic characterization and functional analysis of the GID1 gibberellin receptors in Arabidopsis. Plant Cell 18(12):3399-3414 doi:DOI 10.1105/tpc.106.047415

Harberd NP, King KE, Carol P, Cowling RJ, Peng JR, Richards DE (1998) Gibberellin: inhibitor of an inhibitor of ... ? Bioessays 20(12):1001-1008 doi:10.1002/(sici)1521-1878(199812)20:12<1001::aid-bies6>3.0.co;2-o

Hartl FU, Hayer-Hartl M (2002) Protein folding - Molecular chaperones in the cytosol: from nascent chain to folded protein. Science 295(5561):1852-1858 doi:10.1126/science.1068408

Hartweck LM, Olszewski NE (2006) Rice GIBBERELLIN INSENSITIVE DWARF1 is a gibberellin receptor that illuminates and raises questions about GA signaling. Plant Cell 18(2):278-282 doi:10.1105/tpc.105.039958

Hauvermale AL, Ariizumi T, Steber CM (2012) Gibberellin Signaling: A Theme and Variations on DELLA Repression. Plant Physiology 160(1):83-92 doi:10.1104/pp.112.200956

Hebsgaard SM, Korning PG, Tolstrup N, Engelbrecht J, Rouze P, Brunak S (1996) Splice site prediction in Arabidopsis thaliana pre-mRNA by combining local and global sequence information. Nucleic Acids Research 24(17):3439-3452 doi:10.1093/nar/24.17.3439

Hedden P (2003) The genes of the Green Revolution. Trends in Genetics 19(1):5-9 doi:10.1016/s0168-9525(02)00009-4

Hedden P, Croker SJ (1992) REGULATION OF GIBBERELLIN BIOSYNTHESIS IN MAIZE SEEDLINGS, vol 13,

Hedden P, Kamiya Y (1997) Gibberellin biosynthesis: Enzymes, genes and their regulation. Annual Review of Plant Physiology and Plant Molecular Biology 48:431-460 doi:10.1146/annurev.arplant.48.1.431

Hedden P, Thomas SG (2012) Gibberellin biosynthesis and its regulation. Biochem J 444:11-25 doi:Doi 10.1042/Bj20120245

Hirano K, Asano K, Tsuji H, et al. (2010) Characterization of the Molecular Mechanism Underlying Gibberellin Perception Complex Formation in Rice. Plant Cell 22(8):2680-2696 doi:10.1105/tpc.110.075549

Hirano K, Kouketu E, Katoh H, Aya K, Ueguchi-Tanaka M, Matsuoka M (2012) The suppressive function of the rice DELLA protein SLR1 is dependent on its transcriptional activation activity. Plant Journal 71(3):443-453 doi:10.1111/j.1365-313X.2012.05000.x

Hooley R, Beale MH, Smith SJ (1991) GIBBERELLIN PERCEPTION AT THE PLASMA-MEMBRANE OF AVENA-FATUA ALEURONE PROTOPLASTS. Planta 183(2):274-280

Hosseini SM, Poustini K, Siddique KHM, Palta JA (2012) Photosynthesis of barley awns does not play a significant role in grain yield under terminal drought. Crop & Pasture Science 63(5):489-499 doi:10.1071/cp11256

Hsieh WP, Hsieh HL, Wu SH (2012) Arabidopsis bZIP16 Transcription Factor Integrates Light and Hormone Signaling Pathways to Regulate Early Seedling Development. Plant Cell 24 (10):3997-4011.

Ikeda A, Ueguchi-Tanaka M, Sonoda Y, et al. (2001) slender rice, a constitutive gibberellin response mutant, is caused by a null mutation of the SLR1 gene, an ortholog of the height-regulating gene GAI/RGA/RHT/D8. Plant Cell 13(5):999-1010 doi:10.2307/3871359

Isshiki M, Morino K, Nakajima M, et al. (1998) A naturally occurring functional allele of the rice waxy locus has a GT to TT mutation at the 5 ' splice site of the first intron. Plant Journal 15(1):133-138 doi:10.1046/j.1365-313X.1998.00189.x

Itoh H, Matsuoka M, Steber CM (2003) A role for the ubiquitin-26S-proteasome pathway in gibberellin signaling. Trends in Plant Science 8(10):492-497 doi:10.1016/j.tplants.2003.08.002

Itoh H, Sasaki A, Ueguchi-Tanaka M, et al. (2005) Dissection of the phosphorylation of rice DELLA protein, SLENDER RICE1. Plant Cell Physiol 46(8):1392-1399 doi:10.1093/pcp/pci152

Itoh H, Ueguchi-Tanaka M, Sentoku N, Kitano H, Matsuoka M, Kobayashi M (2001) Cloning and functional analysis of two gibberellin 3 beta-hydroxylase genes that are differently expressed during the growth of rice. Proceedings of the National Academy of Sciences of the United States of America 98(15):8909-8914 doi:10.1073/pnas.141239398

Iuchi S, Suzuki H, Kim YC (2007) Multiple loss-of-function of Arabidopsis gibberellin receptor At GID1s completely shuts down a gibberellin signal. Plant Journal 50(6):958-66

Jacobsen SE, Olszewski NE (1993) MUTATIONS AT THE SPINDLY LOCUS OF ARABIDOPSIS ALTER GIBBERELLIN SIGNAL-TRANSDUCTION. Plant Cell 5(8):887-896 doi:10.1105/tpc.5.8.887

Johnson LR, Scott MG, Pitcher JA (2004) G protein-coupled receptor kinase 5 contains a DNA-binding nuclear localization sequence. Molecular Cell Biology 24: 10169-10179.

Karniol B, Chamovitz DA (2000) The COP9 signalosome: from light signaling to general developmental regulation and back. Current Opinion in Plant Biology 3(5):387-393 doi:10.1016/s1369-5266(00)00101-1

Kim JS, Jung HJ, Lee HJ, et al. (2008) Glycine-rich RNA-binding protein7 affects abiotic stress responses by regulating stomata opening and closing in Arabidopsis thaliana. Plant Journal 55(3):455-466 doi:10.1111/j.1365-313X.2008.03518.x

Kornblihtt AR, Schor IE, Allo M, Dujardin G, Petrillo E, Munoz MJ (2013) Alternative splicing: a pivotal step between eukaryotic transcription and translation. Nature Reviews Molecular Cell Biology 14(3):153-165

Lanahan MB, Ho THD (1988) SLENDER BARLEY - A CONSTITUTIVE GIBBERELLIN-RESPONSE MUTANT. Planta 175(1):107-114 doi:10.1007/bf00402887

Larkin PD, Park WD (1999) Transcript accumulation and utilization of alternate and non-consensus splice sites in rice granule-bound starch synthase are temperature-sensitive and controlled by a single-nucleotide polymorphism. Plant Mol Biol 40(4):719-727 doi:10.1023/a:1006298608408

Lee S, Cheng H, King KE, et al. (2002) Gibberellin regulates Arabidopsis seed germination via RGL2, a GAI/RGA-like gene whose expression is upregulated following imbibition. Genes Dev. 16: 646-658.

Lechner E, Achard P, Vansiri A, Potuschak T, Genschik P (2006) F-box proteins everywhere. Current Opinion in Plant Biology 9(6):631-638 doi:10.1016/j.pbi.2006.09.003

Lester DR, Ross JJ, Smith JJ, Elliott RC, Reid JB (1999) Gibberellin 2-oxidation and the SLN gene of Pisum sativum. Plant Journal 19(1):65-73 doi:10.1046/j.1365-313X.1999.00501.x

Levesque MP, Vernoux T, Busch W, et al. (2006) Whole-genome analysis of the SHORT-ROOT developmental pathway in Arabidopsis. Plos Biology 4(5):739-752 doi:10.1371/journal.pbio.0040143

Li A, Yang W, Li S, et al. (2013) Molecular characterization of three GIBBERELLIN-INSENSITIVE DWARF1 homologous genes in hexaploid wheat. Journal of Plant Physiology 170(4):432-43 doi:10.1016/j.jplph.2012.11.010

Li YY, Xiao JH, Wu JJ, et al. (2012) A tandem segmental duplication (TSD) in green revolution gene Rht-D1b region underlies plant height variation. New Phytologist 196(1):282-291 doi:10.1111/j.1469-8137.2012.04243.x

Liang DC, Wu CY, Li CS, et al. (2006) Establishment of a patterned GAL4-VP16 transactivation system for discovering gene function in rice. Plant Journal 46(6):1059-1072 doi:10.1111/j.1365-313X.2006.02747.x

Libbenga KR, Mennes AM, Vantelgen HJ, Vanderlinde PCG (1986) CHARACTERIZATION AND FUNCTION-ANALYSIS OF HIGH-AFFINITY CYTOPLASMIC AUXIN-BINDING PROTEINS. Journal of Cellular Biochemistry:9-9

Locascio A, Blazquez MA, Alabadi D (2013) Dynamic Regulation of Cortical Microtubule Organization through Prefoldin-DELLA Interaction. Curr Biol 23(9):804-809 doi:10.1016/j.cub.2013.03.053

Lovegrove A, Barratt DHP, Beale MH, Hooley R (1998) Gibberellin-photoaffinity labelling of two polypeptides in plant plasma membranes. Plant Journal 15(3):311-320 doi:10.1046/j.1365-313X.1998.00209.x

Maydup ML, Antonietta M, Guiamet JJ, Graciano C, Lopez JR, Tambussi EA (2010) The contribution of ear photosynthesis to grain filling in bread wheat (Triticum aestivum L.). Field Crops Research 119(1):48-58 doi:10.1016/j.fcr.2010.06.014

McGinnis KM, Thomas SG, Soule JD, et al. (2003) The Arabidopsis SLEEPY1 gene encodes a putative F-box subunit of an SCF E3 ubiquitin ligase. Plant Cell 15(5):1120-1130 doi:10.1105/tpc010827

Menz I (2010) Australian Barley Varieties: A Reference Guide. Barley Australia, Adelaide

Miyazawa M, Tashiro E, Kitaura H, et al. (2011) Prefoldin Subunits Are Protected from Ubiquitin-Proteasome System-mediated Degradation by Forming Complex with Other Constituent Subunits. Journal of Biological Chemistry 286(22):19191-19203 doi:10.1074/jbc.M110.216259

Monna L, Kitazawa N, Yoshino R, et al. (2002) Positional cloning of rice semidwarfing gene, sd-1: Rice "Green revolution gene" encodes a mutant enzyme involved in gibberellin synthesis. DNA Research 9(1):11-17 doi:10.1093/dnares/9.1.11

Moore MJ (2000) Intron recognition comes of AGe. Nature Structural Biology 7(1):14-16 doi:10.1038/71207

Motzo R, Giunta F (2002) Awnedness affects grain yield and kernel weight in near-isogenic lines of durum wheat. Australian Journal of Agricultural Research 53(12):1285-1293 doi:10.1071/ar02008

Murase K, Hirano Y, Sun T-p, Hakoshima T (2008) Gibberellin-induced DELLA recognition by the gibberellin receptor GID1. Nature 456(7221):459-U15 doi:10.1038/nature07519

Nakajima M, Shimada A, Takashi Y, et al. (2006) Identification and characterization of Arabidopsis gibberellin receptors. Plant Journal 46(5):880-889 doi:10.1111/j.1365-313X.2006.02748.x

Ner-Gaon H, Fluhr R (2006) Whole-genorne microarray in Arabidopsis facilitates global analysis of retained introns. DNA Research 13(3):111-121 doi:10.1093/dnares.dsl003

Newman AJ (1997) The role of U5 snRNP in pre-mRNA splicing. Embo Journal 16(19):5797-5800 doi:10.1093/emboj/16.19.5797

Newman AJ, Norman C (1992) U5 SNRNA INTERACTS WITH EXON SEQUENCES AT 5' AND 3' SPLICE SITES. Cell 68(4):743-754 doi:10.1016/0092-8674(92)90149-7

Ni M, Tepperman JM, Quail PH (1999) Binding of phytochrome B to its nuclear signalling partner PIF3 is reversibly induced by light. Nature 400(6746):781-784

O'Keefe RT, Newman AJ (1998) Functional analysis of the U5 snRNA loop 1 in the second catalytic step of yeast pre-mRNA splicing. Embo Journal 17(2):565-574 doi:10.1093/emboj/17.2.565

Ogawa M, Kusano T, Katsumi M, Sano H (2000) Rice gibberellin-insensitive gene homolog, OsGAI encodes a nuclear-localized protein capable of gene activation at transcriptional level. Gene 245(1):21-29 doi:10.1016/s0378-1119(00)00018-4

Oh E, Zhu J-Y, Wang Z-Y (2012) Interaction between BZR1 and PIF4 integrates brassinosteroid and environmental responses. Nature Cell Biology 14(8):802-U64 doi:10.1038/ncb2545

Pearce S, Saville R, Vaughan SP, et al. (2011) Molecular Characterization of Rht-1 Dwarfing Genes in Hexaploid Wheat. Plant Physiology 157(4):1820-1831 doi:10.1104/pp.111.183657

Pedersen C, Rasmussen SK, LindeLaursen I (1996) Genome and chromosome identification in cultivated barley and related species of the Triticeae (Poaceae) by in situ hybridization with the GAA-satellite sequence. Genome 39(1):93-104 doi:10.1139/g96-013

Peng JR, Carol P, Richards DE, et al. (1997) The Arabidopsis GAI gene defines a signaling pathway that negatively regulates gibberellin responses. Genes & Development 11(23):3194-3205 doi:10.1101/gad.11.23.3194

Peng JR, Richards DE, Hartley NM, et al. (1999) 'Green revolution' genes encode mutant gibberellin response modulators. Nature 400(6741):256-261

Phillips AL, Ward DA, Uknes S, et al. (1995) Isolation and Expression of 3 Gibberellin 20-Oxidase Cdna Clones from Arabidopsis. Plant Physiology 108(3):1049-1057 doi:DOI 10.1104/pp.108.3.1049

Plackett ARG, Ferguson AC, Powers SJ, et al. (2014) DELLA activity is required for successful pollen development in the Columbia ecotype of Arabidopsis. New Phytologist 201:825-836

Potts WC, Reid JB, Murfet IC (1985) INTERNODE LENGTH IN PISUM GIBBERELLINS AND THE SLENDER PHENOTYPE. Physiol Plantarum 63(4):357-364 doi:10.1111/j.1399-3054.1985.tb02310.x

Pysh LD, Wysocka-Diller JW, Camilleri C, et al. (1999) The GRAS gene family in Arabidopsis: sequence characterization and basic expression analysis of the SCARECROW-LIKE genes. Plant Journal 18: 111-119

Qi L, Echalier B, Friebe B, Gill BS (2003) Molecular characterization of a set of wheat deletion stocks for use in chromosome bin mapping of ESTs. Functional & integrative genomics 3(1-2):39-55

Ramos JM, Delmoral LFG, Recalde L (1985) VEGETATIVE GROWTH OF WINTER BARLEY IN RELATION TO ENVIRONMENTAL-CONDITIONS AND GRAIN-YIELD. Journal of Agricultural Science 104(APR):413-419

Rayburn AL, Gill BS (1986) Isolation of a D-genome specific repeated DNA sequence from Aegilops squarrosa. Plant Mol Biol(4):102-109

Reddy ASN, Marquez Y, Kalyna M, Barta A (2013) Complexity of the Alternative Splicing Landscape in Plants. Plant Cell 25(10):3657-3683 doi:10.1105/tpc.113.117523

Richards DE, Peng JR, Harberd NP (2000) Plant GRAS and metazoan STATs: one family? Bioessays 22(6):573-577 doi:10.1002/(sici)1521-1878(200006)22:6<573::aid-bies10>3.0.co;2-h

Richards RA (1992) THE EFFECT OF DWARFING GENES IN SPRING WHEAT IN DRY ENVIRONMENTS .1. AGRONOMIC CHARACTERISTICS. Australian Journal of Agricultural Research 43(3):517-527 doi:10.1071/ar9920517

Rieu I, Eriksson S, Powers SJ, et al. (2008a) Genetic Analysis Reveals That C-19-GA 2-Oxidation Is a Major Gibberellin Inactivation Pathway in Arabidopsis. Plant Cell 20(9):2420-2436 doi:DOI 10.1105/tpc.108.058818

Rieu I, Ruiz-Rivero O, Fernandez-Garcia N, et al. (2008b) The gibberellin biosynthetic genes AtGA20ox1 and AtGA20ox2 act, partially redundantly, to promote growth and development throughout the Arabidopsis life cycle. Plant Journal 53(3):488-504 doi:DOI 10.1111/j.1365-313X.2007.03356.x

Robertson M, Swain SM, Chandler PM, Olszewski NE (1998) Identification of a negative regulator of gibberellin action, HvSPY, in barley. Plant Cell 10(6):995-1007 doi:10.1105/tpc.10.6.995

Sadowski I, Ma J, Triezenberg S, Ptashne M (1988) GAL4-VP16 IS AN UNUSUALLY POTENT TRANSCRIPTIONAL ACTIVATOR. Nature 335(6190):563-564 doi:10.1038/335563a0

Sadras VO, Egli DB (2008) Seed size variation in grain crops: Allometric relationships between rate and duration of seed growth. Crop Science 48(2):408-416 doi:10.2135/cropsci2007.05.0292

Sakai M, Sakamoto T, Saito T, Matsuoka M, Tanaka H, Kobayashi M (2003) Expression of novel rice gibberellin 2-oxidase gene is under homeostatic regulation by biologically

active gibberellins. Journal of Plant Research 116(2):161-164 doi:10.1007/s10265-003-0080-z

Sakamoto T, Kobayashi M, Itoh H, et al. (2001) Expression of a gibberellin 2-oxidase gene around the shoot apex is related to phase transition in rice. Plant Physiology 125(3):1508-1516 doi:10.1104/pp.125.3.1508

Sambade A, Pratap A, Buschmann H, Morris RJ, Lloyd C (2012) The Influence of Light on Microtubule Dynamics and Alignment in the Arabidopsis Hypocotyl. Plant Cell 24(1):192-201 doi:10.1105/tpc.111.093849

Sasaki A, Itoh H, Gomi K, et al. (2003) Accumulation of phosphorylated repressor for gibberellin signaling in an F-box mutant. Science 299(5614):1896-1898 doi:DOI 10.1126/science.1081077

Satou A, Taira T, Iguchi-Ariga SMM, Ariga H (2001) A novel transrepression pathway of c-Myc. Recruitment of a transcriptional corepressor complex to c-Myc by MM-1, a c-Myc-binding protein. Journal of Biological Chemistry 276(49):46562-46567 doi:10.1074/jbc.M104937200

Sears ER (1954) The aneuploids of common wheat. Research Bulletin Missouri Agricultural Experiment Station(572):58 pp.-58 pp.

Sears ER (1966) Chromosome mapping with the aid of telocentrics. Hereditas 2:370-81

Shimada A, Ueguchi-Tanaka M, Nakatsu T, et al. (2008) Structural basis for gibberellin recognition by its receptor GID1. Nature 456(7221):520-U44 doi:10.1038/nature07546

Shimada A, Ueguchi-Tanaka M, Sakamoto T, et al. (2006) The rice SPINDLY gene functions as a negative regulator of gibberellin signaling by controlling the suppressive function of the DELLA protein, SLR1, and modulating brassinosteroid synthesis. Plant Journal 48(3):390-402 doi:10.1111/j.1365-313X.2006.02875.x

Silverstone AL, Mak PYA, Martinez EC, Sun TP (1997) The new RGA locus encodes a negative regulator of gibberellin response in Arabidopsis thaliana. Genetics 146: 1087-1099

Silverstone AL, Ciampaglio CN, Sun TP (1998) The Arabidopsis RGA gene encodes a transcriptional regulator repressing the gibberellin signal transduction pathway. Plant Cell 10(2):155-169 doi:10.1105/tpc.10.2.155

Silverstone AL, Jung HS, Dill A, Kawaide H, Kamiya Y, Sun TP (2001) Repressing a repressor: Gibberellin-induced rapid reduction of the RGA protein in Arabidopsis. Plant Cell 13(7):1555-1565 doi:10.1105/tpc.13.7.1555

Silverstone AL, Tseng T-S, Swain SM, et al. (2007) Functional analysis of SPINDLY in gibberellin signaling in Arabidopsis. Plant Physiology 143(2):987-1000 doi:10.1104/pp.106.091025

Simpson GG, Filipowicz W (1996) Splicing of precursors to mRNA in higher plants: Mechanism, regulation and sub-nuclear organisation of the spliceosomal machinery. Plant Mol Biol 32(1-2):1-41 doi:10.1007/bf00039375

Singh RK, Cooper TA (2012) Pre-mRNA splicing in disease and therapeutics. Trends in Molecular Medicine 18(8):472-482 doi:10.1016/j.molmed.2012.06.006

Smith VA, Knatt CJ, Gaskin P, Reid JB (1992) THE DISTRIBUTION OF GIBBERELLINS IN VEGETATIVE TISSUES OF PISUM-SATIVUM L .1. BIOLOGICAL AND BIOCHEMICAL CONSEQUENCES OF THE LE MUTATION. Plant Physiology 99(2):368-371 doi:10.1104/pp.99.2.368

Spielmeyer W, Ellis MH, Chandler PM (2002) Semidwarf (sd-1), "green revolution" rice, contains a defective gibberellin 20-oxidase gene. Proceedings of the National Academy of Sciences of the United States of America 99(13):9043-9048 doi:10.1073/pnas.132266399

Sreenivasulu N, Borisjuk L, Junker BH, et al. (2010) Barley Grain Development: Toward and Integrative view. International Review of Cell and Molecular Biology. Elsevier (281) doi:10.1016/S1937-6448(10). 81002-0

Sreenivasulu N, Schnurbusch T (2012) A genetic playground for enhancing grain number in cereals. Trends in Plant Science 17(2):91-101 doi:10.1016/j.tplants.2011.11.003

Staiger D, Brown JWS (2013) Alternative Splicing at the Intersection of Biological Timing, Development, and Stress Responses. Plant Cell 25(10):3640-3656 doi:10.1105/tpc.113.113803

Stamm S, Ben-Ari S, Rafalska I, et al. (2005) Function of alternative splicing. Gene 344:1-20 doi:10.1016/j.gene.2004.10.022

Sun T-p (2010) Gibberellin-GID1-DELLA: A Pivotal Regulatory Module for Plant Growth and Development. Plant Physiology 154(2):567-570 doi:10.1104/pp.110.161554

Sun TP, Gubler F (2004) Molecular mechanism of gibberellin signaling in plants. Annual Review of Plant Biology 55:197-223 doi:10.1146/annurev.arplant.55.031903.141753

Sun X, Jones WT, Harvey D, et al. (2010a) N-terminal Domains of DELLA Proteins Are Intrinsically Unstructured in the Absence of Interaction with GID1/Gibberellic Acid Receptors. Journal of Biological Chemistry 285(15):11557-11571 doi:10.1074/jbc.M109.027011

Sun Y, Fan X-Y, Cao D-M, et al. (2010b) Integration of Brassinosteroid Signal Transduction with the Transcription Network for Plant Growth Regulation in Arabidopsis. Developmental Cell 19(5):765-777 doi:10.1016/j.devcel.2010.10.010

Swain SM, Tseng TS, Olszewski NE (2001) Altered expression of SPINDLY affects gibberellin response and plant development. Plant Physiology 126(3):1174-1185 doi:10.1104/pp.126.3.1174

Tait S, Moody D, Emebiri L Physiological parameters associated with grain plumpness in a barley mapping population. In: The 16th Australian Barley Technical Symposium, Melbourne, 2013.

Talon M, Koornneef M, Zeevaart JAD (1990) Accumulation of C19-Gibberellins in the Gibberellin-Insensitive Dwarf Mutant Gai of Arabidopsis-Thaliana (L) Heynh. Planta 182(4):501-505 doi:Doi 10.1007/Bf02341024

Tanaka N, Itoh J-I, Nagato Y (2012) Role of rice PPS in late vegetative and reproductive growth. Plant signaling & behavior 7(1):50-2 doi:10.4161/psb.7.1.18533

Thiel J, Mueller M, Weschke W, Weber H (2009) Amino acid metabolism at the maternal-filial boundary of young barley seeds: a microdissection-based study. Planta 230(1):205-213 doi:10.1007/s00425-009-0935-1

Thiel J, Weier D, Sreenivasulu N, et al. (2008) Different Hormonal Regulation of Cellular Differentiation and Function in Nucellar Projection and Endosperm Transfer Cells: A Microdissection-Based Transcriptome Study of Young Barley Grains. Plant Physiology 148(3):1436-1452 doi:10.1104/pp.108.127001

Thomas SG, Phillips AL, Hedden P (1999) Molecular cloning and functional expression of gibberellin 2-oxidases, multifunctional enzymes involved in gibberellin deactivation. Proceedings of the National Academy of Sciences of the United States of America 96(8):4698-4703 doi:10.1073/pnas.96.8.4698

Thomas SG, Rieu I, Steber CM (2005) Gibberellin metabolism and signaling. Vitam Horm 72:289-338 doi:Doi 10.1016/S0083-6729(05)72009-4

Toledo-Ortiz G, Huq E, Quail PH (2003) The Arabidopsis basic/helix-loop-helix transcription factor family. Plant Cell 15(8):1749-1770 doi:10.1105/tpc.013839

Ueguchi-Tanaka M, Ashikari M, Nakajima M, et al. (2005) GIBBERELLIN INSENSITIVE DWARF1 encodes a soluble receptor for gibberellin. Nature 437(7059):693-698 doi:10.1038/nature04028

Ueguchi-Tanaka M, Hirano K, Hasegawa Y, Kitano H, Matsuoka M (2008) Release of the Repressive Activity of Rice DELLA Protein SLR1 by Gibberellin Does Not Require SLR1 Degradation in the gid2 Mutant. Plant Cell 20(9):2437-2446 doi:10.1105/tpc.108.061648

Ueguchi-Tanaka M, Nakajima M, Motoyuki A, Matsuoka M (2007) Gibberellin receptor and its role in gibberellin signaling in plants Annual Review of Plant Biology. Annual Review of Plant Biology, vol 58, p 183-198

Varbanova M, Yamaguchi S, Yang Y, et al. (2007) Methylation of gibberellins by Arabidopsis GAMT1 and GAMT2. Plant Cell 19(1):32-45 doi:10.1105/tpc.106.044602

Wahl MC, Will CL, Luehrmann R (2009) The Spliceosome: Design Principles of a Dynamic RNP Machine. Cell 136(4):701-718 doi:10.1016/j.cell.2009.02.009

Weiss D, Ori N (2007) Mechanisms of cross talk between gibberellin and other hormones. Plant Physiology 144(3):1240-1246 doi:10.1104/pp.107.100370

Wells L, Kreppel LK, Comer FI, Wadzinski BE, Hart GW (2004) O-GlcNAc transferase is in a functional complex with protein phosphatase 1 catalytic subunits. Journal of Biological Chemistry 279(37):38466-38470 doi:10.1074/jbc.M406481200

Wen CK and Chang C (2002) Arabidopsis RGL1 encodes a negative regulator of gibberellin responses. Plant Cell 14: 87-100.

Wen W, Deng Q, Jia H, et al. (2013) Sequence variations of the partially dominant DELLA gene Rht-B1c in wheat and their functional impacts. Journal of Experimental Botany 64(11):3299-3312 doi:10.1093/jxb/ert183

Weston DE, Elliott RC, Lester DR, et al. (2008) The pea DELLA proteins LA and CRY are important regulators of gibberellin synthesis and root growth. Plant Physiology 147(1):199-205 doi:DOI 10.1104/pp.108.115808

White O, Soderlund C, Shanmugan P, Fields C (1992) INFORMATION CONTENTS AND DINUCLEOTIDE COMPOSITIONS OF PLANT INTRON SEQUENCES VARY WITH EVOLUTIONARY ORIGIN. Plant Mol Biol 19(6):1057-1064 doi:10.1007/bf00040537

Will CL, Luehrmann R (2011) Spliceosome Structure and Function. Cold Spring Harbor Perspectives in Biology 3(7) doi:10.1101/cshperspect.a003707

Willige BC, Ghosh S, Nill C, et al. (2007) The DELLA domain of GA INSENSITIVE mediats the interaction with the GA INSENSITIVE DWARF1A gibberellin receptor of Arabidopsis. Plant Cell 19(4): 1209-20

Wilson RN and Somerville CR (1995) Phenotypic suppression of the gibberellin-insensitive mutant (*gai*) of Arabidopsis. Plant Physiol 108:495-502

Wu J, Kong X, Wan J, et al. (2011) Dominant and Pleiotropic Effects of a GAI Gene in Wheat Results from a Lack of Interaction between DELLA and GID1. Plant Physiology 157(4):2120-2130 doi:10.1104/pp.111.185272

Wu N, Matand K, Wu HJ, et al. (2012) Natural rules for Arabidopsis thaliana pre-mRNA splicing site selection. Central European Journal of Biology 7(4):620-625 doi:10.2478/s11535-012-0060-1

Xu YL, Li L, Wu KQ, Peeters AJM, Gage DA, Zeevaart JAD (1995) THE GA5 LOCUS OF ARABIDOPSIS-THALIANA ENCODES A MULTIFUNCTIONAL GIBBERELLIN 20-OXIDASE - MOLECULAR-CLONING AND FUNCTIONAL EXPRESSION. Proceedings of the National Academy of Sciences of the United States of America 92(14):6640-6644 doi:10.1073/pnas.92.14.6640

Yamaguchi-Shinozaki K, Shinozaki K (2006) Transcriptional regulatory networks in cellular responses and tolerance to dehydration and cold stresses Annual Review of Plant Biology. Annual Review of Plant Biology, vol 57, p 781-803

Yamaguchi S (2008) Gibberellin metabolism and its regulation Annual Review of Plant Biology. Annual Review of Plant Biology, vol 59, p 225-251

Yamaguchi S, Smith MW, Brown RGS, Kamiya Y, Sun TP (1998) Phytochrome regulation and differential expression of gibberellin 3 beta-hydroxylase genes in germinating Arabidopsis seeds. Plant Cell 10(12):2115-2126 doi:Doi 10.2307/3870788

Yamamoto Y, Hirai T, Yamamoto E, et al. (2010) A Rice gid1 Suppressor Mutant Reveals That Gibberellin Is Not Always Required for Interaction between Its Receptor, GID1, and DELLA Proteins. Plant Cell 22(11):3589-3602 doi:10.1105/tpc.110.074542

Yeaman SJ (2004) Hormone-sensitive lipase - New roles for an old enzyme. Biochem J 379:11-22 doi:10.1042/bj20031811

Zentella R, Zhang Z-L, Park M, et al. (2007) Global analysis of DELLA direct targets in early gibberellin signaling in Arabidopsis. Plant Cell 19(10):3037-3057 doi:10.1105/tpc.107.054999

Zhang Z-L, Ogawa M, Fleet CM, et al. (2011) SCARECROW-LIKE 3 promotes gibberellin signaling by antagonizing master growth repressor DELLA in Arabidopsis. Proceedings of the National Academy of Sciences of the United States of America 108(5):2160-2165 doi:10.1073/pnas.1012232108

Zhu YX, Tepperman JM, Fairchild CD, Quail PH (2000) Phytochrome B binds with greater apparent affinity than phytochrome A to the basic helix-loop-helix factor PIF3 in a reaction requiring the PAS domain of PIF3. Proceedings of the National Academy of Sciences of the United States of America 97(24):13419-13424 doi:10.1073/pnas.230433797

Zhu YY, Nomura T, Xu YH, et al. (2006) ELONGATED UPPERMOST INTERNODE encodes a cytochrome P450 monooxygenase that epoxidizes gibberellins in a novel deactivation reaction in rice. Plant Cell 18(2):442-456 doi:10.1105/tpc.105.038455